Long-life HTP Depot Refuelling Interface

A Preliminary Investigation

Žilvinas Vinskas

Delft University of Technology

TU Delft

Long-life HTP Depot Refuelling Interface

A Preliminary Investigation

by

Žilvinas Vinskas

to obtain the degree of Master of Science
at the Delft University of Technology,
to be defended publicly on Wednesday February 1, 2023 at 9:00 AM.

Student number:	4353242	
Project duration:	May 9, 2022 – February, 2023	
Thesis committee:	Dr. ir. B.V.S. Jyoti,	TU Delft, supervisor
	Dr. A. Cervone,	TU Delft, chair
	Ir. R. Noomen,	TU Delft, examiner

This thesis is under embargo and cannot be made public until January 31, 2025.

Cover: ”Testing Satellite Servicing Technologies” by NASA Goddard/Rebecca Roth under CC BY-NC 2.0

An electronic version of this thesis is available at `http://repository.tudelft.nl/`.

TU Delft

Preface

I wish to thank dearly all the people who challenged my assumptions with their vivid imagination.

Žilvinas Vinskas
Delft, January 2023

Abstract

Highly concentrated hydrogen peroxide, known as high-test peroxide (HTP), is widely regarded as a greener and safer alternative to traditional hypergolic fuels. A recent development demonstrated the potential to manufacture HTP in-orbit, bypassing prolonged storage challenges associated with the substance. This sparked interest in development of a space resident HTP manufacturing depot which could enable a next generation of satellites powered by greener propellants capable to routinely refuel. One of the missing pieces is a refuelling interface that could be utilized in such a system. In this work, an initial set of conceptual requirements for the device are proposed together with a potential design based on existing solutions. The design is partially implemented and studied in simulations to verify the major components are feasible to develop. Out of the components, the development of an all-aluminium construction quick-insert fluid coupler is found to be an important immediate target for future research. While assumptions are made, this work eliminates an area of otherwise pure speculation within the depot concept by establishing a feasible set of capabilities of the interface as well as identifying specific targets for future developments.

Contents

List of Figures

List of Tables

Nomenclature

Abbreviations

3D	Three-dimensional
ASPIN	Augmentation System Port Interface
CAD	Computer-aided design
CONFERS	Consortium for Execution of Rendezvous and Servicing Operations
COTS	Commercial off-the-shelf
DOF	Degree of Freedom
EOL	End of Life
EROSS	European Autonomous Robotic Vehicle for On-Orbit Servicing
FEA	Finite Element Analysis
FKM	Fluoro-rubber
GEO	Geo-stationary Earth Orbit
GPS	Ground Positioning System
HST	Hubble Space Telescope
HTP	High-test Peroxide
IR	Infrared
LEO	Low Earth Orbit
LIDAR	Light Detection and Ranging
LINUSS	Lockheed Martin's In-space Upgrade Satellite System
LTL	Liquid Transfer Lines
MEOP	Mean Operating Pressure
MEP	Mission Extension Pod
MEV	Mission Extension Vehicle
MI	Mating Interface
MRV	Mission Robotic Vehicle
PID	Proportional, integral, derivative
PLA	Polylactic Acid
prox	Proximity
PTFE	Polytetrafluoroethylene
RAFTI	Rapidly Attachable Fluid Transfer Interface
RFNA	Red Fuming Nitric Acid
RNS	Relative Navigation System
RRM	Robotic Refuelling Mission
RSGS	Robotic Servicing of Geosynchronous Satellites
sat	Satellite
SIROM	Standard Interface for Robotic Manipulation
spec	Specification
SIS	Space Infrastructre Servicing
SSO	Sun-synchronous Orbit
TBD	To be Determined
UMHD	Unsymmetrical Dimethylhydrazine

Symbols

Symbol	Definition	Unit
$\vec{}$	Vector	-
$\hat{}$	Unit vector	-
$\mathbf{q}$	Quaternion	-
$\mathbf{q}(n)$	Conversion of axis-angle vector n to a quaternion representation	-
e_n	extension length n	[m]
$\vec{L}$	Length vector	[m]
l	length	[m]
$\vec{P}$	Position vector	[m]
P_{MPa}	Numerical value of pressure in MPa	-
r	Radius	[m]
v	Velocity	[m/s]

1

Introduction and Research Goals

1.1. Introduction

A recent development of a new technology at TU Delft that allows for greatly simplified production of highly concentrated hydrogen peroxide has unbound the substance from complexities of previous production techniques. In principle, the production now only requires water and electricity to be available. The concentrated hydrogen peroxide itself, also known as high-test peroxide (HTP), has been shown to be a viable propellant in low thrust applications like maneuvering thrusters even before turn of the century[1][2]. Recent advancements combining HTP with secondary fuels, such as Ethanol, suggest HTP-based combinations are also viable in other applications which utilize hypergolic propellants. HTP offers a basis for green and much safer alternative to traditional hypergolics, such as systems utilizing UDMH-RFNA combination which are highly toxic and carcinogenic[3]. One of the challenges of utilizing HTP is its tendency to slowly decay over time. This has been discussed since the early works and is a natural property of HTP[2]. While careful material selection for components such as storage tanks may reduce the rate of decay, it is impossible to fully eliminate and complicates use of HTP on long-life missions.

Here, the HTP producer-depot concept comes together. The novel production technology allows for HTP to be generated on-orbit and on demand, alleviating the storage life issues. As long as the producer is supplied with water, it could, in principle, endlessly generate propellant to fuel other HTP powered spacecraft. Enabled by the opportunity to regularly refuel, the latter would likewise not have to tackle the issue of storing HTP for extreme periods of time. In its entirety, the concept could result in next-generation satellite systems powered by much safer propellants and having lifetimes not limited by fuel capacity.

Perhaps similar to a regular fuel station, for the HTP producing depot to function it requires three fundamental capabilities: capability to source fuel, capability to store it, and the capability to transfer it to another spacecraft. The availability of the first sparked the concept, while the latter two are still to be developed. The storage solution is already in development, whereas the transfer capability is to be explored in this study.

A particular challenge herein is the fact the refuelling interface design study project starts from a blank slate. Initially, even the definition of what is 'a refuelling interface' is not known aside from it should somehow suitably transfer propellant. As such, there are two major aspects to the project: first, define the functionality of a refuelling interface in this context and second, generate a conceptual design that satisfies the definition in order to investigate its feasibility. Ultimately the expected outcome is some initial design of such a system which could serve as a basis for future work. Being one of the mission critical subsystems that would drive capabilities of the entire system, this would provide the first stepping stone for attempts to design a mission or vehicle around it, and a starting point for likely plentiful further improvements.

This document details an early design study performed on a plausible construction of such device. This first chapter introduces the problem and defines the research questions and goals. Following the introduction, the first part of this report attempts to solve the challenge of defining the required functionality of such an interface device. Chapter 2 details background investigations performed in search

of a reference system or a well-defined set of required capabilities. This search found limited success and thus chapter 3 details how expected requirements for such a device were constructed by collecting ideas scattered through various literature. The latter part of the document focuses on providing a conceptual solution to the identified problem and investigates if said solution is realistic to implement. In chapter 4 a conceptual solution is proposed by combining elements from existing successful designs in a manner that, at least in principle, would be capable of satisfying the proposed requirements. It is argued that a system comprised of a minimised clamp-secured liquid transfer interface assisted by an optional docking mechanism would allow for a flexible and scalable solution. To verify the assumptions behind this proposition, the following chapters 5, 6 and 7 investigate implementation of the three major elements of the proposed design: the liquid transfer lines, the clamp-based connector, and the docking mechanism. In these chapters, the fundamental functionalities required for the concept are demonstrated and critical components of each subsystem are sanity checked for feasibility.

1.2. Research Questions and Objectives

In order to achieve the goal of this research and answer the need for a conceptual design of a refuelling interface suitable for the HTP depot application, two critical questions have to be answered. First is knowing what a refuelling interface even implies in this context and what functionality does it require. A strict definition of the device is not yet available and any assumptions should be made with caution. The second is perhaps more natural and asks how could we make one.

Therefore, the boundaries of the what is considered the refuelling interface must be established first. Once that is known, the question of the required functionality can be raised, combined with a search for possibly existing solutions. Afterwards, the work can finally focus on providing a specific solution to the application. The critical need is to understand what capabilities such a device could offer as well as how it would integrate into spacecraft carrying it. These are important pieces of information in order to be able to kick start the iteration process on the entire HTP depot concept.

The following research questions are thus raised for this work:

1. What is the required functionality?
    (a) What defines a refuelling interface system in the context of HTP depot system?
    (b) What are the expected technical requirements for such a device?
    (c) Were such devices previously developed and if so, are they suitable?
2. How could such an interface be implemented?
    (a) What could be a suitable design concept?
    (b) What are the limiting factors, if any?
    (c) What would be the approximate mass and volume of such a device?

These research questions are aimed directly at the underlying need of having an initial design reference for such an interface. This project is not yet concerned about optimisation but rather finding a solution that would enable the concept in the first place. As a consequence, the objectives are focused on providing a single, likely viable solution that could later be iterated on. The research objectives formulated to answer the research questions are following:

1. Based on existing works, define the scope of the refuelling interface system functionality.
2. Based on existing works, generate a list of high level requirements for a refuelling interface system suitable for HTP depot application.
    (a) Formulate expected functional requirements.
    (b) Formulate expected reliability requirements.
3. Propose a conceptual solution.
4. Identify limiting factors by implementing a proof of concept design.
5. Demonstrate suitability of the solution by means of proof of concept simulations.
6. Provide an estimate of size and mass for such a device based on the proof of concept design.

2

Background and Literature Study

This chapter covers background investigation on the topic of space servicing and with special focus on refuelling attempts. Section 2.1 discusses the general topic of space servicing, the reasons behind interest in it and a typical mission. Section 2.1.4 more specifically reviews existing attempts at in-orbit refuelling systems in search of a conceptual reference for the depot system for this investigation. Section 2.2 provides a brief review of advances in supporting technologies. Finally, section 2.3 gives short summary of the chapter.

2.1. Background on Space Servicing

This section provides background information on the general topic of space servicing. It serves primarily to build context on the commonplace trends in satellite design, especially to understand the value and practicalities of servicing satellites.

2.1.1. Life of a satellite

The availability of spacecraft technology has provided humanity with communication tools and observational capabilities which would likely outclass even the wildest dreams of generations just a century prior. Unfortunately, these advanced technologies often come with a high monetary and even environmental cost. Typically satellite systems are objects of immense expense, commonly reaching into hundreds of millions per launch of a GEO (Geostationary Earth Orbit) satellite[4]. This only worsens as one includes the fact that a system is often is comprised of multiple satellites and requires extensive development before even getting to launch. To illustrate, the widely known GPS (ground positioning system) had an estimated initial cost of 14 billion dollars in 1995 and even decades later, the newer GALILEO system is expected to cost around 6 billion for development and initial operations[5].

Once developed and built, a satellite's life can typically be sectioned into four distinct phases: launch, deployment, operations and decommissioning. First, the launch phase is rather self-explanatory and includes the initial lift-off followed by insertion and release into the target orbit. The second is the deployment phase, which typically includes unfolding of structures such as solar arrays, final orbital corrections and other preparations required for the system to begin operations. Next, the satellite unsurprisingly spends most of its life in the operations phase, performing its primary function. Lastly, once end of life (EOL) is reached, the satellites are generally disposed of in a manner designed to minimise potential risk to other spacecraft. For LEO (low earth orbit) operations, the spacecraft are typically simply left to gradually descend due to drag from trace amount of gasses from the upper atmosphere and eventually de-orbit by burning up in the atmosphere. GEO satellites, however, are not feasible to fully de-orbit. As such, they are generally moved to a 'graveyard' at EOL from which they pose minimal risk of interfering with other satellites in GEO.

All of these mission phases carry significant risks due to technical or environmental challenges. The primary risk during launch phase is the failure of the launch vehicle in reaching the target orbit. Approximately 5% of GEO satellite launches fail here, and the number is slightly higher at 6% for LEO[4][6]. The following deployment phase carries risks of malfunctioning devices, such as failed extensions of solar panels or communication antennas, or discovery of irrecoverably failed components,

such as the central computer. A study on beginning of life failures of GEO satellites presented an estimate of 3-4% for experiencing a total failure and another 3-4% for a partial failure during this phase[7]. After entering the operational phase various failures are often experienced due to either component failure or space weather events. The space weather term absorbs various dangers in space - meteoroids and other micro-bodies, electrostatic charge buildup, highly energetic cosmic particles, and atomic oxygen corrosion are a few suggested by a study[8]. The said study also mentions an interesting figure that only 8% of the operational failures are due to 'human error', that is can be attributed to obvious mishaps in operation or design stage. Even when it comes to the decommissioning stage, where failure of the spacecraft may not seem to pose a direct threat to its (now completed) mission, a failure becomes a threat to other spacecraft. Derelict spacecraft can potentially break up or even worse, impact others, creating a threat of microbodies or catastrophic collisions. A worst-case outcome of such events is an exponential cascade where collision fragments from satellites cause a chain reaction of destruction, filling large areas of earth's orbit with so much 'junk' as to make it infeasible for a spacecraft to survive in, or even cross. The concept was first proposed in 1978 by Donald J. Kessler and has since become known as the Kessler syndrome[9]. While critically important for LEO operations, the same fundamental concept also applies in GEO.

Overall, about one in seven GEO spacecraft fail to survive to designated EOL[4]. Since the risks of failure during mid-life operations are relatively low, there is an industry trend to minimize launch and deployment failures by simply launching fewer, longer-lived spacecraft built with older 'proven' technologies. This is illustrated in figure 2.1 from a dissertation paper on on-orbit servicing[10]. This immense focus on reliability, redundancy and longevity results in both increasing complexity, mass and thus cost, but arguably also in reduced capability. The latter is just a consequence of avoiding cutting-edge technologies and having lifespan of over a decade - in the later stages of the mission the satellite might be severely outdated as suggested by the study on value of space servicing[4].

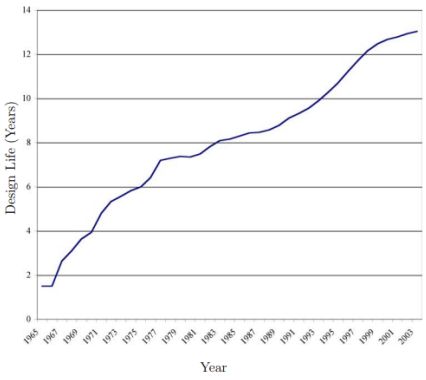

Figure 2.1: GEO satellite planned lifetime vs. launch year [10]

The same study also highlights an important point that the surviving six out of seven spacecraft do not instantaneously malfunction the moment EOL is reached. These spacecraft are often still perfectly functional, albeit the simple fact that some consumable has been exhausted, forcing to seize operations. The most straightforward example is often the propellant for the attitude and orbital thrusters, although other liquids (such as coolant for IR camera on Hubble Space Telescope[11]) or even batteries degrade under use and are viewed as consumables. As such, if a satellite survives to EOL, it could often be revitalized for years of further operation by simply refuelling or replacing worn batteries. Simple solution, if not for the incredibly inconvenient reality that the satellite is practically inaccessible due to being in orbit. As a footnote, the situation is lovingly summarized by a tongue-in-cheek quote found on the preface of the prior mentioned dissertation - "Looks like your vehicle is out of gas. Would you like to buy a new one?"[10].

2.1.2. Autonomous space (on-orbit) servicing

The need for performing maintenance or upkeep on spacecraft is by no means a novel concept. *The* canonical celebrated example of space servicing is the successful repair of the Hubble Space Telescope, which launched with an incorrectly manufactured mirror and thus had to be subsequently repaired in orbit[12]. The repair was performed by astronauts by installing additional optical components to correct for the flaw. In the period of 1993-2009 five servicing missions were performed by astronauts, maintaining and upgrading the HST[13]. However the manned missions such as servicing of the HST are infeasible outside of LEO. The manned spacecraft are simply too large, as such the costs are simply prohibitive.

Consequently, autonomous on-orbit servicing missions are a highly active topic in the industry. If a spacecraft does not experience an irrecoverable loss during launch, a lot of common faults can potentially be addressed via servicing. A reliability study suggests that approximately half of failed satellites could have been recoverable given even limited servicing capabilities[14]. With advancements to guid-

ance, tracking and maneuvering capabilities of satellites, performing autonomous service is actively pursued as a viable technology. The service tasks considered in the literature are fairly consistent, however are often referred to by different names due to lack of consistent vocabulary[15]. The areas of service discussed in literature can be grouped into the following eight categories with little loss of generality: inspection, orbit maintenance, refuelling, upgrade, repair, assembly and debris mitigation[16][15][17][18][19][14].

These common servicing areas cover the entirety of a satellite's mission profile starting from deployment through to end of life.

Inspection

The description of inspection missions is widely shared amongst the sources. Inspection is primarily discussed in terms of its diagnostic or identification value. Examples include analysing a failed satellite for incomplete deployment or damage, identifying uncooperative or unknown objects, and general preparations for other servicing. In most sources the reason for distinguishing inspection as a separate service comes from the fact that the servicing spacecraft does not have to make any physical contact with or even closely approach the target.

Orbit Maintenance

While in principle similar to refuelling in the achieved goals, orbit maintenance is often singled out as its own category. This class of service is described as the use of a servicing spacecraft to provide external support to a target vehicle. Boosting to maintain orbit or attitude control assistance are two most common functions mentioned. Because the thrust and control (station-keeping) is provided by the external spacecraft alone, this allows to potentially recover even truly failed targets.

Refuelling

Rather self explanatory, the refuelling services are commonly defined as the transfer of propellant or other consumable items to the client vehicle. Although the end goal is the same (i.e. allow the target to retain orbit and attitude) the critical distinction from orbit maintenance tasks arises in the fact that material transfer takes place between the vehicles.

Upgrade

Upgrading tasks are defined as addition or exchange of hardware, usually with the goal of improving the system's performance. The distinction between upgrade and repair tasks is commonly made despite both typically being envisioned as swapping hardware on the target system. Most common area of interest is modular upgrading of sensors to keep fleets of satellites equipped up to date as technologies advance.

Repair

The repair services are the most varying in descriptions. Repairs that involve swapping modules such as batteries are sometimes lumped together with upgrading and referred to as augmentation. Most common feature appears to be the availability of some level of robotic manipulation and changeable, multi-purpose tooling.

Assembly

This is a common category that refers specifically to building up of larger structures from independently launched modules. The despite the complexity, the value proposition described arises from reduced launch costs and risks as well as potential circumvention of launch size limits. The launch risks are said to be reduced as in case of failure not an entire satellite system is lost, rather only individual modules.

Debris mitigation

This is the last of the common categories. Although the classification varies between sources, the distinctive repeating feature is the ability to capture and recover or remove uncooperative targets. These range from minor debris pieces to derelict satellites.

2.1.3. Anatomy of on-orbit servicing missions

Investigation efforts under Consortium for Execution of Rendezvous and Servicing Operations (CONFERS) aim at establishing a common vocabulary and practices with the ultimate goal of laying foundation for future developments of safe and reliable on-orbit servicing technologies[20]. In pursuit, they sought to define common vocabulary and ethos for design efforts, especially surrounding safe approach of targets. The paper splits up a servicing mission into four large parts: ascent, quiescent, orbital servicing, and disposal. The illustration from the paper is included in figure 2.2. Of particular interest here are not the mission phases themselves, which are self-explanatory, but rather the clear demarcation of transitions between them. Especially those of rendezvous, proximity ('prox') operations and the triplet of capture, servicing and release. These terms appear to be used somewhat interchangeably in other literature. As such, to lessen confusion the following definitions based on the CONFERS work will be used in further discussions in this study:

- *Rendezvous* - the transition between idling and proximity operations. This refers to the approach maneuver that takes the service vehicle from its idling orbit to close proximity of the target client.
- *Proximity operations* - precise movements in the vicinity of the target without influencing it, such as making physical contact.
- *Capture* - establishment of sufficient physical influence on the target such that servicing operations are enabled. Most commonly docking, but non-contact alternatives are proposed for some applications (i.e. electrostatic capture).
- *Servicing (fluid transfer)* - execution of the primary servicing task. In the context of this study it refers to establishment and later safe separation of fluid transfer lines.
- *Separation* - the transition between captured and proximity operation states.

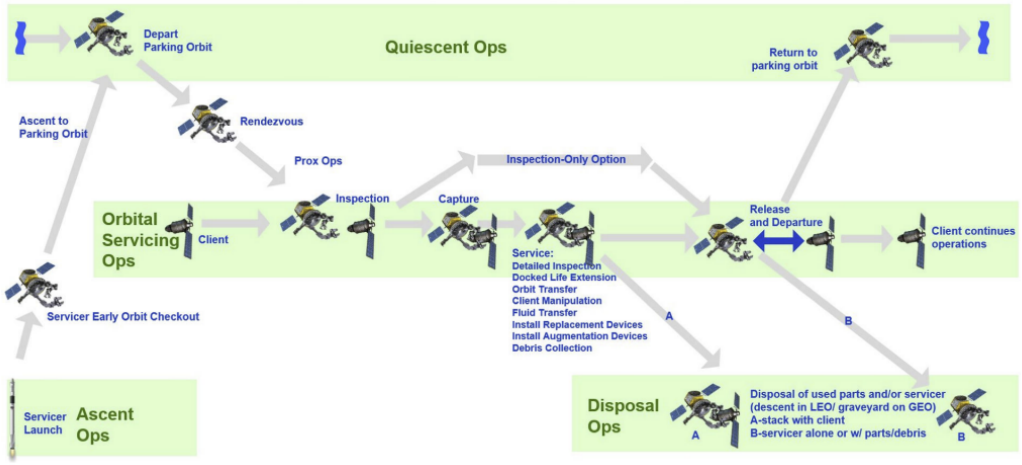

Figure 2.2: CONFERS proposed operational breakdown [20]

These five events comprise the sequence of actions necessary to perform a servicing mission. Once again owing to flaky vocabulary a distinction can be made between a servicing interface system and a service interface. The latter encompasses only the means relating to physically connecting two spacecraft (capture through to separation), whereas the prior also includes systems required for approach and proximity operations.

2.1.4. Contemporary and landmark autonomous space servicing missions with refuelling

Following the definition of core terminology, this subsection provides a short summary of most recent or milestone space servicing programs and missions that have officially announced to target providing refuelling services.

Unfortunately, a significant amount of the information presented here comes from less than ideal sources. Due to the nature of the projects being fairly secretive due to their commercial or even military nature, often times only breadcrumb information from official press releases is available. This

overview is an attempt to piece together the fragmented disclosed information into short summaries of the programs. Rather disappointingly, only a minority of them indicate any detailed technical plans or capabilities for refuelling, regardless of statements made.

Tanker-001 Tenzing

Orbit Fabs's Tanker-001 Tenzing is in principle similar to the concept under investigation. It is stated to be the first commercially available fuel depot satellite, launched as a demonstrator in 2021 and carrying HTP and oxidizer to SSO (sun-synchronous orbit)[21]. Docking to the client satellite and subsequent refuelling is accomplished by Orbit Fab's own RAFTI (rapidly attachable fluid transfer interface), which had previously been demonstrated to successfully transfer liquid water in ISS[22]. Tanker-002 is planned to be launched in ca2022-23, carrying Hydrazine propellant to GEO[23].

These missions are dedicated refuelling missions that have not shown any interest in providing other kinds of servicing, which makes them unique in the field. Although Orbit Fab have made statements that the company will open-source the design of the RAFTI interface, there is no indication it has done so as of yet[24].

LINUSS by Lockheed Martin

The LINUSS (Lockheed Martin's IN-space Upgrade Satellite System) is a demonstrator mission for feasibility of providing satellite servicing in Geosynchronous Earth Orbit (GEO) by small satellites[25]. The initial pair of 12U CubeSats were planned to be launched in late 2021, but appear to be have been delayed to first half of 2022[26]. This mission is primarily focused on demonstrating maneuvering performance and capability for proximity operations of the developed 3D sensing and tracking technologies [25]. It appears to be designed to target Lockheed's own LM 2100 satellite bus, which are GEO satellites in the range of 2.3-6.5 tons in mass [27].Currently the mission mentions use of AS-PIN (Augmentation System Port Interface), which appears to be a docking adapter with only electrical connections for modular expansion of the system. Under the LINUSS program, Lockheed Martin expressed interest in providing refuelling capability as well, and has invested in Orbit Fab, the company behind RAFTI refuelling connector, with the latter mentioned as a potential option for providing refuelling capability[28]. In practice, as of time of writing, the LINUSS mission is only targeting upgrade and modular repairs capability. The refuelling capability is only conceptual and even if committed to, would likely use the same system as Tanker-001.

MEV/MEP/MRV by Northrop Grumman, DARPA

Northrop Grumman's MEV (Mission Extension Vehicle), MEP (Mission Extension Pods) and MRV (Mission Robotic Vehicle) are considered among the market leaders of on-orbit servicing[15].Developed by Space Logistics (a subsidiary of Northrop Grumman) the MEV-1 and MEV-2 satellites are designed to attach themselves to Intelsat communication satellites via hooking onto their main propulsion thruster. Once fully attached, the MEV vehicle provides maneuvering and pointing control to the client satellite by using its engine, thus circumventing the fact that the client satellite is out of propellant. Both vehicles have successfully attached to their clients in 2020 and 2021, respectively[29]. The MEV vehicles are designed to last 15 years and potentially provide such support for multiple clients during this time. The MEV-1 is mentioned to support its current client for five years before moving on to others[30].Meanwhile, the MEP's are expected to be launched in 2024 and will serve a similar purpose of the MEV, albeit more cost-optimized. Instead of docking the entire service vehicle to the client, only the MEP (a miniaturized propulsive unit) will be attached to the client satellite, thus keeping the service MRV itself free and available[31]. Although envisioned for the MRV mission, there does not appear to be any intent of planned capability of refuelling as of yet, outside the functionally similar auxiliary MEP attachment. The MEV/MEP/MRV missions are thus orbital maintenance services. Potentially this confusion arises from lack of established universal vocabulary and orbital boosting sometimes being lumped with refuelling, a previously described problem in section 2.1.2.

LEXI by Astroscale

Astroscale's LEXI (Life EXtension In-orbit) project intends to use servicer vehicles that are in principle similar to the MEV and MEP from Northrop grumman. The service vehicle is intended to attach itself to the client vehicle and provide orbit and attitude control via its own thrusters[32]. This would classify it as a orbital maintenance servicer, just as the MEVs and MEPs.

However, an interesting feature of LEXI system is the fact the service craft themselves are intended to be refuelled to prolong their life. At start of 2022 Astroscale announced partnership with the prior mentioned Orbit Fab to provide refuelling capability of the service vehicles which are planned for launch in 2026[33].While it brings a second mission with dedicated refuelling capabilities to the table, is unfortunately yet another system utilizing the same RAFTI connector from Orbit Fabs.

EROSS by ESA
EROSS (European autonomous Robotic vehicle for On-Orbis Servicing) is a joint European project to demonstrate robotic capabilities[34]. It is still in development and is planned to carry and demonstrate various newly developed technologies. Among them two are peculiarly interesting to this research: the ASSIST docking system and SIROM modular expansion interface. The prior is meant to standardise and demonstrate refuelling capabilities while the latter is a highly capable inter-connect solution including liquid transfer (although for cooling purposes only)[34]. The ASSIST system is specifically interesting as it is a dedicated refuelling interface.

SIS (Space infrastructure servicing) by Maxar, DARPA, NASA
Originally started by MDA (now Maxar Technologies) of Canada, it was intended as a refuelling service mission for GEO satellites in partnership with IntelSat in 2011. The vehicle was planned to dock to a client satellite via hooking onto its primary thruster. The propellant was then intended to be delivered via robotic manipulators accessing the fuel system by reaching into the internals of the engine[35]. As such, the SIS is fundamentally a repair servicing mission. Even though its intended purpose was refuelling, that would have been achieved by the virtue of advanced general repair capability and in a complex fashion.

The program struggled achieving government-backed contracting through NASA or DARPA and was abandoned. After DARPA's own similar satellite servicing program, Project Pheonix, was reformed into RSGS (Robotic Servicing of Geosynchronous Satellites), the initial contract was awarded to SSL (a subsidiary of Maxar) in 2017[36]. In 2019 SSL left the project[37] and consequently the DARPA's contract was awarded to Northrop Grumman, giving rise to the prior mentioned MEV program[38].

OSAM-1/RESTORE-L by NASA, Maxar
Although SSL(Maxar) dropped out of the RSGS project by DARPA, they apparently continued work on the NASA's descendant of the SIS mission. Originally by the name of RESTORE-L, later renamed to OSAM-1, the vehicle is intended to demonstrate performing complex servicing on LEO satellites. Namely, perform assembly and deployment of structures on-orbit as well as refuelling of satellites which were not designed with this capability. The latter is achieved by use of advanced robotic arm and tooling, essentially disassembling the client satellite in order to access propellant filling ports which were used to originally fill the tanks before launch[39]. The mission is planned to begin preparations for launch in late 2022 [40].

In 2022, Northrop Grumman Licensed technologies from the NASA's OSAM-1 mission for their MRV project[41] , perhaps as a possible alternative to their vague plan of incorporating the previously mentioned RAFTI.

RRM by NASA
Nasa's RRM (Robotic Refuelling Mission) was a demonstrator mission launched in 2011. It successfully demonstrated operation on demo valve and plug assembly on the ISS (international space station). During its operations until 2013, it managed to validate the ability for its robotic manipulator to change and use various tools to open bolts, fuel caps, valves, and to transfer fluids[16]. It was the precursor that demonstrated the viability of, and kicked off interest in what became SIS project and lead to most of the prior mentioned programs.

Orbital Express
Orbital Express mission was amongst the earliest of such kind and consisted of two spacecraft: ASTRO and NextSat. Meant as a demonstrator of various space servicing tasks and as an evaluation of viability of such services it was proposed c.a. 2000 [19]. The mission successfully launched and operated in 2007, demonstrating cooperative in-orbit servicing capabilities. A long list of demonstrations included docking and separation, servicing of a battery module and a series of successful fluid transfers between the two spacecraft in both directions, testing various flow control methods[42].

Being a demonstrator platform, the refuelling interface was quite auxiliary to the docking solution and relied on the docking to be already completed. Since mission was amongst the earliest attempts and two decades passed since its inception, it is unique in quality of published documentation. This provides valuable reference for how such systems are expected to function and what characteristics it should posses.

DEOS
Perhaps merely an honorable mention due to its early cancellation, the DEOS mission was intended as technological demonstrator for recovery and de-orbiting of uncooperative satellites. Secondary role was also planned as a servicing demonstrator. Consisting of two spacecraft, one acting as the client, one as the servicer. The servicer was to demonstrate the ability of capture of a tumbling target and performing servicing tasks, which also included discussions for potential refuelling capability[43]. The project was cancelled after the initial exploration and definition phase in 2010[44].

2.1.5. Summary of space servicing

Most missions are (or were) focused on the proximity operation or demonstrating a mix of tracking, capture and manipulation technologies. While the missions highlight maneuverability advancements, advanced ability to manipulate tooling and perform complex tasks, only few of them actually mention refuelling as more than an afterthought or expected emergent ability. Likewise, no true analog for the long-life depot concept was found.

The entire family of missions that have lineage from NASA's RRM mission rely on a specific feature of a family of mechanically related GEO satellites where the primary thruster provides a structurally convenient place to attach the servicing spacecraft. From there, the servicing, if any, is intended to be carried out by robotic manipulators in a similar fashion as would a human mechanic. This group of missions (RRM, OSAM-1, SIS, MEV) do not have any indication of having a standardized refuelling interface. This makes logical sense, as the last (or current) generation of satellites were not developed with any expectation of servicing to be feasible. As the technologies matured and recently made on orbit service possible, an obvious immediate client of interest are the numerous already deployed satellites. This pushes immediate efforts towards complicated generic servicing capabilities or highly situational solutions targeting a single family of related satellites.

As of today, it seems that achieving viable proximity operations has traditionally been the 'hard' part of on-orbit servicing concepts. This is further reflected in the fact that even MEV-1 and MEV-2 vehicle missions released a follow-up report which focused solely on the tracking and data gathered prior to the docking[45].To some extent the celebration of successful docking and servicing seems shunned by the victory that was proving the rendezvous and proximity operations.

When looking towards next generation developments it seems that the challenge to demonstrate proximity operations has been overcome and now multiple players in the field state interest directly pursuing refuelling in orbit. For this, companies are searching for a standardized or at least common way to provide a refuelling interface on their upcoming satellite busses. However there is an extremely limited selection of refuelling interface solutions. From the reference missions only the Orbit Fab related missions and the European EROSS have a clearly defined interface that could both provide the docking *and* liquid transfer capabilities. Given the Orbit Fab's solution is the only one available commercially and even proven in missions, there is no surprise that it was adopted by other major efforts as the go-to solution.

It is worth noting further that the Orbit Fab's Tanker spacecraft stand out as the exception here and are by far the closest to the concept application considered in this study. Not only is the spacecraft claimed as the first truly dedicated fuel tanker, its development is based around a specific, integrated interface that provides both the docking and refuelling capabilities for the spacecraft. They are designed with the sole purpose of refuelling and have no planned intention to provide other services. As of time of writing, Orbit Fab claim to be the only commercially available refuelling interface on the market. The recently announced LEXI mission from Astroscale brings another exciting dimension to this, potentially marking start of a new ecosystem. However, the reason this effort is hard to consider a true analog to the long-life depot concept under investigation is the fact that fuel tankers are more akin to disposable shuttles than a would-be permanent resident. Still, the concept itself is a very viable reference for a solution that could support the depot.

2.1.6. Lack of standardisation of refuelling

Given the novelty of the concept it is not unexpected that there was no direct analog mission found. As such, the interest shifts to whether or not more conceptually broad works exist that could be used as a credible reference for the capabilities of such system. In particular, have there been prior efforts that established general guidelines or recommendations for autonomous spacecraft refuelling systems.

An immediate finding in this area is the lack of published works of such nature. Lending credibility to this observation, the previously mentioned Consortium for Execution of Rendezvous and Servicing Operations (CONFERS) under funding from DARPA attempted a multi-year effort to document requirements and best practices for satellite servicing missions with the findings presented at the 70th International Astronautical Congress in 2019. Although successful in categorizing critical areas, the actual conclusions mostly consist of 'TBD' (to be determined) when listing any practical parameters[20]. Additionally, out of 24 interfaces the effort identified, only a single one was suitable for satellites (i.e. not human-sized) and capable of refuelling - RAFTI by Orbit Fab, which was already identified in the reference missions.

Overall these findings agree with those from section 2.1.5 in that existing solutions are highly specific and likely no works have been published which would generalize well to the concept under investigation. The literature investigation performed is by no means extensive enough to truly declare that no such works exist, but between the efforts of this work and especially those by CONFERS it can be said with confidence that this specific problem has not been widely studied in detail, at least in published works.

2.2. Advancements in Autonomous On-Orbit Service

Missions discussed in section 2.1.4 lead to a disparity where the apparent amount of work on service docking interfaces is remarkably low given the high effort in on-orbit servicing itself. While perhaps explained by economical factors, it still raises a suspicion that there is a potential technological hurdle that is reached before the projects get to interface designs. To investigate this line of thought, a short review of related technologies was conducted to answer if there are more critical pieces missing. In particular, which parts of the rendezvous, proximity operations and capture sequence should be considered as critical in this development.

2.2.1. Reference point - a 2005 summary of rendezvous and docking in space technologies

A convenient starting point here is a rather concise review of the state of autonomous rendezvous and docking as of 2005. The proceedings paper published by researchers at NASA explores what technology advancements were required for autonomous docking and consequent servicing of spacecraft to be viable[46]. The study highlighted that as of 2005, there was little feasibility of fully autonomous docking, especially outside of LEO. The three development areas critical to success, yet lacking in available solutions were identified as follows: long range navigation systems, proximity sensing and pose estimation, and mating mechanisms. In general, the conclusion was that at the time technology was not yet capable of reliably and efficiently tracking a distant spacecraft, it was difficult to safely and precisely approach a target, and there were no docking mechanisms that lend themselves to minimization. Regarding the latter, the discussion was about larger, human-sized docking solutions. However, it was highlighted that the issue was the reliance on impact docking to achieve capture. The fundamental concept applies to small vehicles as well.

2.2.2. Advancements in long-range navigation and rendezvous

The 2005 study proposed that navigation systems should be capable of safely tracking and approaching another spacecraft from 100's of kilometers. At the time, the discussed solutions like RF beacons or radar would become too impractical due to power and size requirements in the range of 10's of kilometers. The ground-based tracking technologies were not sufficient either, as 1km position accuracy was stated even in LEO, with support of GPS[46].

As an example of state of the art, the previously discussed reference mission spacecraft MEV-1 and MEV-2 have successfully demonstrated rendezvous and docking with a commercial satellites in 2020 and 2021. A following review report on the mission discussed how accurate and continuous tracking of both spacecraft was successfully achieved using a complex system of dozens of observation stations and advanced control algorithms fusing data from first party and even a large number of amateur

stations[45]. Another paper mentioning the MEV-1 mission suggests that the ground-based tracking system had a performance requirement of 50-100m in position accuracy[47].This capability is already an order of magnitude greater in accuracy than in the 2000's, even before considering this accuracy is achieved in GEO orbits rather than LEO.

The same study which mentioned the position accuracy of MEV-1 tracking also proposes a RNS (relative navigation system) capable of guiding a spacecraft to its target from around 80km range, without the need ground tracking support. The system uses optical cameras and LIDAR sensors in various regimes. Existing LIDAR-only systems are also presented, the best of which offer millimeter to centimeter accuracy ranging at a distance 1m to 10km [47].

Given these advancements in performance as well as successful GEO demonstrations of autonomous rendezvous and docking in reality, it can be argued that this limiting factor has been addressed by recent developments. As such, the navigation and the mid-range approach to a target in GEO is no longer a critical limiting factor.

2.2.3. Advancements in short-range navigation

According to the 2005 study, the complicated and massive system used on the Space Shuttle consisting of star trackers, radar, laser rangers, cameras, and the astronauts using hand-held instruments caused complications with discontinuities and accuracy, although no direct figures are provided[46]. It also identified a need for a single-sensor solution as a critical development for safe autonomous final approach. The review further described that despite being extremely experimental at the time, camera NFIR (natural feature image recognition) and LIDAR combination systems held great potential for excellent performance in a small package. The review concluded that although such systems were seen as a technological risk, these technologies would bring great benefits given sufficient development resources. This turned out to be a remarkable prediction, as all current developments hinge on this exact combination.

Currently, when using dedicated features such as distinct reflective or illuminated targets, these optical systems can achieve immense accuracy at shorter ranges. For example, VBS optical rendezvous system for PRISMA satellite stated typical 0.1mm (100 micrometer) position and <1°attitude accuracy at a distance below 5m back in 2010[48].Another more recent (2018) system discussed in a design of a cubesat is stated to be capable of <0.1mm accuracy and <0.2°attitude accuracy [49].In addition, such systems do not suffer from discontinuities and switch-over issues, as the accuracy naturally increases as the distance to target decreases. Overall, as wished by the 2005 study, the camera and lidar systems have reached maturity and have taken over as the de facto standard. As an example, they are relied upon in Orbit Fab Tanker-001[50], the ASSIST interface[51], the EROSS mission[34], and were to be used on the DEOS mission if it were not cancelled[52].

With improvement in machine learning technologies and processing power, the camera based systems have been dramatically improving in other areas as well. One area of specific interest is non-cooperative pose estimation. This refers to measuring the position and orientation of a satellite which has no special tracking features (i.e. reflective targets) and offers no useful information about itself such as telemetry. A paper published in 2020 discusses a recently held competition where teams competed to develop the most accurate computer vision algorithms for estimating the pose of a satellite from a single image frame. Described as a key technology for on-orbit servicing and debris removal missions, the best team achieved mean accuracy of 3cm in position and 0.41°in attitude [53].

Similarly to the long-range navigation, the short-range sensing is arguably a solved problem. While non-cooperative situations will undoubtedly see further progress, the systems utilizing dedicated tracking markers have since surpassed any realistic requirement for accuracy. To illustrate, the RAFTI interface described in section 4.1.1 has an alignment requirement of +-1cm, which is two orders of magnitude more lax than the accuracy of modern optical sensing systems. As such, there is no need to specifically develop a tracking system for a docking interface, as the needed accuracy can be assumed to be easily achieved if optical markers are included.

2.2.4. Advancements autonomous in mating solutions

The 2005 review made an observation that unfortunately the mating interfaces are often neglected in design due to a misconception of them being a simple mechanism. The study highlighted four critical features: the solutions of the time could not be minimized, the mating system should require minimal contact forces rather than relying on impact to self-align, the systems are not dual-fault tolerant in

mating and de-mating, and a docking interface should preferably be androgynous as to not limit cross-compatibility (i.e. not require active and passive sides) and potentially increase redundancy. The latter principles are incredibly important in manned missions where reliability in extreme situations is paramount, but in principle apply the same for autonomous missions where reliability is critical.

Between the published efforts of the SIROM, ASSIST and RAFTI interfaces discussed in chapter 4, the highlighted concerns have been partially addressed. First of all, these systems have been successfully minimized to suitable degree to suit use on even small spacecraft. Next, all these systems have some capacity to self-align after the initial capture and even prefer near zero-velocity docking situations rather than requiring an impact. In fact, for these miniaturized systems any excess velocity is now detrimental and the risk of rebounding and failing the docking sequence is a critical concern or even the primary area of focus in case of ASSIST. Out of the selection, only SIROM is specifically designed to be androgynous as its intended self-chaining purpose requires it. In the case of RAFTI and ASSIST, they have been specifically chosen to have active and passive sides to save weight and complexity on the client. The dual-fault tolerance for connection and release also shows little indication of being addressed with neither of the three indicating any design features for it.

It would be amusing to conclude that perhaps the study's observation of mating interfaces being neglected still stands. Especially considering the limited amount of reference docking solutions as shown in chapter 4, when compared to the amount of missions in section 2.1.4 where they would seem necessary. However, the reality is different - the years old high value satellites which are in need of service today were designed before there was any practical (or even potential) need for a mating interface to be included. As such, many servicing applications are developing towards generic robotic servicing such as OSAM-1 or use bespoke, target-specific solutions like the MEV-1 and MEV-2. Dedicated mating and refuelling interfaces are only of interest to next generation developments. As discussed in section 2.1.4, these efforts seem to have adopted ASSIST on the European side and RAFTI over in American developments. Each only address the 2005 study's concerns partially, and in different areas.

2.2.5. Summary of remaining challenges

From the review of recent developments it can be concluded that in fact rendezvous and proximity operations have been historically challenging. However, the technical solutions in these areas have been overcome and even proven in real-life deployments. Critically for this investigation is the knowledge that rendezvous and proximity operations do not currently pose technical challenges in interface design. Additionally, the systems which provide these solutions are easy to integrate independently of the interface. This luckily narrows the scope of interest to just the physical mating structure.

2.3. Summary of the Literature Study

The literature study identified that there is a lack of direct analogues to the long-life depot concept of interest. Nearly all the refuelling missions reviewed operate in a fashion that would not generalize well to the depot concept. These missions either achieve the propellant transfer in complicated means almost emulating groundservice or simply emulate the results of a would-be refuelling by externally assisting a target rather than transferring propellant. Aside from specific technology demonstrator missions, an integrated solution to the problem has only been demonstrated by the RAFTI interface developed by Orbit Fabs. Even for the latter, the concept of operations of the refuelling missions has sufficient differences from that of a long-life depot. As such, no sufficiently complete solution has been found existing, at least in the reviewed efforts.

A robust general definition of what a refuelling interface for a long life depot should be capable of was also not found in published literature. A recent attempt by a credible body to produce a generic set of requirements for a satellite refuelling interface has likewise not managed to define it sufficiently. However, the said effort did successfully define an operations sequence for a generic servicing mission.

The operations sequence defined by CONFERS when combined with a summary of outstanding challenges in autonomous servicing of spacecraft was used to finally define the functional scope for the interface to that of the capture and mating systems. Existing solutions were found that satisfy technical capability for the rendezvous and proximity operations phases of the servicing mission with a high degree of independence from the rest of the system. As such, the capture and mating are deemed the areas of interest for this concept.

3

Conceptual Requirements

This chapter focuses on the attempt to define the expected required functionality of a refuelling interface suitable for the long-life depot concept. As discussed previously in Chapter 2, no clear analog which would suggest a full definition of such parameters was found in the existing literature. As a consequence, this effort is left in a highly undefined state. As the long-life depot is merely a conceptual idea at this stage, there are no specifications whatsoever, leaving the project in a chicken and egg situation. In order to break this viscous cycle, hypothetical requirements are constructed based on fragmented information and considerations found in various existing works. Due to the fragmented nature of the information and the highly conceptual status of this project, the aim is not to achieve overly precise requirement definitions but rather encapsulate plausible extreme bounds in critical areas of the system. The intent is to later attempt and suggest a conceptual solution which would offer scalibility within these bounds. As a result, the performance figures are mostly taken as order of magnitude or based on extreme values encountered in the literature.

While there is little work implementing the such devices directly, more plentiful works have been published on various other aspects of servicing missions. These works draw conclusions on various sets of assumed operational conditions which can be used to theorize requirements, if not already so suggested by the studies. Combined, these fragments draw a picture of what a hypothetical interface should be capable of.

3.1. Baseline Requirements - HTP Depot Concept

There is a mere handful of high level requirements stemming directly from the concept itself. They are as follows: the interface shall be able to transfer liquid HTP or water, the interface shall be suited for extended life, and a soft requirement of the interface being easily adaptable for various missions. The latter is not strict in definition and in principle implies that a design should consider not resisting small modifications. Finally, based on the conclusions of section 2.2 there is no obvious technical need to consider systems for rendezvous and proximity navigation as part of the refuelling interface. Therefore, the bounds for functionality of the interface can be constrained: the interface shall provide means of mating, transferring fluid, and separating two spacecraft.

3.2. Expected Applications

An interesting source of insight here are economic studies of space refuelling. While they rarely offer any engineering details, the works theorize on how to make on-orbit refuelling services commercially viable. A major component of the value proposition for the clients is to allow reduction in initial launch mass and all associated costs[4]. While not directly stated as such in the literature, it can be safely assumed that minimal mass and cost for client-side integration are thus important features.

The core issue tackled by the economic investigations is the availability of clients and how to best utilize the servicer spacecraft. There is a general consensus that LEO servicing is not a viable interest due to the high ΔV requirements and disposable nature of satellites deployed there[4]. Multiple studies identify medium and large GEO satellites as the only viable target[4][10][17][54]. From here other works

expand in terms delivery optimization. Two major lines of thought diverge: one is providing a refuelling-only service by multiple small spacecraft [55], and the other is deployment of few but capable generic servicing spacecraft[47][43].

Studies considering dedicated refuelling missions suggest operation based on hub-and-spoke[19] or peer-to-peer models[55]. The fundamental optimization problem explored is efficient delivery of the propellant with minimal launch risks. The hub-and-spoke model utilizes simplistic ferry spacecraft shuttling fuel to and from a centralised depot. The peer-to-peer model bypasses a centralized depot by cooperation between the shuttles. In both concepts either the depot or lowest altitude shuttles are resupplied by consumable ferries. Because such arrangements call for numerous spacecraft, unit cost and simplification of each is favorable. As a consequence, the refuelling interface is highly standalone - it serves as both a docking and fuel transfer solution. Out of existing missions (section 2.1.4), the LEXI and TANKER missions are similar in operation. Both use RAFTI interface which appears to have been designed for such purpose.

The high capability servicing approach leans towards large and complex servicers which are capable of hosting integration of robotic manipulators. In this case, the refuelling interface is expected to only offer berthing capabilities rather than docking. By being mounted on a robotic manipulator operating between two already secured vehicles, the interface does not require to handle large misalignment or impacts. However, the overall minimization and mating forces are critical for efficient integration as an end-effector of a manipulator[56]. Out of the reference missions from section 2.1.4, the EROSS, SIS, RRM and potentially MRV use this approach.

Applying these observations in the context of a refuelling interface for a propellant producing depot is straightforward. For widest commercial viability the refuelling interface shall support medium and large GEO satellites and shall have minimal impact on the clients' design. In addition, the client shall be accessible for direct-docking shuttles and robotic manipulators via the same interface. It can also be expected that such a device will spend most of its life in GEO orbits and as such shall have suitable lifetime in GEO environment.

3.3. Lifetime

An immediate point of interest is to identify what would specify as suitably long life and translate it to a targetable figure. In the literature a very specific figure of 15 years is widespread when considering long-lasting satellites. Although not clear if it an actual or just de facto standard, it is found in multiple sources and multiple satellite systems[4][7][14][57].One of these studies elaborates further that it is the target design life of satellites manufactured by Intelsat which are common and have actual life of 12-15years, with 1/3 surviving 15-20years [4]. One of the other papers states that 30 years is an extremely long lifetime that would only be achievable with regular servicing and in the context of a communication satellite[15].But such lifespan would seem unlikely to be a practical target for a more dynamic system such as a servicing vehicle. Continuing with 15 years, a reliability study also used this figure as the cut-off point in its analysis without further elaboration as to the reasons why[58].Out of the reference missions described in section 2.1.4 only the MEV servicing vehicles had a clearly stated design lifespan and it is once again at 15 years. Following the apparent consensus the lifespan for the interface shall be at least 15 years.

In practice the refuelling interface would only operate occasionally and spend most of its lifespan in an idle state. For such applications it is more convenient to express lifetime requirements in cycles rather than operational hours. If a cycle taken as a complete mating-unmating sequence, the lifetime figure will correspond to number of servicing operations. Luckily the expected yearly count of refuelling clients in GEO have been previously estimated in at least two on-orbit servicing studies. A study comparing space-tug and refuelling concepts estimated 20 refuelling opportunities per year[57].Some thesis work has concluded at a similar figure of 25 when doing a broader analysis of serviceability of space systems[54]. The two estimates would place the lifecycle requirement in the region of 300 to 375 over 15 years. However if some margin is considered, for the uses of this project the lifecycle requirement can be estimated as 1000. This somewhat arbitrary increase is suggested with the intention of future-proofing the design for future market growth (more opportunities), respecting that the hub-and-spoke model of operations potentially could increase of cycles experienced, and finally simply collapsing the figure to an order of magnitude.

To conclude, in order to be suitable for long-life fuel depot application the refuelling interface shall

have a lifespan of at least 1000 cycles and 15 years.

3.4. Mating

An obviously critical function of the refuelling interface is safe connection and disconnection of the two spacecraft. In order to understand the expected requirements the following questions need to be answered: what is the range of masses expected and what are the expected approach conditions.

First, values for expected mass properties of GEO refuelling missions were collected and are presented in table 3.1. While there is no singular value, the literature proposing servicing of GEO satellites is in general agreement that both spacecraft are expected to be in the range of a few tons and have propellants capacity in range of a few hundred kilograms. The common trend is to estimate servicer mass around 1000kg of dry mass and multiple tons of propellant. One paper in particular draws a distinction between medium (2.5 - 4 tons) and large (4 - 8 tons) GEO satellites[51]. This distinction could explain why the most common range for client masses considered is around 2 to 4 tons. In order to maximise compatibility, the interface thus shall be designed to support the entire range of proposed masses. Therefore a requirement can be established that the interface shall support capture between any combination of spacecraft in the range of 1 to 10 tons. It can also be assumed to be expected to transfer up to 1000 kilograms of propellant per refuelling.

Table 3.1: Mass properties for refuelling missions. Fields marked with '-' indicate that data was not listed

servicer mass [kg]	client mass [kg]	propellant [kg]	source
-	3300	1100	[59]
6276	-	-	[4]
2300	-	-	[60]
2000 - 4000	1800-4200	-	[61]
4494 - 4899	2605 - 3010	122	[62]
2000 - 5000	-	600-850	[55]
-	500 - 2000	-	MEV spec
-	2500 - 8000	200 - 1000	[51]
1000 - 9000	2000 - 3000	-	[63]

Next, alignment performance is considered such that approach and capture limits could be established. There is some discussion of theoretical missions and previously proposed requirements available, which are presented in table 3.2. Although the estimates are once again scattered, the order of magnitude is fairly consistent. For example, a docking capture is expected to require a few centimeters and couple of degrees of tolerance. When operated on a precise robotic manipulator only a few millimeters and less than one degree is tolerance is expected. It is practically impossible to further analyse the data as none of the sources provide the reasoning on how these figures were achieved. Own attempts at re-estimating the values were not successful as there is lack of published data of similar nature. One paper was found that has shown that the actual docking precision is expected to be much higher, in the order of millimeters [49]. There is clearly large contingency in the estimates yet the reasoning behind it remains largely unclear. It could be theorized that such contingency is better respected by a refuelling mission, as it is not difficult to imagine a situation where the target of refuelling is in some form of contingency mode due to low propellant and thus experiences limited station keeping. Due to fairly common agreement, the middle range values shall be taken as the expectation, whereas the extremes shall be combined to form the worst possible case.

Consequently the following requirements are proposed for the interface:

- The interface shall be designed to capture targets within bounds of $+-50mm$ and 5° of alignment, and residual velocities of up to $30mm/s$ and $0.4^\circ/s$.
- The interface shall be designed to not be damaged by impact events up to $+-50mm$ and 5° of alignment, with residual velocities of $100mm/s$ axial, $50mm/s$ lateral and $1^\circ/s$ angular.
- The interface shall support robotic manipulator applications with precision of $5mm$ and 1°.

In addition to the approach envelope two other requirements have been occasionally mentioned in reviewed literature. First, the capture mechanism should support zero-impact operation [46][51]. This refers to the ability of bringing the spacecraft together from close proximity and zero relative velocity. The second is that the interface shall not require external force to initiate and hold connection[42][64].

Table 3.2: Collated estimates of docking conditions. Fields marked with ' - ' indicate that data was not listed.

offset [mm]	angular offset <axial, planar> [°]	linear velocity <axial, lateral> [mms^{-1}]	angular velocity [$^{\circ}s^{-1}$]	envelope (occurance)	source
50	5 ; 5	100; 50	0.25	expected	[63]
20	5 ; 5	15 ; 10	-	expected	[51]
20	11.3 ; 11.3	50; -	-	limit	[61]
5	1 ; 1	-	-	limit	[64]
- (0)	2 ; 2	100; 4	0.4	limit	[65]
50 (2")	5 ; 5	30; -	-	limit	[66]
50	1 ; 0.5	-	1	limit	[20]

Both of these are similar in nature, essentially the mating mechanism must be self sufficient to complete and hold the connection when positioned accordingly, with no additional support from other systems.

How the interface is expected to handle separation events is barely ever discussed. The most detailed mention, just a few sentences, was found in work related to EROSS mission. It is stated that the mechanism shall be able to impart an impulse during separation in order to safely distance the two spacecraft[34][51]. The magnitude of required velocity is not mentioned, but the fundamental functionality is clear.

3.5. Fluid Transfer

A fairly detailed design report about the liquid transfer system of Orbital Express mission has been published and covers fundamental considerations of such system[42]. It describes various liquid transfer techniques and there is a need for two fluid transfer lines even if a single liquid is transferred. Depending on the technique, the uses of each line differ but they are always utilized. Therefore the refuelling interface shall include two fluid lines for each transfer circuit.

Another major sizing parameter is the operational pressure. The intended operational pressure of the HTP depot is not yet known, however a rough figure can be estimated by referencing more widespread hydrazine systems for which the HTP is envisioned as a fairly direct replacement. A particular value of 20bar is a figure commonly seen in various systems. It is mentioned in the papers describing Orbital Express mission[42] and the COTS hydrazine storage tanks manufactured by Rafael cluster their pressure ratings in the 20-25bar range. As such, the value is adopted as the approximate target figure for operational pressure.

When considering transfer rate, no clear value for how long the liquid transfer process should take has been established. One study suggested that a reasonable mark is less than 8 hours so that the process can be completed under supervision of single shift of ground control operators[67]. Considering section 3.4 identified 1000kg of propellant as the expected maximum amount to transfer, the transfer rate should be around 125kg/hr or 35g/s. A similar number (same order of magnitude) is reported by Orbital Express mission which transferred fluid at 94.5g/s [42]. 100g/s figure was also assumed in a refuelling simulation thesis of GEO satellites, with satisfactory results [62]. Considering 35g/s rate would leave no time for approach, docking and pre-tests in the 8 hour window, the adoption of 100g/s is preferable. Therefore the liquid transfer rate shall be at least 100g/s, however this is perhaps a soft requirement given this is envisioned as an autonomous system.

Although the amount of liquid lines required per liquid transferred is known, the amount of different liquids to transfer over a single interface is another consideration. The entire space-deployed system is envisioned to be based around a permanent HTP depot which manufactures the propellant using water as a raw material. As such, there are two materials that would potentially be transferred. The depot spacecraft would inevitably require resupply of the raw material, most likely from earth. The rest of the system would likely utilize orbit-resident servicers that ferry the produced propellant from the depot to clients and are powered by the same substance. It can further be argued that the depot would likely have internally separate storage systems for both the raw H20 and the produced HTP. Therefore, it is reasonable to assume that a single transfer would not require simultaneous transfer of both H20 and HTP, or, at the very least, the 'space-resident' side of the system would only care about transferring HTP. Under this assumption, the required fluid transfer lines would remain at two.

3.6. HTP Handling

There are two areas to consider when considering HTP handling: HTP's harshness on materials and HTP's own stability when in contact with materials and surfaces[1]. The specific details appear limited and lacking in literature, and this lack of information has likewise been directly mentioned by a paper describing development of Tanker-001 spacecraft which was a HTP tanker[50]. These issues were especially critical to the storage system, but the impact on the transfer system is not highlighted aside from generic material compatibility. In general, the compatibility of valves, seals and tubing components must not be assumed, although compatible solutions are mentioned to exist as COTS.

Rocketdyne (USAF) compiled a detailed technical report about HTP and its physical properties which was finally publicly released in 1971[68]. Albeit old, it is still an exceedingly valuable resource on the topic. Some of the described effects garner immediately identifiable attention: rates of natural decomposition, interactions with construction of components, formation of damaging ice crystals and existence of potentially explosive liquid-vapor phases even at low temperatures below 100°C. First the rate of natural decomposition is reported as relatively low, in the order of few percentage points of mass per year. While this leads to dramatic effects in prolonged storage and is discussed in previously mentioned works, it can likely be ignored during a short transfer in the context of a refuelling interface. Next, the report provides detailed recommendations for valve selection and construction techniques. Regarding the latter, welded or flange construction of piping is recommended, while threaded fittings are to be avoided if at all possible. The report further recommends treatment of wetted surfaces with suitable coatings on top of selecting a highly compatible base material, with aluminium 1060 stated as ideal for piping although in general 1- or 2- series are suitable. Third, peroxide ice is said to be dangerous to material coatings and sensitive components such as valve assemblies. Ice formation can lead to surface scouring damaging coatings, blockage of piping or damage to seals and mechanisms. Finally, depending on pressure and temperature, HTP is reported as forming liquid-vapor phases which are an explosive hazard if contacted with carbon (organic materials or metallic-alloy contaminants). The latter two effects in particular impose a need to have thermal regulation of fluid transfer lines within suitable parameters, at least during operation.

A fundamentally similar set of problems has been encountered in the Orbital Express mission[42]. The spacecraft had capability to refuel by transferring hydrazine, another mono propellant which has similarly unstable and corrosive nature to HTP. The Orbital Express mission identified a requirement to pre-pressurize transfer lines before transfer as well as to completely purge the transfer system prior to undocking. This handling sequence was specifically chosen to minimize stability concerns of the propellant and to avoid prolonged exposure of components to hydrazine.

In summary, to respect the nature of HTP, the transfer system can ignore the slow natural decomposition of the material, but must ensure the following:

- Wetted components shall be HTP compatible. (valves, connectors, seals, etc.).
- The liquid transfer system shall be temperature-controlled during operation to prevent uncontrolled freezing or evaporation of the fluid.
- The lines shall be purgeable and ventable to avoid prolonged exposure to HTP.

3.7. Other Requirements

In literature the critical functions for docking and refuelling were considered no leakage [42] and separation of the docking mechanism[46]. Among many functional areas, the criticality of these stems from the possibility of losing the entire spacecraft rather just some functionality. For example, leaking propellants can damage spacecraft as the propellants are usually aggressive to spacecraft surface materials [19]. Meanwhile, if a mated interface fails to separate it may lead to loss of both vehicles [46]. Therefore interface shall be dual-fault tolerant against leaking, and the docking mechanism shall be dual-fault tolerant in separation.

Finally the operational temperature should be considered. Typically temperature requirements for space-grade components are fairly extreme, with -110-50°C range proposed for SIROM project [64]. However, such conditions are aimed at completely independent operation in space. In reality, some level of thermal management is usually provided by the spacecraft bus. For example LM2100 bus is common between GEO satellites and maintains temperature range of -24 to 61°C for its payload [69]. Assuming the liquid storage system of the HTP depot would require more delicate thermal management,

it is safe to assume that the operational conditions will be controlled to some extend, rather than design for absolute limits. Therefore the refuelling interface shall be designed to operate between -21 and 61°C.

3.8. Summary and Definition of High Level Requirements

Within previous sections various features required for long-life HTP depot have been identified from analysing published literature. This allows to define what a hypothetical refuelling interface should be capable of for such application. As a conclusion, these features are compiled into a list of higher-level requirements presented here:

1. The mating interface (MI) shall be comprised of the mating mechanism and fluid transfer lines.
2. The MI shall contain minimal active components on client side.
3. The MI shall be suitable flexible servicing of medium-large GEO satellites
   (a) The MI shall be capable of direct docking between medium-large GEO satellites
      i. The MI shall allow capture between two spacecraft of 1-10 tons in mass.
      ii. The MI shall have a capture tolerance of at least 50mm and 5°.
      iii. The MI shall allow approach velocities from zero up to 30mm/s and 0.4°/s.
      iv. The MI shall not be damaged by impact in the following conditions: up to 50mm position error, up to 5°orientation error, up to 100mm/s axial and 50mm/s lateral approach velocity, and up to 1°/s relative rotation.
      v. The MI shall be able to exert a repelling force during docking separation.
   (b) The MI shall be suited for manipulator driven berthing.
      i. The MI shall complete mating from 5mm and 1° of misalignment without application of external force.
      ii. The MI shall maintain the connection without application of external force.
4. The MI shall have suitable reliability
   (a) The MI shall have a lifecycle count of at least 1000.
   (b) The MI shall have lifetime of at least 15 years.
   (c) The MI shall be dual-fault tolerant against uncontrolled leaking.
   (d) The MI shall be dual-fault tolerant in separation.
5. The liquid transfer lines (LTL) of the MI shall be suited for transfer of liquid HTP and water.
   (a) The MI shall allow for at least 100g/s of flow rate.
   (b) The MI shall contain at least two transfer lines.
   (c) The LTL shall have MEOP of at least 20bar.
   (d) The LTL shall prevent uncontrolled freezing or boiling of HTP or water during operation.
   (e) The LTL and the wetted components therein shall be compatible with HTP and water.

4

Reference Interfaces and the Proposed Concept

Based on available literature the requirements for a hypothetical refuelling interface have been estimated in section 3.8. Now that the essential definition of a refuelling interface is known, a small number of similar devices can be found within servicing missions discussed in section 2.1.4.

In this chapter additional information gathered on these developments is presented. General functionality and capabilities of the interfaces are discussed. The goal is to establish commonalities, differences and solved or faced technical challenges of the designs to form a proposed conceptual solution for the interface.

4.1. Reference Interfaces

This section provides a review of discovered interfaces that were found to specifically target or, at the very least, mention refuelling of satellites as their application. Only four such devices were discovered: RAFTI, ASSIST, SIROM and the demonstrator system used in Orbital Express mission.

4.1.1. RAFTI (Rapidly attachable fluid transfer interface)

The RAFTI integrated docking and refuelling interface is currently claimed to be the only commercially available device of such nature (or at least discussed in public domain). The interface has been on the market since c.a. 2018 and has been demonstrated to successfully transfer water to the ISS in 2019, establishing a TRL (technology readiness level) of eight, raising it out 'experimental' status and becoming flight qualified[22]. TRL of 8 is generally accepted as the threshold for technologies to be integrated as part of baseline spacecraft bus[4]. It is therefore not surprising that contemporary space servicing missions have jumped to express interest in, or stated commitment to, adopting RAFTI as the solution for refuelling.

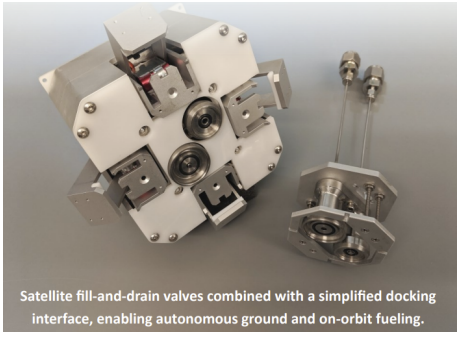

Figure 4.1: Early RAFTI design [70]

The RAFTI interface consists of an active (servicer) half and a passive (customer) side. The active side provides the clamping mechanism for the docking and initial alignment. The passive side only contains an attachment structure and fluid couplers to reduce cost and mass requirements for the customer [71]. Figure 4.1 shows both sides together for reference. During the docking, the active side's latching mechanism provides the initial berthing capture and alignment correction before retracting fully to rigidly clamp the two halves together and connecting the fluid couplings [72].

The interface comes in two variants - low and high pressure, depending on the fuel requirements. The low pressure interface lists compatibility with a wide range of liquid propellants, including HTP and water, whereas the high

pressure variant is intended for gaseous propellants, such as Xenon. The physical housing is maintained between the two variants, the only difference being the equipped quick-connect valves [71].

Manufacturer specifications [71](as stated as of time of writing) for the low pressure variant of the RAFTI interface are provided in table 4.1 below, with the exception of approach velocity which comes from earlier presentation[73].

Table 4.1: RAFTI specification

mass	0.5 kg (receiver side)
operating pressure	<650 psig
flow rate	4l/min ($\sim$96 g/s HTP)
cycle life	200
operational temp	-40 to 60°C
alignment req.	+- 10mm; +- 10°
approach velocity	5mm/s

By tracing the history of RAFTI an interesting observation can be made - the interface has been severely down-rated in terms of its lifespan. Initially, the interface was stated as capable of more than a thousand docking cycles. This figure is featured in old spec-sheets and was presented by Orbit Fab during the 2019 CubeSat Developers Workshop [73]. Such a drastic reduction in lifespan by nearly an order of magnitude is worrying, especially considering the peculiar interest of this research in the long-life space fuel depot use case. Unfortunately there appears to be no published reason for this downgrade, so it is up to speculation whether the design has been changed or the original life expectancy was over estimated.

Similarly to the cycle life of RAFTI, the self alignment capabilities have been drastically down-rated as well. The previously stated company's presentation showed 30°as the allowable limit for rotational misalignment around longitudinal axis[73] . Later spec-sheets state this value as 20°[70], and finally the most recent spec has dropped it to 10°. Once again, there is no clear indication as to why this happened.

In regards of suitability, RAFTI addresses many of the requirements proposed in section 3.8. It satisfies all the requirements to be manipulator mounted due to its minuscule size and latching design. However RAFTI fails to address some critical requirements as well. In particular, it falls short in requirements of life cycle endurance and capture characteristics.

4.1.2. ASSIST

The ASSIST interface is an effort by ESA to standardise and simplify OOS (on orbit service) operations by providing a common docking and service interface. It is worth highlighting that the ASSIST system encompasses more than just the connector itself, it also defines approach and guidance sensors[51], but these components lie outside of what requirements from section 3.8 defined as the scope of refuelling interface.

Similar to prior discussed RAFTI, this interface is also comprised of two distinct sides. The servicer side is once again the active side, containing all the mechanically active components and the receiver side is passive, both are shown in figure 4.2 for reference.The active side is intended to be mounted on a robotic manipulator as the end-effector [51].

The interface targets compatibility with GEO telecommunication satellites in the range of 2.5-8 tons specifically [51][61]. One of the primary design goals is to feature zero-force capture to avoid bumping the client spacecraft away during berthing, and to perform full alignment of the mating spacecraft before they are even brought together for latching. These capabilities are achieved using a complex mechanism in a multi-stage process shown in figure 4.3. The first stage of soft capture begins by the pantograph entering the oversized drogue cavity without yet making physical contact between the spacecraft. It is then expanded larger than the opening, resulting in the spacecraft being loosely connected and no longer in danger of drifting apart, completing the soft capture. Next, the clamping collar is extended such that it presses into the alignment ridge on the fixture with enough force to produce a rigid connection. This process also forces both spacecraft into relative alignment except for rotation around the longitudinal axis. This alignment is achieved by rotation of the clamping collar assembly and once aligned, the entire assembly is retracted such that the electrical and fluid couplings are engaged.

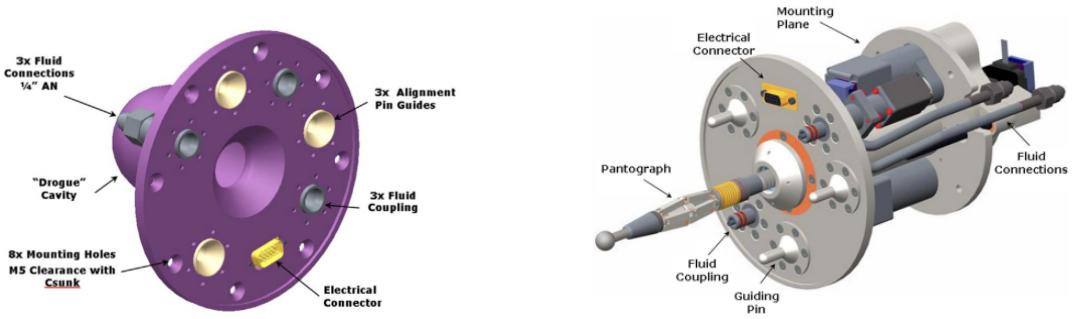

(a) Passive fixture **(b)** Active end-effector

Figure 4.2: The ASSIST interface passive and active sides [51]

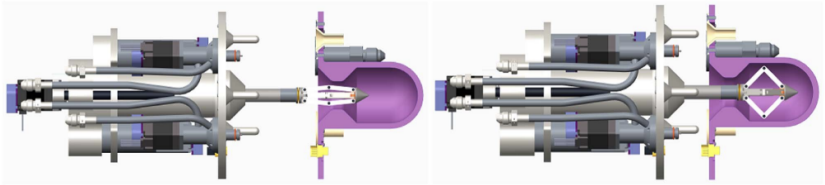

(a) Left: pantograph enters the drogue. Right: pantograph is deployed

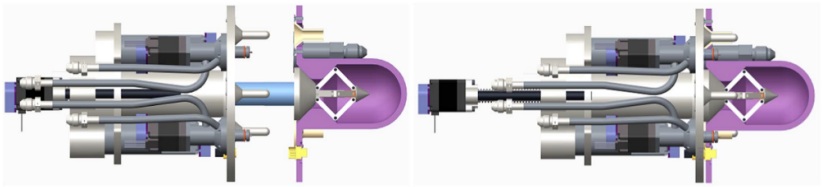

(b) Left: clamping collar pressed into the fixture. Right: collar is retracted to complete docking

Figure 4.3: The ASSIST capture sequence [51]

The publications describing the design of the ASSIST system focus heavily on the mechanical and structural design of the interface as well as development of simulations used in the design process. Unfortunately, they only mention other capabilities in passing. It is described to be capable of transferring monopropellants, MMH and xenon gas, but more detailed specifications are not mentioned. Hence operational pressures, mass flow rates, expected life or even operational temperatures are not known.

This unfortunately leaves the specification summary rather vacant, as shown in table 4.2. Nonetheless, the papers, and especially the project summary report [51], provide valuable hints and practices for design of such a system.

Table 4.2: ASSIST specification

mass	-
operating pressure	- (xenon transfer capable)
flow rate	-
cycle life	-
operational temp	-
alignment req.	+- 20mm; +- 11°
approach velocity	+-10mm/s lateral, 15mm/s axial

One piece of information provided by this project is that is of high value is that lenient capture and fluid coupler connection is difficult to combine, effectively requiring two separate mechanisms or stages of operation [51]. This fact should be considered when attempting to design a refuelling interface.

As a final thought, perhaps of note is the fact that in spite of great increase in mechanical complexity, the ASSIST system is not stated to have a significantly greater misalignment tolerance than the RAFTI. This is perhaps even more striking considering the ASSIST interface is specifically designed for soft capture and misalignment tolerance.

4.1.3. SIROM (Standard Interface for Robotic Manipulation)

Admittedly, the SIROM interface is not intended for refuelling purposes, but it is interesting to consider nonetheless. The SIROM connector is designed as a modular 'building block' for space robotics. Amongst the requirements imposed on the design is the capability for high capacity heat transfer for thermal management purposes between modules[64].This requirement is satisfied by inclusion of connectors for liquid transfer in the interface, such that the individual modules can link up and share a closed-loop liquid coolant system[74]. Although not intended as the primary function, a report mentions that it is feasible to repurpose the liquid transfer interface for future refuelling capability[56].Besides the (optional) liquid interface, SIROM carries multiple electrical connectors for data and power connections. A picture of the connector is shown in figure 4.4

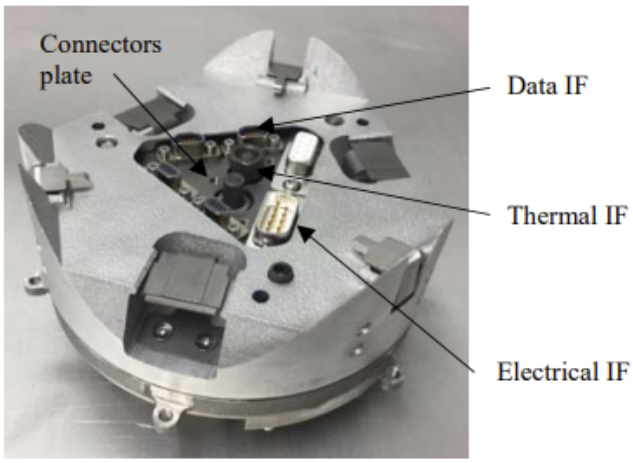

Figure 4.4: SIROM interface- SENER © [56]

One of the distinct features of this design is that is androgynous. Unlike the previously discussed interfaces, both 'halves' of SIROM are identical. While this feature is a necessity for the purposes of being used in multi-module chains, it still provides interesting benefits. For example, if one of the halves malfunctions after attachment, the remaining half can disconnect both modules on its own, improving fail-safe operation [56].

Operationally SIROM functions similar to RAFTI - the capture and securing of the connection is handled by latches that grab and compress the two sides together once roughly positioned. Both interfaces rely on final alignment occurring naturally as the clamps are engaged. Unlike the RAFTI design, SIROM features prominent alignment structures that gently guide the structure into alignment. Figure 4.5 shows a photo of two SIROM units approaching latching during a demonstration.

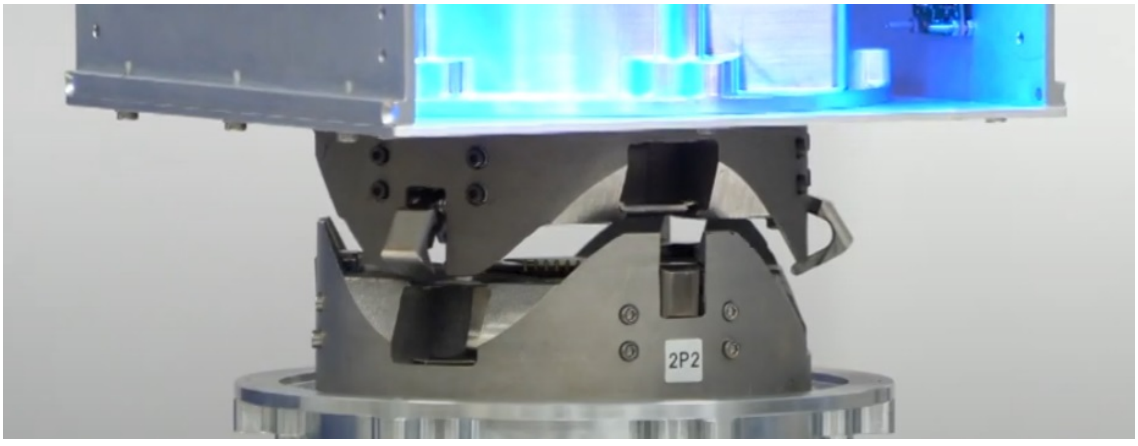

Figure 4.5: Two halves of SIROM positioned together for final latching. (Cropped still from [75])

Similar to the ASSIST interface, SIROM is intended to be mounted on a robotic manipulator. It is not intended to dock two free-floating spacecraft together and thus has much tighter alignment tolerances

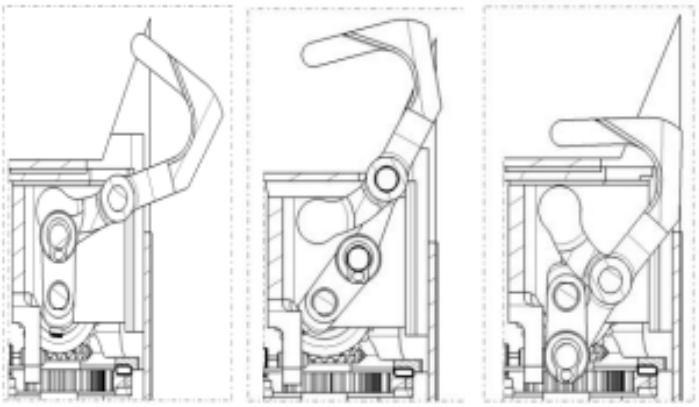

Figure 4.6: SIROM latching mechanism. Left to right: ready to capture, captured, final engagement[64].

when compared to previously discussed solutions. A lot of the specifications of interest can be found in the overview paper [56], an exception being the flow rate - it is a rough estimate translated directly from 2.2L/min capacity of the cooling loop pump intended to circulate coolant through the liquid interface [74]. The data is presented in table 4.3.

Table 4.3: SIROM specification

mass	<1.5 kg
operating pressure	-
flow rate	$\sim$ 2.2 l/min ($\sim$ 53g/s HTP)
cycle life	10000
operational temp	-110 to 50°C
alignment req.	+- 5mm; +- 1°
approach velocity	-

What makes SIROM project unique is the fact there are published works about the earliest stages of its inception, including earliest conceptual tradeoffs of technologies. In particular, the clamp mechanism has been identified as the superior option among many concepts when considering final mating which includes fluid couplers[76].In addition a report on later development stages provided a clear graphic on how the latching mechanism works, which is included as figure 4.6. This provides great technical guidance for future works, as there is a known optimal solution. Perhaps not surprising, the same approach is used in RAFTI as well.

4.1.4. Orbital Express fluid transfer system

The Orbital Express mission successfully demonstrated various cooperative servicing capabilities in 2007 including bidirectional transfer of hydrazine between two spacecraft and is well document in a report which will be summarized here[42]. In this case the refuelling interface was quite auxiliary, being connectable independently of the main docking port. However, the it did not feature any capability to reposition relative to the craft. As such, it can be argued as simply an interesting configuration choice for practicalities of the demonstrator vehicle.

Once the primary docking was complete and the two spacecraft were securely attached as seen in figure 4.7, the fluid coupler on the active side would extend to complete the connection for fluid transfer.

Conceding to the fact that the brunt of the complexity of connecting two spacecraft is carried by the primary docking port, the fluid transfer interface itself is unsurprisingly minimalist. Following or, perhaps, setting the trend it has two distinctive sides - active and passive. The passive side effectively only contains the female side of the fluid couple, whereas the active side contains the male counterpart and an extension mechanism. The active part is designed to extend the coupler by 3” and thus initiate the connection. The two sides can be seen in figure 4.8. According to data provided in the overview paper the connector contains two independent fluid transfer lines, but there is no clear indication as to how this is achieved.

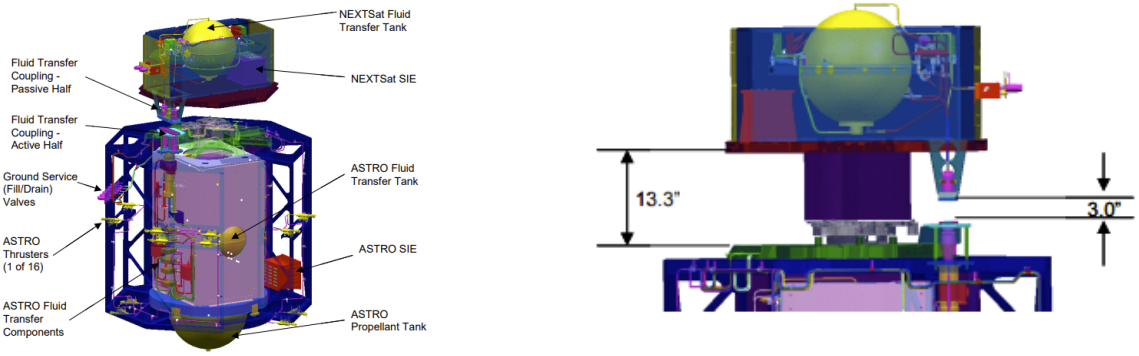

(a) Orbital Express' spacecraft (ASTRO and NEXTSat)

(b) Orbital Express' sideview, the structures separated by the 3" dimension are the liquid transfer interfaces

Figure 4.7: Orbital Express spacecraft in docked configuration [42]

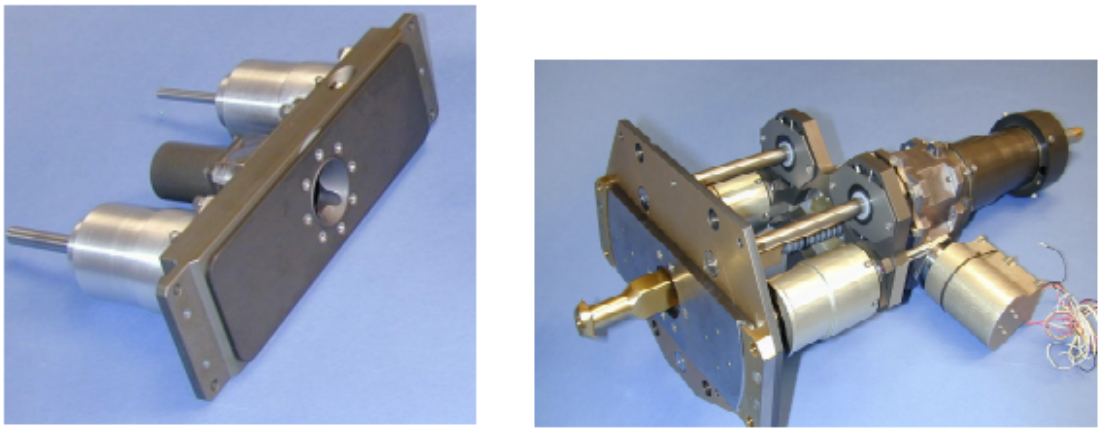

(a) Passive half

(b) Active half

Figure 4.8: Orbital Express liquid transfer interface [42]

There is likewise some published work on the external docking system used in the mission[66]. In the latter work some design elements of the docking capture mechanism are discussed, in particular that the endurance is over 200 cycles. The mechanism is based around three enlarged latch-like structures to widen capture window to 2" and 5°, although it is directly reported as being unsuitable for all but micro-sat applications due to structural integrity limitations.

Table 4.4: Orbital Express liquid transfer interface spec summary

mass	-
operating pressure	-
flow rate	0.0945 kg/s
cycle life	>200
operational temp	-
alignment req.	2" (51mm), 5° ; 2.5mm for liquid coupler
approach velocity	30 mm/s

4.1.5. Summary of interface projects

None of the reviewed developments fully satisfy the requirements proposed in section 3.8. However, these projects do provide valuable information. Tradeoffs performed for SIROM project identified that clamp-and-latch mechanisms are ideal to support liquid coupling for manipulator based operation and can achieve sufficiently robust life. However these solutions struggle with capture leniency and thus are not well suited for direct-docking, especially in impact conditions. The findings form ASSIST project

make it clear that a dedicated capture structure is required for higher degrees of leniency. Regardless of intent, all designs use a two-stage mechanism where the target is first trapped and then gently pulled into alignment. Such mechanism is thus the key to supporting zero-force capture operation.

One key area that is clearly lacking when compared to the proposed requirements is the capability of direct docking at higher approach velocities.

4.2. Proposed Conceptual Solution

This section proposes a conceptual solution to the requirements.

4.2.1. First proposition - independent 'inner' and 'outer' elements

The first major conceptual proposition is made as an answer to the requirements 3a and 3b. These call for the following: 'the MI shall be capable of direct docking with medium-large GEO satellite' and 'The MI shall be suited for manipulator driven berthing', respectively. If taken as-is, the requirement 3a appears as a strict super-set of requirement 3b as it calls for much greater misalignment allowance as well as for handling potentially significant impact conditions between two large spacecraft. However, the sole adoption of 3a as the target performance figure for the interface without regards to the need of minimising the bulk of the end effector for manipulator operations would oppose the intent of this project.

The works detailing the ASSIST design already suggested that a single mechanism that is capable of both sufficient capture tolerance during docking and precise post alignment of connectors is not practical. As such, multiple stages are expected to be required.

It is thus proposed that the interface should be comprised of two independent elements rather than a single, staged mechanism as in ASSIST. One tasked with handling the initial capture, arrest and rough positioning of the spacecraft, and the other to perform the final liquid connection. For clarity these will be referred to as the capture element and the mating element. The mating element would remain a constant between both direct docking and manipulator assisted situations. The capture element, however, could be made entirely optional, if it were to be designed in such manner that it does not interfere with operation of the mating element.

The relative placement of the two elements does not offer many options. It has been established that if the capture element is to be made optional the precondition exists that it must not interfere with the functioning of the mating element. There are two fundamental ways to place the two elements: surrounding each other or adjacent. The first option further presents a choice between which element resides centrally. For the purposes of this discussion the location of the mating element is considered. The configurations are thus the following: adjacent, central (mating element in the center) and outward (capture element in the center). Figure 4.9 illustrates the conceptual footprints of such setups and how they would reduce with the capture element omitted. It is clear that in order to achieve the size benefits of such arrangement, the two elements must be positioned in either the central or adjacent configuration.

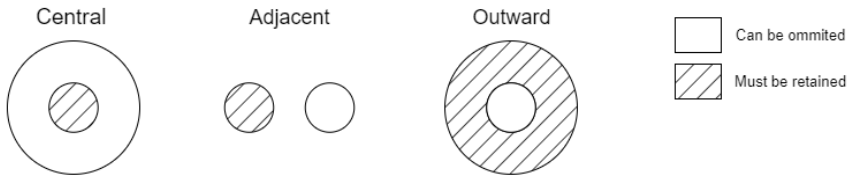

Figure 4.9: Conceptual footprint reduction by omitting the capture element when mounted on a manipulator

Further, the adjacent configuration can be eliminated on the basis of how it would amplify alignment errors of the capture element. Expecting that the capture element will just meet the positioning accuracy as proposed by requirement 3b, it is allowed to have 5mm and 1° of residual error. Very approximately, this could result in $sin(1°) \approx 0.0175$ additional offset per meter of separation, or 17.5mm. Such adjacent configuration would place stringent alignment requirements on the capture element or require excess tolerance from the mating element, eliminating one of the major benefits of the two element concept. Consequently, the most viable configuration to pursue is the one where the mating element is located centrally.

It is thus proposed that a desirable configuration for the conceptual interface is that consisting of a centrally located mating element with the capture element implemented around it. Given the positions and the expected size of each element, they will be referred to as the 'inner' and the 'outer' interface or element for the rest of this work.

4.2.2. Second proposition - clamp latch based inner interface

One of the fundamental functionalities the inner interface must provide is to successfully align the liquid couplers such that they could be safely inserted. Although the mechanism is expected to operate in an environment where precision manipulation is available, perfect alignment is not a viable assumption. The expectation as captured by requirement 3b is $+-5mm$ and 1°. In comparison, the tolerances for inserting liquid couplers are expected to be an order of magnitude lower [42]. Thus the alignment capabilities are a critical area to address in order to achieve reliable operation. Additionally, as per requirement 3b.i successful connection shall be achievable by the mechanism without external assistance, given it begins within the acceptance window.

The existing RAFTI and SIROM designs are excellent solutions to this problem and are thus good reference designs for the inner element of the interface.

Table 4.5: Pros and cons of types of latches [76]

Latch type	Advantages	Disadvantages
Hook	Rigid Connection	Naturally male
	Small misalignment correction	Multiple moving parts
	Passive retention	Point contacts
		Active (de)couple
Roto-Lock	Rigid Connection	Little / no lateral misalignment correction
	One moving part	Active (de)couple
	Passive retention	
	Potentially fail-safe	
Clamp	Rigid Connection	Multiple moving parts
	Naturally male or female	Active (de)couple
	Fail-safe	
	High strength	
	Passive retention	
	High misalignment correction	
Carribena	High misalignment correction	Naturally female
	Passive couple	Multiple moving parts
		May require push part
		Active decouple

The previously mentioned published works regarding early developments of the SIROM interface are again of interest in this discussion. Considering the context of that problem was very similar to that of this work, their conclusions are thus considered highly valuable. Four types of latching mechanism were condensed from existing designs and further discussed as an option to secure the interface: carabiner, rotating, clamp and hook[76]. The table summarizing their findings is presented in table 4.5. For the purposes of this work, out of the four options only the clamp design comes with no deal-breaker drawbacks. Hook-based design offers little misalignment correction, as does the rotating lock. The carribena based designs have a crucial flaw that they are passive and as such are not self sufficient in closing the interface, failing requirement 3b. Further, the fail-safe and passive retention features of the clamp design are welcome additions in the context of designing a robust interface for handling propellant. This leads to the clamp mechanism as the one proposed as the most viable use in this work.

With the clamp style latch decided on as the means to close and secure the interface from a misaligned state, a remaining consideration is the timing of when the final alignment is achieved. If the mechanism relies only on the mechanical tolerance of the latch to nudge it into final alignment, then rather expectedly this might not happen until the latch is fully closed. This would be sufficient if the

two mating surfaces were planar but it poses a challenge when considering connectors which have to be aligned and *then* inserted. By their nature the liquid couplers are expected to have some degree of interference between the two sides of the interface as there is typically a protruding element on at least one of the halves which inserts into the other. This forms the new seal and commonly actuates mechanisms to open the two halves to flow. As a consequence, the inserting mechanism must achieve lateral alignment before the insertion point of the connectors is reached. Otherwise, jamming of the mechanism along with damage to the protruding components is a likely possibility.

This, of course, is not a novel observation and has been accounted for in the two designs. The SIROM and RAFTI designs solve it differently however. The RAFTI design relies on the latching mechanism alone to align the two halves [72]. However, both sides of the interface are in fact designed to be planar with no protruding elements. The RAFTI design then includes actuators which extend the couplers after the latching is completed [72]. On the other hand, the SIROM interface has very prevalent passive alignment petals which guide the two halves of the interface into alignment as the axial separation between them decreases. This allows for staged operation of lock-align-connect using only a latch mechanism and passive structures which could be used to avoid the need of extension mechanisms. Due to requiring fewer active components it is proposed that the general principles of the SIROM design should be adopted as the more viable solution for a long-life refuelling interface.

An additional benefit provided by such arrangement is the trivial scalability of the number connectors and the ability to mix different types of connectors. If the consistent alignment of the entire mating faceplate is assured then a design could easily support the inclusion of additional connectors for data and power without having to repeatedly solve the associated insertion challenges.

To summarize, the proposed concept for the inner interface is to utilize a clamp style latch mechanism assisted by passive alignment structures. This arrangement has been successfully used in the SIROM interface, and the combination offers high initial misalignment tolerance, can finalize the connection without external assistance, is robust, and offers the opportunity to guarantee lateral alignment before the interface is fully inserted. The latter would enable easy scalability of the design if required, which is a great benefit to the concept given an exact specification is not yet known.

4.2.3. Third proposition - back-drivable hexapod platform as capture mechanism for the outer interface

The capture mechanism to be implemented by the outer interface is primarily faced with the problem of capturing and safely arresting two spacecraft of potentially significant sizes and in non-trivial approach conditions. Additionally the expected conceptual requirements also call for the capability of zero impact capture, minimisation of active components on the client side and the ability to safely separate the two spacecraft. Answering these challenges would require any conceptual solution to offer considerable degree of compliance in all six degrees of freedom for the impact situations as well as to posses some degree of mobility.

The flexible boom solution used by the ASSIST system would not be suited to package into the concept as it would not implement well as an outer element. It was already discussed that to allow the capture element to be optional, it must not be contained within the inner element. If the flexible boom approach were to be pursued, the non-central placement would immediately result in excessive complications. For example, the use of multiple booms would now be required in order to achieve rotational alignment. Even aside the likely triplication of all elements, this leads to further complications on how to ensure simultaneous contact of all the booms. This would imaginably require introduction of additional positioning stages for the ability to control the booms independently, further reducing any potential mass savings of such approach. The limited mobility grasping mechanism as utilized in Orbital Express mission is likewise already known to offer extremely limited impact tolerance which makes it only suitable for micro-sat applications and not a promising solution for this concept.

Taking a departure from satellite specific systems, it is proposed that the capture device could utilize a stewart platform. Famously, this solution utilized by the docking system developed for the ISS[77]. The primary argument being that this system solves a highly similar problem. In particular, such system has been successfully utilized to enable docking of two large spacecraft with significant tolerance in all six degrees of freedom, one side of the system is almost entirely passive, the device packages well as an outer element, and the repositioning capabilities are leveraged to position a hermetically-tight secondary connector. Scale aside, the existing solution is an excellent match to the conceptual requirements. Additionally, the stewart platform itself is a highly efficient mechanism in terms of strength

and mass to achieve 6DOF actuation and is widely used at various scales[78]. Due to these features this solution is good candidate for a docking system concept that could be scalable.

There are, however, caveats to address. This system utilizes carribena style latches to secure the connection and thus requires a degree of impact to secure the capture ring[77]. For the concept at hand this design would have to be changed slightly to utilize active securing means as to enable zero force capture of the target. By leveraging the mobility of the platform to preposition the capture rings, the target capture ring could be restrained by means of a series of simple hook mechanism. This could provide a fast actuating, rigid contact and require no components aside from a passive capture ring on the target.

Another problem is that of managing impact forces. A solution to this problem is to construct the linear actuators in a manner that allows them to be highly backdrivable [79]. The construction of such actuators is based around a linear ballscew and brushless motor rather than a more typical worm screw and a stepper motor.

Overall the stewart platform based capture system is proposed as a possible solution for use in the concept due to its scalabity, mobility, structural efficiency and the ability to generate forces in all six degrees of freedom.

4.3. Conclusions

Certain conceptual principles were adopted as the most likely to yield a viable solution to the conceptual problem. In particular, it is proposed to base the design on a two-stage solution: an ’inner’ interface targeting manipulator assisted operation and an ’outer’ interface that is designed to handle docking operations. This combination was deemed beneficial to yield a compromise and optimization opportunities for both shuttle and manipulator-equipped services while maintaining cross-compatibility between the two options on any given client vehicle.

The inner element is proposed to be designed similar to the existing solutions of RAFTI and SIROM. The use of clamp mechanism and passive alignment structures would enable an easily scalable and robust design that is inherently capable of achieving and sustaining high preload without active power requirements. In addition, if align-insert behavior is achieved, the design would not inherently put restrictions on compatible connectors.

The outer element is proposed to be based on a stewart platform on the active side and a simple passive structure on the passive side. This would allow to achieve minimal complexity on the interfaces deployed on the clients, and allow trivial omission of the unnecessary active part of the docking structure for manipulator deployments. In addition the fully actuated platform presents a compact means to achieve both capability to reach out for zero force capture, and actively control impact in all degrees of freedom.

So far these propositions are largely based on known or assumed achievable properties of such arrangement and its suitability is only a claim based on this potential. The inner and outer element are implemented as partial proof of concept designs in chapters 6 and 7 to verify the correctness of these assumptions and the overall feasibility of the proposed solution.

5

Fluid Transfer

This chapter proposes a conceptual design of the fluid transfer lines which would likely be the core subsystem around which everything else is designed in order to support its operation. The approximate expected requirements such as lifetime and operational pressure have been estimated in chapter 3. This chapter investigates how the system could be implemented and if any of the components require additional future development.

5.1. The Conceptual Element

In order to implement the functionality as called for by the requirements, a naive arrangement of a pair of transfer lines for a single fluid would consist of a considerable number of elements. This is because the system is expected to support leak checking, purging, preconditioning in addition to fluid transfer, with the additional requirement of being doubly-redundant against leaking. Finally, the system should utilize minimum active components on the client side. Assuming the cause of leakage as likely to arise from a worn out or otherwise malfunctioning active component (i.e. valves) rather than a passive connection, this effectively requires ensuring three inhibiting stages in series for every branch between a storage tank and an outlet leading to space. Ignoring performance requirements for now, the expected redundancy could be implemented by an arrangement presented in Figure 5.1.

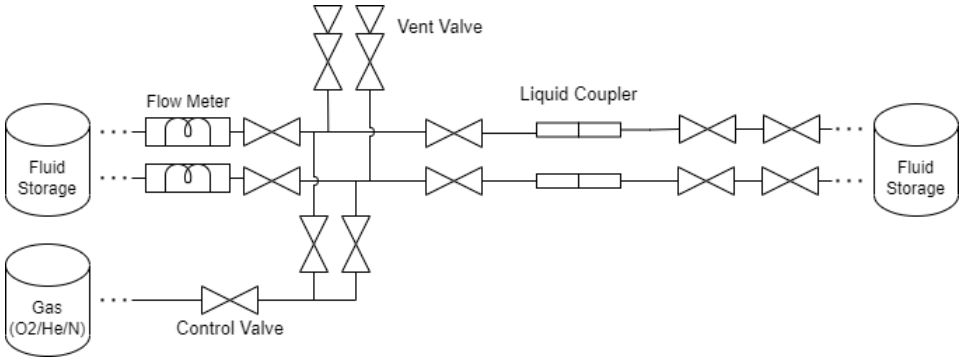

Figure 5.1: A diagram of a full set of components that would naively implement a transfer line

With the assumed presence of some master shut-off valve located near the storage tanks, this arrangement places the minimum required inhibits for both the purging and venting system as well as the liquid transfer lines. However, there is argument to be made that such an arrangement has a lot of duplicate elements when considered in the context of being integrated into a full propellant storage system.

Diagrams of two storage systems from existing designs are presented in Figure 5.2. In the diagrams it can be seen that the example storage systems have a significant overlap with the naive element from Figure 5.1. Particularly, the means of flow metering and venting reside within the storage systems. Both arrangements likewise feature a master shut-off valves that are positioned before the interface.

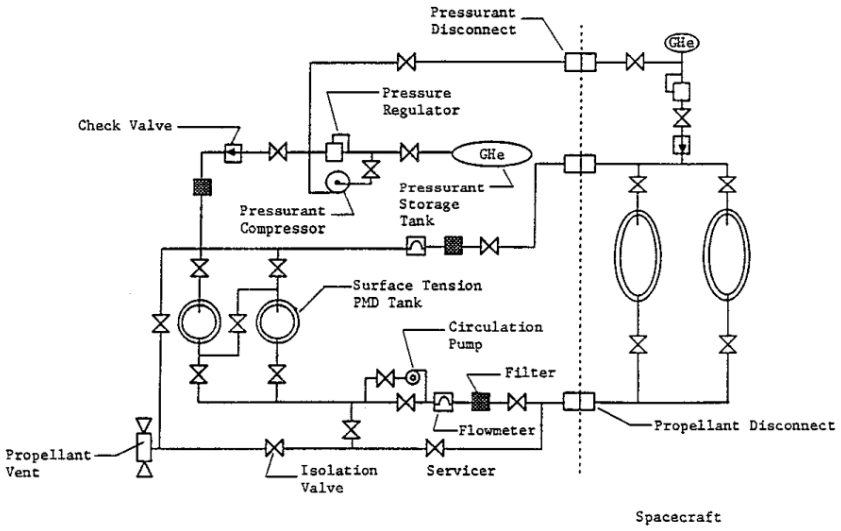

(a) Orbital Spacecraft Consumables Resupply System (OSCRS)[80]

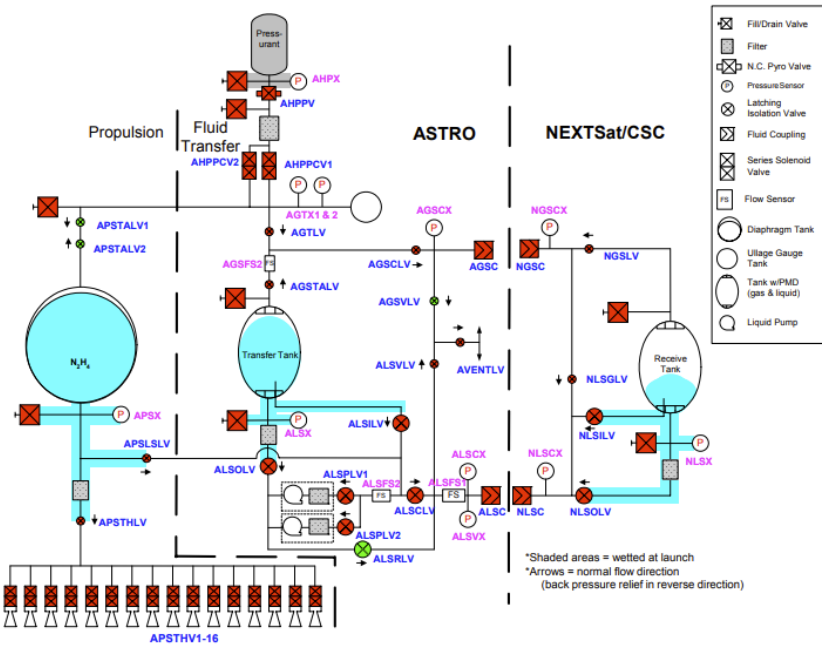

(b) Orbital Express [42]

Figure 5.2: Storage systems implementing fluid transfer

I can be argued that if the the conceptual interface were to simply replace the coupling element in these systems the entire integrated solution would posses all the required functionality. This offers the opportunity to greatly reduce the set of components comprising the individual fluid lines and slightly changes the definition of the functionality required from the interface. Based on these observations it is proposed that the interface requires only to implement a reduced coupling element that would enable preconditioning of the transfer lines, not *inhibit* purging or venting, and provide a dual redundancy against leaking once paired with a master shut-off residing upstream of the interface.

Such a reduced element could consist of the following set of five components per side of the interface: a control valve, an over-pressure relief valve, a pressure sensor, conditioning heaters, and the liquid coupler. The conceptual element is shown in a minimalist diagram form in Figure 5.3. The liquid couplers are self-explanatory and serve as basic means to establish a connection for the liquid transfer between two spacecraft. The relief valves would be required to respect the requirement of controlled discharge in overpressure conditions and should exist on both sides of the interface in order to provide safety against either side of the transfer experiencing such condition, regardless of which valves are possible stuck closed. The control valve serves as an additional means of inhibition against leakage as well as to provide flow rate and pressure control. The pressure sensors are required in order to not make the element opaque during leakchecking by providing feedback on the conditions within the element. The feedback from the pressure sensors would also enable a degree of environmental control within the transfer lines when paired with a set of heater elements that condition the system to above a certain temperature. The latter would enable the system to avoid temperature shock on the peroxide entering the transfer lines as well as to control the ambient pressure during venting. This is called for in the requirements under the need to prevent uncontrolled evaporation or freezing of the liquid being transferred.

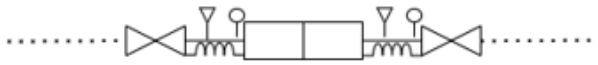

Figure 5.3: The reduced transfer element consisting of a control valve, an over-pressure relief valve, a pressure sensor, pipe conditioners and a liquid coupler per each side of the interface

This suggests the minimal set of components that must be comprise the fluid transfer lines of the interface. The question remains what materials must these components be manufactured of and whether or not they are available.

5.2. HTP Material Compatibility

The subject of material compatibility with HTP appears to be exceptionally complicated and further made more confusing by an apparent lack of consensus. The disagreement between and general incompleteness of various sources has been directly expressed by OrbitFab researchers when documenting their design of an HTP tanker spacecraft[50]. The recommendation made by these researchers was to directly validate any chosen combination of materials, and only to select those materials that universally recognized as highly HTP compatible to seed this testing. Otherwise, the published data is too inconsistent to directly predict a choice.

It so appears that the major point of confusion in this area is the fact that industry and space applications define materials as compatible with HTP differently. This is not immediately obvious as research from both contexts utilize identical language to describe largely qualitative observations of compatibility and the findings are often presented as ’good’ or ’bad’ on a non obvious scale. In space applications, the critical concern is that of the HTP itself not being chemically affected by contact with a given material[2][1], whereas the industrial applications are much more concerned about the material itself not being damaged by exposure to HTP. A particularly vivid example of such conflict was discovered in a technical directive document listing materials compatibility with Hydrogen Peroxide by a medical manufacturer[81]. The particular document ranks copper as compatible with peroxide at the same time as reporting it as a strong catalyst and that it will experience excessive oxidation if exposed to peroxide. Such material, of course, would not in any way represent a sensible choice for the space depot application.

Various available online sources such as material compatibility tables were rarely found to provide their sources, and all the ones that did referred to a specific document AD819081. This is an extensive report detailing qualities of concentrated Hydrogen Peroxide dating back to 1967 that was produced by US Airforce Rocket propulsion laboratories[68]. To the author’s understanding this appears to be the most detailed and credible document published on the topic. In particular, the research effort experimented with various materials to categorize their compatibility in terms of both being affected by peroxide and their catalytic affects on the peroxide. The materials were assigned compatibility classes, out of which class 1 was defined as suitable for excessively long contact and class 2 allowing transient

contact in the timescales of days. These most suitable materials are therefore used as the reference in this work. The lower rated materials in the ranges of hours to seconds are deemed of no interest to this conceptual investigation.

The materials rated as highly peroxide compatible were further filtered down by referencing another old yet highly detailed technical report from JPL regarding vacuum compatibility of materials[82]. Admittedly also ancient, dating back to 1961, it was the only reputable source discovered that extensively tested a wide set of materials that overlapped well with those tested by[68]. This allowed for cross-validation of materials between the two reports to narrow down a list of desired materials that are both highly vacuum and peroxide compatible.

The result of cross-comparison between the two reports is listed in Table 5.1. This list of materials is almost entirely confined to aluminium alloys that are nearly pure in composition with the exception of stainless steel, although the latter represents a significant tradeoff in the compatibility. A few extremely chemically inert plastics and elastomers also remain, such as PTFE or FKM. While likely not viable construction materials due to much lower strength than the aluminium options, these do present an opportunity to be utilized in seals or similar components.

Table 5.1: List of suitable construction materials generated by cross-comparison between [68] and [82]

Material	Type	Pros	Cons	Notes
Alu 1xxx	Almost pure Al	Best compatibility	Lower strength	-
Alu 5xxx	Low Cu Al alloy	Higher strength than 1-series	Slightly lower HTP compat.	-
Alu 356	Low Cu Al alloy	Castable, weldable; suitable for valve bodies	Slightly lower HTP compat.	-
Steel 300-series	Stainless Steel	Very high strength; no AlOx contamination	Cast parts require surface treatment; Lower HTP compatibility	Class 2 HTP compatibility
PCTFE	Plastic	Can be used as coating	Low tensile strength	-
PTFE	Plastic	Very low friction; Can be used as coating	Very low tensile strength	-
FKM	Elastomer	Good seal material	limited <66° C	Lower vacuum compat.
PTFE Nickel/Tin plating	Surface Coating	Can protect otherwise incompatible materials	HTP penetrates imperfections, reacts with undersurface	Primarily splash protection

These findings allow to conclude on a very specific set of desired materials for all the components that are present in the fluid transfer lines. In order to even feasibly achieve the required lifetime of 15 years, the couplers and the valves would likely have to be constructed purely out of specific grades of aluminium and utilize PTFE seals.

As a last mention and perhaps verification of these findings, the particular problem has been raised by SSTL in a somewhat recent call to arms competition in 2014. Amongst the set of national engineering challenges was that of a development of an aluminium-bodied valve for long-life HTP applications[83]. The problem formulation behind this challenge was that existing valve designs typically utilize stainless steel construction which does not posses sufficient endurance. While high degree of compatibility with HTP is achieved, the expected lifetime of existing components was stated as less than 5 years. This problem formulation is highly consistent with the findings on suitable materials from this section. Unfortunately there was no direct information found on whether there were entries in this category, nor were there published works discovered that directly address this problem or hint at an attempt to solve it. The three winning entries were revealed publicly, however none of the winning entries focused on this particular problem.

5.3. Limitations of Existing Components

Literature and COTS catalogues were scouted for components or solutions that satisfied the requirements in an attempt to identify missing areas that would have to be addressed for this depot's interface concept to be implementable in reality. Existing works on similar systems set an initial expectation

that sufficient components should exist COTS, and a limitation was of lead times[50]. However, two important missing components were found: a sufficient fluid coupler and a bidirectional control valve.

5.3.1. Fluid couplers

A search in COTS catalogs and literature failed to find a fully suitable fluid coupler that would satisfy the construction material and lifetime requirements. However, there was a relatively close analog discovered that suggest such a component is fundamentally feasible to build to the required specification.

First of all, an unsuitable feature shared between COTS fill-drain connectors is a low cycle count for repeated connections and the mode of operation. The latter issue refers to these connectors featuring a threaded or otherwise manually operated mechanism to secure the connection which would be hardly viable to utilize in a quick-insert fashion in an automated system. Regarding the cycle life, fill-drain connectors produced by Nammo are rated only for 100 insertions[1][2] for example, which falls short of the required 1000. Fill-drain connectors from another manufacturer have an even lower rating of only 40 cycles [3].

The smaller of the mentioned fill-drain produced by Nammo is the only one discovered specifically targeting HTP applications. Although the specific component is designed for only 10bar of operational pressure and not 20, it is made from aluminium and uses PTFE seals. This confirms that the materials found required to achieve HTP compatibility can in fact yield a viable fill drain valve, although the design would have to be slightly upscaled and modified to support quick insertion.

Overall, this search revealed that a suitable fluid coupler does not readily exist. The HTP specific valve from Nammo proves that the all(mostly) aluminium construction and use of PTFE seals still allows to construct a functional valve. However, this project would require development of a custom connector design.

It is also important to acknowledge that at least Orbit Fab have seemingly solved this design challenge proving such design is achievable. Presumably, they have developed a highly HTP compatible fill-drain connector that is suitable for quick insertion and with operational pressures suitable for this concept[70]. However, they are a commercial body and have not shared the design specifics publicly. Based on their published paper[72], this seems to be *the* critical know-how of their entire RAFTI interface and consequent demonstrator missions. The fact OrbitFabs seemingly hold the only current solution to this specific problem makes the earlier observation from section 2.1.4 that major industry players seemingly defaulted into buying the RAFTI system a lot less surprising. As such, it is highly unlikely Orbit Fabs would give up their unique position. A press release has been made suggesting the RAFTI specifications would become public domain as part of standardisation but even well past the expected date this has not come to fruition. Regardless, based on the available information their design appears limited to 300 cycles.

To conclude, a limiting factor for the depot interface concept is identified. A required development or acquisition is that of a quick insert fluid coupler that reaches 1000 insertion cycles, has MEOP of at least 20bar, and features aluminium and PTFE construction.

5.3.2. Flow control valves

First, control valves that only allow for flow in a single direction were found to readily exist COTS and constructed out of sufficient materials. These are once again manufactured by Nammo for use in their seemingly uniquely HTP oriented propulsion solutions. The manufacturer offers two throttle valves that are constructed entirely out of aluminium and use PTFE seals. These are an apogee motor throttle valve [4] and a dual-inline throttle valve for smaller applications[5].

The first, although rather bulky at 440g, is almost an absolutely perfect match to the proposed performance requirements for the concept: MEOP of 22bar, aluminium construction, flowrate rating of 95g/s and cycle of life 8000. The only requirement that barely fails is flowrate not reaching 100g/s but the difference is insignificant.

The second option is a much smaller unit having a lower mass of 210g. Interestingly, this valve is a compound unit of two independent valves that could provide useful by introducing an additional stage

[1] https://www.nammo.com/product/mini-fdv/

[2] https://www.nammo.com/product/fdv-fvv/

[3] https://www.space-propulsion.com/spacecraft-propulsion/valves/fill-drain-valves.html

[4] https://www.nammo.com/product/engine-flow-control-valve/

[5] https://www.nammo.com/product/dual-inline-thruster-valve/

of redundancy in a highly compact fashion. The component likewise satisfies operational pressure requirement by being rated for 25.4bar MEOP. This valve also offers exceedingly long life with a cycle rating of a million. However, this valve has drastically lower flow rate rating of only 2g/s, or 8g/s if the same pressure drop as for the first valve is assumed.

During the estimation of flowrate requirements in chapter 3 the original rough estimate before rounding to an order of magnitude was that of 35g/s. If this more specific figure were to be readopted, these two valves would similarly over and under achieve the requirement. Likewise, the 35g/s estimate was based on the maximum expected transfer volume which would only truly apply to the most massive client spacecraft or the depot itself.

These two options thus perhaps offer a point of easy scalability in the system. As long as the external interface and the connectors remain the same, the valves utilized within could be selected for the size of the spacecraft at hand. Small clients and shuttle vehicles which would transfer lower amounts of propellant and be more sensitive to mass constrains could reasonably utilize the dual inline valve and leverage the fact this component in combination with a self-sealing coupler already provides all three inhibits for dual-redundancy against leaking. The large spacecraft would require the larger valve to achieve reasonable transfer times, but they would likewise much more easily absorb the added mass and volume requirements.

While the two discovered components already promise a high degree of feasibility, the fact that both of the valves are directional is perhaps a complication that should be addressed by future works. Based on existing assumptions, the directionality of the the valves would not pose an issue during ressuply of the depot or refuelling of a client spacecraft. However, the potential complication arises when considering an orbit resident ferry shuttling propellant from the depot to a client. In such case, it would be highly beneficial for at least the ferry spacecraft to be able to support bidirectional transfer of propellant as to allow operation while equipped with a single interface.

A ball or a three-way valve would likely be required to enable such bidirectional flow. An example of such a valve has actually been found offered by OmideaRTG[6]. This high pressure 3-way valve has MEOP of 200bar and a flowrate rating of 200g/s at a mass of 350g and volume comparable to the two previous valves. However, its cycle life rating is 300 and the utilized construction materials are primarily stainless steel. Importantly, the sealing material used is the desired PTFE.

It is thus suggested that perhaps future efforts could attempt to modify such design to make it better suited for this application. It might be reasonable to assume that a tenfold reduction in operational pressure would allow to replace the steel construction with aluminium and bump the endurance to 1000 cycles up from 300 while retaining comparable dimensions and overall mass.

5.4. Stand-in Coupler Utilized in Further Conceptual Investigation

While plausible analogs for the control valves were found that provide a somewhat realistic substitute of components that could later be utilized in the interface's construction, the case is not the same for the fluid coupler. It has been identified that such coupler would have to be developed by future efforts and thus does not yet exist. It is, however, effectively the critical element that the rest of the system is built around to support. As such, in order to make it possible to proceed with even a proof of concept design of the rest of the interface, an approximation for the coupler's behavior needs to be found.

A temporary stand-in for the couplers was chosen to be Cupla MALC-SP medium pressure connector offered by Nitto Kohki[7]. This is a high flow rate, medium pressure connector specifically intended for automated industrial applications. The component functionally satisfies all the needs of the concept except for construction materials. The stainless steel construction and the FKM seals were found to not be ideal materials in section 5.2. However these were still amongst the a possible choices even if the least desirable. Taken as is, such connector would not be suitable to achieve 15 years of lifetime but it perhaps could be modified by future efforts.

Another important reason behind this specific choice is the fact that the specification rather uniquely list the required force to insert as well the required preload to maintain the connection. These two parameters are critical in defining the mechanical properties of the rest of the interface.

[6] http://www.omnidea-rtg.de/site/images/stories/Downloads/Omnidea-RTG_Catalogue_Feb2016.pdf

[7] http://www.nitto-kohki.eu/en/products-en/quick-connect-couplings/multi-port-connection/item/multi-cupla-malc-sp.html

The following bullet point list summarizes the important features of this coupler that make it a reasonable approximation for the would-be developed custom coupler:

- MEOP 20bar
- ≈0.2bar pressure loss at 100g/s flowrate of H2O
- Body material is stainless steel
- Seal material uses FKM
- Dual shut-off (both connectors sealed when disconnected)
- Specification includes insertion requirements
- Industrial automation part with long endurance

5.5. Summary

In this chapter the conceptual set of components required to implement the fluid transfer lines was proposed. It was found that the scope of fluid line elements required to implement the proposed functionality had a large degree of overlap with components already resident in existing propellant storage system. As a consequence, it is proposed that the interface device needs only to implement a greatly reduced set of functionality.

The resulting reduced element was proposed to consist only of a control valve, a fluid coupler, a relief valve, a pressure sensor, and to contain heaters for the piping. This combination of elements in principle satisfies all the required functionality once integrated with the rest of the storage system. Viable choices for materials of construction of these components were found to be almost exclusively that of aluminium alloys and PTFE in order to achieve sufficient lifetime and compatibility with HTP.

When investigating existing designs for these components it was discovered that the fluid couplers and potentially the control valve do not yet have sufficient solutions. The fluid couplers constructed out of sufficiently compatible materials were found to exist but the existing designs do not posses sufficient insertion cycle endurance for the predicted 15 years of the interface's lifetime nor obviously allow for automated insertion. Thus the development of a suitable aluminium quick insert coupler was identified as critical area to address by future works. The case of the control valves was also found potentially problematic. Sufficient control valves were found to exist albeit they are directional which could lead to complications in the design of propellant ferries. Consequently, a second area of future interest was identified in the need of developing an aluminium bidirectional valve.

Finally, in order to continue with an approximate conceptual design, COTS stand-in component for the coupler was selected. It will be used to provide core parameters for a proof of concept design while hopefully somewhat resembling plausible solutions which would be produced by future works.

6

Proof of Concept of Inner Interface Element

This chapter documents the attempt to partially implement the proposed concept for inner interface with intent to achieve proof of concept of the major design choices proposed. In particular, this chapter focuses on verifying the expected self-alignment behavior of the proposed mechanical arrangement. The experience gained during the 0th-iteration design of the device is also utilized in estimating an approximate scale of the device.

6.1. Proof of Concept Faceplate

This section details the construction and simulation of a minimalist implementation of the faceplace housing alignment structures and the liquid couplers.

6.1.1. Alignment structure - 3Dxface

A particularly interesting alignment structure has been described in the literature by for application in robotics. Named ’3D X-face’ by the authors, it is proposed as a superior alternative to existing designs [84]. The fundamental geometry is shown in figure 6.1a. As the designers of the 3D X-face report, this geometry offers great simplicity, high misalignment tolerance for a given size, and, most importantly for this work, the designers suggest it has the capability to be tailored to have ’align before insert’ behavior. The latter is achieved by offsetting the sliding surfaces such that the two halves would slot together once aligned. This modification is shown in figure 6.1b. As an additional benefit, this geometry also provides a rigid connection against lateral movement once fully mated.

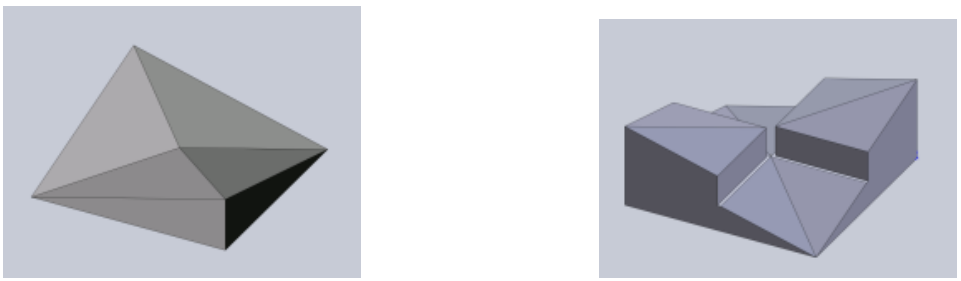

(a) Standard **(b)** Locking

Figure 6.1: Variants of the 3D X-face geometry [84]

Because this geometry satisfies the functionality requirements and comes with further benefits, it was chosen to adopt it for this proof of concept. Considering the authors behind the design of 3D X-face already demonstrated its superiority to traditional ideas, it is questionable if there is value in pursuing improvements in this area, especially so at such an early stage of development.

6.1.2. Minimal implementation

To serve as a proof of concept, a faceplate design consisting of a pair connectors and the proposed stabilizers was implemented in CAD. Three stabilizing structures are located radially at 120° to achieve stability in all six degrees of freedom. Aside from the radial symmetry, the spacing of the features is arbitrary with the outside diameter of the faceplate chosen as 100mm. This dimension takes inspiration from the scale unit in cubesats being a 10x10x10cm cube with the intention of exploring how the rest of the concept would package around this volume. The example design is shown in figure 6.2.

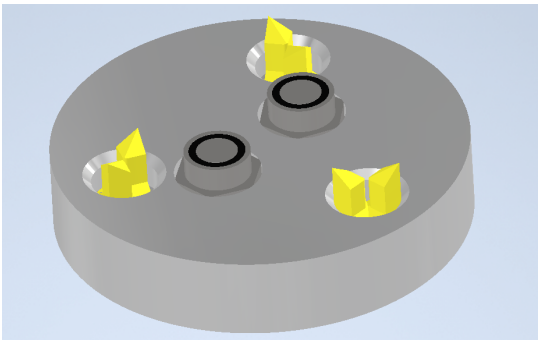

Figure 6.2: Faceplate with liquid connectors and the stabilizing structures. The latter are highlighted yellow for visibility. The only difference between the faceplates of both sides of the interface is the gender of the connectors.

The stabilizing geometry was resized to allow for the desired 5mm of misalignment window and to offer 6mm of final vertical travel once alignment is achieved so as to encompass the insertion distance for the model connectors. In addition, the slope of the sliding surfaces was chosen 45° which is expected to not seize until coefficient of friction approaches 1. Sliding surfaces experiencing heightened friction is one of the effects of operation under vacuum conditions[82] but a friction of coefficient <1 is expected to be achievable using solid lubrication, even accounting for wear.

6.1.3. Droptest simulations using Autodesk Inventor

The Autodesk Inventor CAD software was chosen because of the built-in dynamic simulation capabilities. In particular, it supports simulation of three dimensional contact, friction and impacts between components of complex geometry.

The simulations consisted of two halves of the interface being dropped under gravity or pushed into each other by a vertical force to approximate clamping of the interface. One of the simplifications made by the original authors of the 3Dxface design was that of zero friction[84]. The geometry hence was also simulated with varying friction coefficients to verify its behavior.

The following simulation parameters were used

- 3D contact stiffness - 1e6 N/mm (default)
- 3D contact damping - 1e4 N/mm/s (default)
- 3D contact friction coef. - 0 - 1.5
- Gravity - 0/9.81 m/s^2

The simulations verified the expected behavior - the geometries successfully aligned unless affected by very high friction. An example simulation where the faceplate was dropped under gravity from a height of 23mm with initial 5mm lateral misalignment is shown in figure 6.3. The subfigures show the initial positions, sliding into alignment, and the moment when lateral alignment is achieved. The accompanying figure 6.4 shows the corresponding graph of misalignment. It can be observed that the lateral misalignment (x,y axii) becomes almost zero before the vertical separation of the parts approaches 6mm which was the primary desired effect.

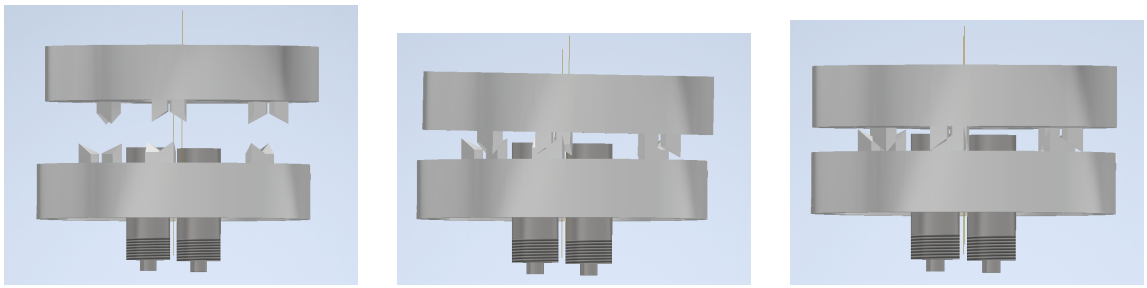

(a) Initial condition **(b)** Sliding into alignment **(c)** Aligned, about to drop in

Figure 6.3: Faceplates aligning during a simulated droptest

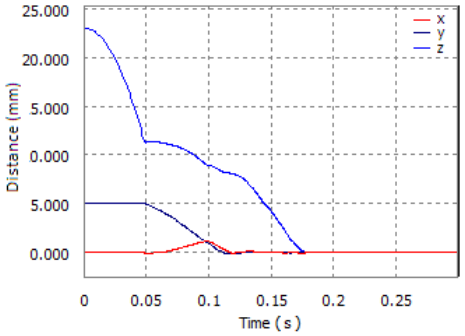

Figure 6.4: Linear separation of the centers of the faceplates during the droptest

To increase confidence that the observed behavior is due to the properties of the geometries involved and not an artifact of the simulation software, additional simulations were performed. First it was confirmed that the faceplates still align if forced together by an external force rather than dropped. Second, it was verified that the interface correctly reacts to friction (i.e. seizing as expected for $\mu > 1$). Lastly it was verified that the alignment fails if the initial misalignment is too high. Examples of alignment graphs from these tests simulations are given in figure 6.5.

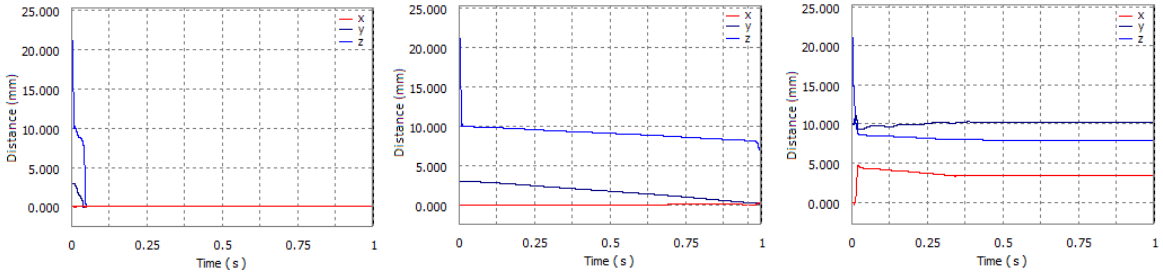

(a) Faceplates pushed together by a force of 100N **(b)** Coefficient of friction set to 1.5 **(c)** Initial misalignment outside acceptable range

Figure 6.5: Simulation verification.

Figure 6.5a Shows that the faceplates still aligned correctly when forced together. In addition, it further confirms that the desired align-insert behavior has been achieved. The faceplates remained at

above 6mm axial separation until fully laterally aligned, and were only then able to continue moving axially. When friction was increased to a degree that should result in the alignment structures being unable to slide, it resulted the geometries effectively seizing upon contact as expected and can be seen in figure 6.5b. Although minute motion remained, a drastic change in behavior is definitely observable. This verifies that the simulation is sufficient to identify that the mechanism might seize. Finally, figure 6.5c shows a sanity test where the faceplates were misaligned well outside the acceptance window. As expected, the two halves simply came to rest on top of each other but did not align or 'clip' through each other.

Sensitivity of the simulation to the stiffness and damping parameters of the contact joint was also investigated, however no significant difference in results was observed unless these parameters were altered by multiple orders of magnitude, and in such cases the simulation would fail. Under very low stiffness the two components would penetrate and seize, whereas extremely high stiffness prevented the simulation from progressing due to convergence issues.

The dynamic simulations predict that the desired self-aligning behavior was successfully achieved with a reasonable degree of confidence. Thus this element of the proof of concept design was frozen.

6.2. Latch Linkages

In this section a proof of concept latch linkage is generated and investigated. The problem of linkage synthesis refers to finding an arrangement of anchor positions and link dimensions which yield a desired trajectory for some element of the linkage[85]. This includes two problems - finding a topology which is the number of links and how they are connected, and sizing the dimensions of said links to achieve a desired kinematic behavior. In this work the lesser problem of dimensional synthesis is tackled as there is a known suitable topology to take as a reference.

First, a plausible geometry of the links was computed by implementing a rudimentary kinematic solver and optimiser based on Frechet distance. Next, the linkage was implemented in CAD to verify the generated geometry's motions, study closing and holding loads, and to verify the feasibility of the components withstanding these loads.

6.2.1. Dimensional synthesis of the linkage using Fréchet distance

The design of the clamp mechanism used in the SIROM interface is taken as the reference for the topology. This is a four-bar linkage with the clamp effectively being just an extension of one of the links. The reference mechanism is shown in figure 6.6a. This arrangement is convenient as the two anchors are generally located on one side of the mechanism and there is only a single driven link. A kinematic diagram of the mechanism is shown in figure 6.6b. In the figure the pivot points are marked with letters and the links will be referred to based on their start and end points. Here only the link AC is directly driven.

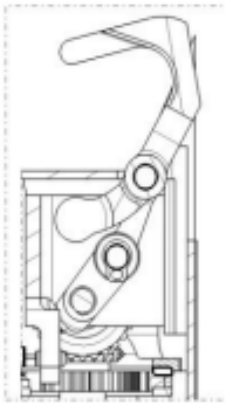

(a) Drawing of the SIROM latch used as the reference[76]

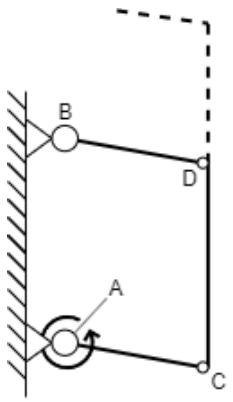

(b) Diagram of the linkage

Figure 6.6: SIROM mechanism and the diagram of the linkage

Kinematic solution

The four-bar mechanism has a singular degree of freedom. Assuming positions of the anchors along with lengths of the links are known, a single angle or position constraint is sufficient to solve for the position of the structure. In this case, the constraint comes from the fact link AC would be driven by a motor or similar means and thus its angle is assumed to be known. Here the interest is in the location of the clamp's endpoint, and the solution for its position is obtained in the following steps:

1. Calculate position of point C based on the anchor A and the known driven link's position
2. Calculate the circle-to-circle intersection of links CD and BD
3. Add the offset vector to the link CD to calculate position of the endpoint

The circle-to-circle intersection calculation is based on example equations by Eric W. Weisstein[86]. A diagram of two intersecting circles in shown in figure 6.7. Given two circles with radii R and r, separated by a distance d, the coordinates of the intersection points are the following:

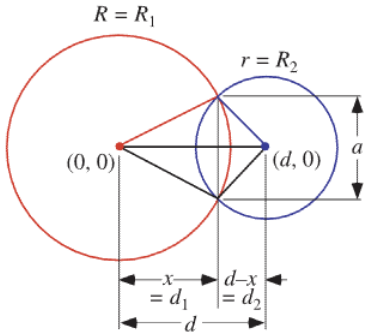

Figure 6.7: Circle intersection[86]

$$x_{int} = \frac{d^2 - r^2 + R^2}{2d} \tag{6.1}$$

$$y_{int} = \pm\frac{1}{2d}\sqrt{4d^2R^2 - (d^2 - r^2 + R^2)^2} \tag{6.2}$$

The equations (6.1) and (6.2) are relative to a line connecting the two circles and as such the intersection points need to be projected back into the frame of the mechanism. This line is the vector $\vec{L}$ separating points C and B of the linkage. Taking the 2D coordinates of these points as $\vec{P_C}$ and $\vec{P_B}$ gives the following:

$$\vec{L} = \vec{P_B} - \vec{P_C} \tag{6.3}$$

The unit vector $\hat{l}$ of this line is then:

$$\hat{l} = \frac{\vec{L}}{|\vec{L}|} \tag{6.4}$$

The normal vector $\hat{n_l}$ is constructed by swapping elements of $\hat{l}$ and inverting the vertical component:

$$\hat{n_l} = \begin{bmatrix} l_1 \\ -l_0 \end{bmatrix} \tag{6.5}$$

Combined with equations equations (6.1) and (6.2), the position $\vec{P_D}$ of this intersection and hence of vertex D in the mechanism is the following:

$$\vec{P_D} = \vec{P_C} + x_{int} \cdot \hat{l} + y_{int} \cdot \hat{n_l} \tag{6.6}$$

The decision to use either the positive or negative solution for y_{int} is taken such that the mechanism is outward facing, that is the x coordinate of $\vec{P_D}$ is greater than that of $\vec{P_B}$. If both y_{int} solutions fail this, that means the mechanism has 'folded' onto itself and is discarded. To illustrate, an example of such condition is shown in figure 6.8.

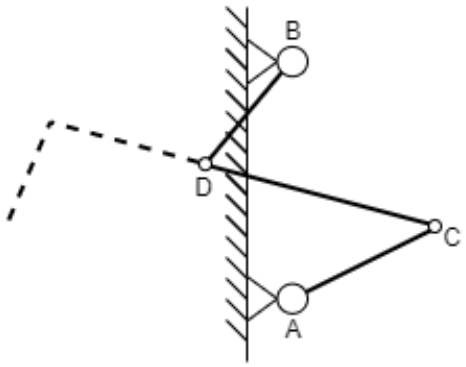

Figure 6.8: Illustration of an invalid solution

At this point the entire mechanism is solved and the remaining step is to calculate the position of the end point. This is done in similar fashion by extending the link CD by the two additional segments which would represent the attached clamp:

$$\vec{P_{tip}} = \vec{P_D} + e_1 \cdot \hat{l_{cd}} + e_2 \cdot \hat{n_{cd}} \tag{6.7}$$

Where $\vec{P_{tip}}$ is the end position of the tip of the clamp, $\hat{l_{cd}}$ and $\hat{n_{cd}}$ are the unit vector and the normal of the link CD, and e_1 and e_2 are the extension lengths.

Parameters of the linkage

In order to optimize the geometry, a set of variable parameters was selected. The anchor point B is taken as the reference of the entire geometry because it would likely be the most critical dimension for integration into the rest of the device. All the dimensional parameters are listed in table 6.1 and illustrated by figure 6.9.

Table 6.1: Parameters of the dimensional synthesis

Parameter	Description
dx	horizontal offset of the second anchor
dy	vertical offset of the second anchor
l_{ac}	length of link AC
l_{bd}	length of link BD
l_{cd}	length of link CD
e_1	parallel extension of link CD
e_2	perpendicular extension of link CD

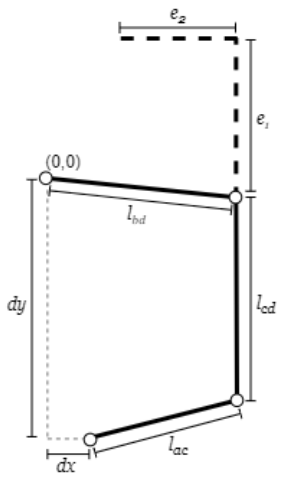

Figure 6.9: Parametric dimensions of the linkage

Synthesis strategy

In order to generate a plausible geometry, the previously described kinematic solution was implemented in Python and used to build a simple optimization script.

Given a set of geometric parameters, the code constructs corresponding linkage and solves it over a range of the driven link's positions. The driven link is assumed to have a range of motion of $\pm 90^\circ$ with $+90^\circ$ as mechanism fully open and -90° as fully closed. At each step, the position of the tip of the clamp is recorded to trace out its trajectory. This trajectory is then compared to the desired motion and is used for parameter optimisation.

Fréchet distance was used as the primary measure of fitness. It is one of the more commonly used metrics for trajectory matching and is a measure of maximum distanced between two curves[87]. An analogy commonly used is that Fréchet distance represents the shortest string required to keep the curves connected, such as a person and their dog walking along. Here it serves as measure of how closely the trajectory of the end point of the linkage matches that of the desired. More advanced techniques exist but this metric was deemed sufficient for the purpose due to availability of implementations and ease of integration into code. In particular it only requires two sets of points rather than full parametric definitions of the paths which greatly simplifies its use. In this work the algorithm's implementation as a module in Python by Spiros Denaxas called FrechetDist was utilized [88].

The optimisation algorithm used was Differential Evolution and is available in the SciPy Python library. It was chosen due to it's capability to support multivariate functions, great coverage of the parameter space and lack of reliance on accurate initial guesses. The trade-off, of course, are the computational costs but they remained within acceptable bounds on modern desktop hardware.

Three additional soft constraints were also introduced by means of punishing the cost function. These constraints were used to discourage unwanted behaviors on the resultant linkage. The first constraint relates to achieving self-locking behavior in the mechanism. This was implemented by requiring the clamp's vertical motion to reverse near the end of travel. Based on an assumption, this makes it such that a resisting vertical force now results in the mechanism closing further rather being backdriven and opened. The second constraint was used to enforce straighter travel at the ends of motion and punish motion in the unwanted axis. Finally the third constraint was used to enforce a minimal amount of travel by the mechanism and maximum deviation from the path. These boundaries are illustrated in figure 6.10.

Based on the dimensions of the previously designed the faceplate, the target trajectory was set as follows: vertical travel of 20mm (with last $\approx$15mm evaluated for straightness), horizontal travel of 10mm (7mm minimum, with last $\approx$5mm evaluated for straightness), and a no-go zones below 10mm above the anchor and 2mm around the trajectory.

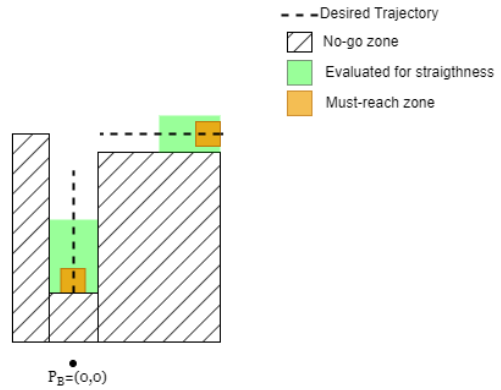

Figure 6.10: Illustration of target trajectory constraints

Synthesis results

The optimising script successfully found a set of parameters that satisfy the requirements for smoothness and travel. A partial exception to this is the horizontal travel when opened, which is sufficient but sadly fails to reach the desired goal. The achieved value is $\sim 8mm$ which correlates well with the maximum allowed deviation from the trajectory endpoints. With further experimentation by tweaking the constraints, it was found that the horizontal travel range seems to be in tension with straightness of the travel and especially achieving the self-locking property. The latter two are deemed far more desirable properties than additional margin on horizontal travel so trade-off was accepted. Overall the found parameters are satisfactory for the proof of concept investigation. However, the overall bulk of the linkage compared to the achieved travel is admittedly lackluster. This should definitely be revisited by future work.

The resultant linkage is shown in figure 6.11 and its dimensional parameters are listed in table 6.2.

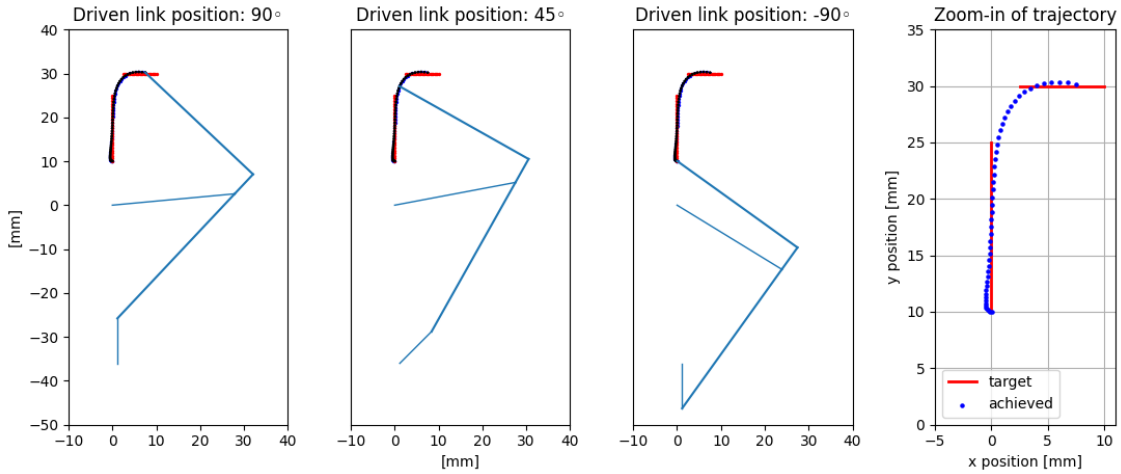

Figure 6.11: Open, 'captured' and closed positions of the linkage, and the overall trajectory of the tip

Table 6.2: Discovered dimensional parameters for the linkage

Parameter	Value[mm]
dx	1.2
dy	36.0
l_{ac}	10.25
l_{bd}	28.0
l_{cd}	39.0
e_1	6.1
e_2	33.8

6.2.2. CAD implementation

The dimensional parameters discovered by the synthesis were used to implement the mechanism in CAD software and verify the solution. As the only dimensions known were the lengths of the links, the remaining dimensions were modified largely arbitrarily as the work progressed. A perspective view of the mechanism in CAD is shown in figure 6.12. The linkage shown in the figure is not the initial version and has already been adjusted by work described in following sections. The connections between the links are assumed to be, or at the very least, behave as pin connections.

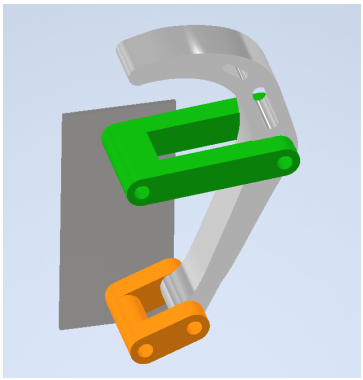

Figure 6.12: Perspective view of the linkage partial assembly. For clarity, the driven link AC is colored orange, link BD is green and the extended link CD is light gray.

An implementation detail that the reader may find confusing is the stark difference between the shapes of the link CD in figures 6.11 and 6.12. In reality no change at all was made to the geometry of the linkage. This is illustrated in figure 6.13. The particular feature to observe is that placement of the endpoint is identical to that as generated in section 6.2.1.

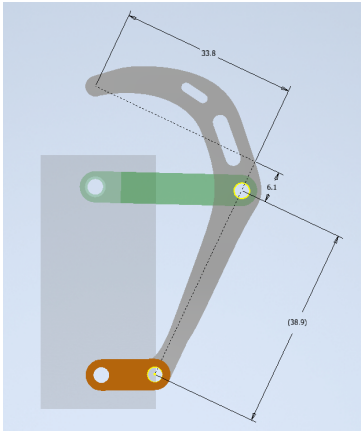

Figure 6.13: The underlying geometry of the extended link CD

The arc-shaped latch is a consequence of iterative tweaking of the design to eliminate unwanted contact points. The curvature near the tip of the clamp was tweaked to result in a larger contact area once the mechanism is fully closed as well as reduce the variation of the tip's height as the clamp slightly rotates during the travel of the mechanism. The mechanism in three stages of motion is shown in figure 6.14 to illustrate. These stages represent the fully open ('ready for capture'), partially closed ('captured') and fully closed stages of the travel. The initial curvature near the tip was then propagated down the rest of the structure for the purposes of a smoother stress distribution over the component as will be explored in section 6.2.3.

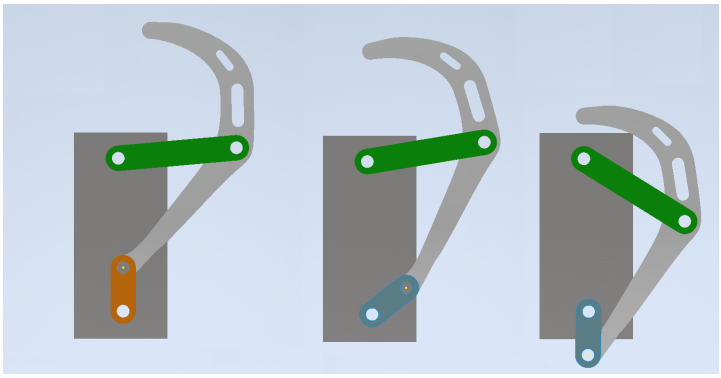

Figure 6.14: The stages of mechanism. Open, captured, closed.

First, the motion of the generated linked was verified by tracing out the trajectory of the center of the nose of the tip. This was done by utilizing the kinematic simulation capabilities of the CAD software and sweeping the driven link across it's range of motion. This process is fundamentally the same as the one described section 6.2.1 to generate the linkage parameters and as such if the generation was implemented correctly, this should yield an identical trajectory. Figure 6.15 shows the resultant trajectory as traced by the CAD software. The achieved trajectory is almost identical to that predicted by script used to find the parameters of the links and the discrepancies are small enough to not be important. For example, the horizontal travel in opened state is a 7.8mm and not 8mm as predicted but it is still sufficient for the purpose. These can be explained by rounding of the dimensions to the nearest tenth of the millimeter when recreating the linkage in CAD. Although this has no meaningful impact on this proof of concept investigation, the sensitivity of such mechanism to manufacturing tolerances would present an important point of consideration for future work.

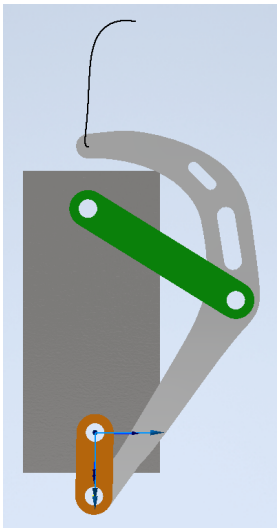

Figure 6.15: Tip trajectory simulated in CAD. The result is a very close match to the predicted one, validating the correctness of synthesis.

Next, the self locking behavior of the latch was verified by dynamic simulation. A vertical force of 1N was applied to the tip at the approximate expected contact point and the driven link was swept through its final $90°$ of travel. The holding torque was directly measured as the effort required to sweep the driven joint of the link. The point of force application and the initial position of the mechanism is shown in figure 6.16. A graph of the measured torque versus position of the driven link is given in figure 6.17 . It can be seen that the mechanism successfully achieves self-locking behavior in the final few degrees of travel as the holding torque crosses zero and slightly reverses direction. This verifies that the desired behavior has been achieved - once closed, the mechanism requires zero actuation to maintain its position. In addition, the region around the fully closed point is of immense mechanical advantage and as such even large preloads should be trivial to achieve, at least in terms of torque requirements.

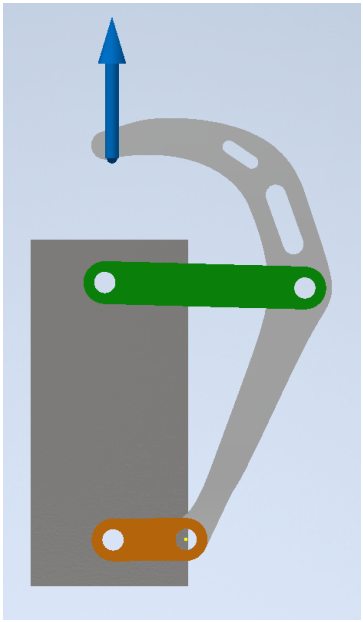

Figure 6.16: The simulation setup to measure torque load on the driven link. A 1N force is applied to the clamp and the driven link (orange) is swept downwards 90 towards its final locked position

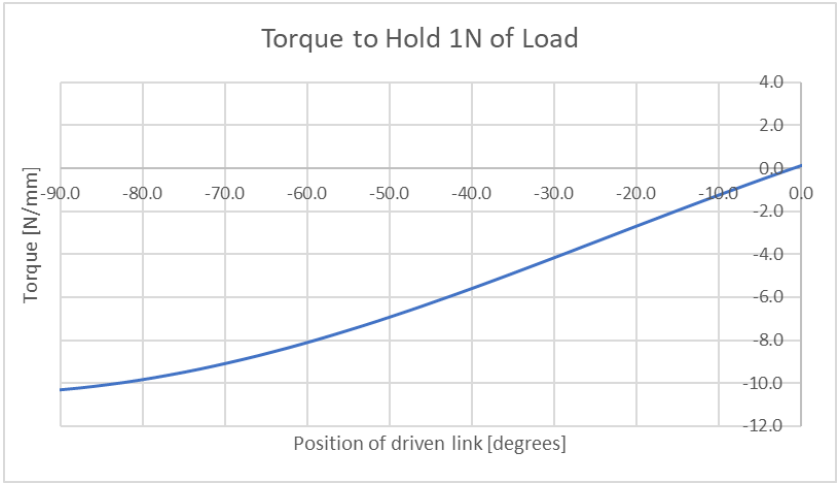

Figure 6.17: The torque required to drive the actuated link

The results of the linkage synthesis have been successfully verified by implementing the predicted parameters in a CAD model. The trajectory had been correctly predicted to a suitable degree and the differences are likely due to manual rounding of the dimensions when building the CAD model. The

self-locking property of the mechanism and a very large degree of mechanical advantage around the fully closed position have also been verified. Overall, the generated parameters successfully achieved the desired goals for the mechanism.

6.2.3. Closing and holding loads

With the basic geometry of the linkage verified, the loads expected on the components were studied next. This was done to sanity check the feasibility of implementing such mechanism at the assumed scale. Due to its overall small stature and expected large loads it needs to verified that the current scale of the mechanism is realistic. If it is not, then the information could be used to adjust synthesis constraints and reiterate the design. A second point of interest is to obtain the expected closing torque requirements such that drive mechanism could later be implemented.

Here two situations are considered: the loading experienced during closing the initial connection and the loading experienced once the interface is in operation. In the first situation, the clamping mechanism has to produce sufficient force over a considerable vertical travel distance in order to seat the liquid couplers, and before the mechanism is fully closed. In the latter case, the mechanism is already fully closed but has to withstand very large loads arising from the liquid couplers being pushed apart once the fluid lines are pressurized.

According to the manufacturer's specification for Cupla MALC coupler, the force required to maintain connection has the following approximation:

$$F \approx P \cdot 170 + 85N \tag{6.8}$$

In equation (6.8), P_{MPa} is operating pressure in MPa and F is the approximate force required in newtons. The assumed pressures for insertion and the operational condition are 0 and 20bar (2MPa), respectively. Plugging the values into the equation results in the expected force requirements to be in the region of $\sim 85N$ to insert and $\sim 425N$ to maintain the connection, per coupler. In this conceptual design there are two liquid couplers and the interface has three latches. It is assumed that the loads will be evenly shared between the three clamps. A safety margin of 2 is also assumed, both as a rule of thumb and because it allows for a once of the three clamps to fail safely. Combining these assumed values gives the following estimates for the expected loads on a single clamp mechanism:

$$F_{ins} \approx \frac{2 \cdot 2 \cdot 85}{3} \approx 113N, F_{hold} \approx \frac{2 \cdot 2 \cdot 425}{3} \approx 567N \tag{6.9}$$

The estimated insertion depth of the connector is 6mm. As such, the mechanism must produce the required insertion force F_{ins} at least over its final 6mm of vertical travel. Based on the CAD model, this corresponds to approximately the last $85°$ of movement of the driven link, which is just under half the motion range. The two cases are summarized in table 6.3.

Table 6.3: Considered operational scenarios for the clamp mechanism

Scenario	Driven link position, °	Clamp vertical load, N
Closing	[-85, 0]	133
Closed	0	567

Both scenarios were simulated in identical fashion as discussed in the previous section, however this time the forces internal to the mechanism were also recorded. Unsurprisingly, the results for the driving torque requirements were identical to simply scaling the unit force graph from figure 6.17 by the new load. The torque requirement for the driven link is identified as 1.33Nm and it is the highest at the very beginning of the insertion. Likewise, the torque needed to drive the mechanism near its locking position remained vanishingly small. Given the driving torque results pose no unexpected outcome they will not be discussed further. The simulated forces internal to the mechanism were exported from the dynamic simulation over to the finite element analysis (FEA) environment. The constructed load cases were used to perform stress analysis on the individual links.

Component simulations

Simple static stress analysis of the individual links was performed by directly exporting load cases from the dynamic simulations. It is important to keep in mind that this is a very early conceptual exploration

and the goal of the stress analysis is by no means structural optimisation. Attempting such at this stage would be foolish at the very least. However, the idea here is to simply investigate how heavily the components are loaded. Although these are simply mocked-up parts, if the stress analysis predicts that they are extremely overloaded (i.e. safety factor <0.1) then it could be deemed that the design is not feasible. If the predicted stress levels would fall within reason, then an argument can be made that such design is a feasible target for future work.

In order to perform the stress analysis, the components must be assigned a material. Detailed decisions about the choice of material cannot yet be made as the rest of the system is simply a proof of concept built on compounding assumptions. The goal here is to verify that the device could be built without resorting to exotic materials.

A material considered representative as a substitute is aluminium 6-series. It is a strong, common material that is suitable for vacuum and is otherwise widely used in aerospace. One of the requirements for the interface mechanism is to have a lifecycle count of at least 1000. This requirement is respected by not assuming fresh aluminium properties. In particular, the yield strength of the substitute material is assumed as that of Al6061-T6 after $\sim$10000 cycles and is $\sim$200GPa [89]. The rest of the aluminium properties were kept at the CAD software defaults for aluminium 6061. The material properties used in these simulations are listed in table 6.4.

Table 6.4: Mechanical properties of material used to represent fatigued aluminium

Property	Value
Young's modulus	68.9 GPa
Yield strength	200 MPa
Density	2700 kgm^{-3}
Poisson's ratio	0.33

Out of the linkage components, only the clamp finger was found experiencing significant stress loads. The geometry of the part was iteratively tweaked until a safety factor of >1 was achieved. The final geometry has a predicted safety factor of 1.19 and this result is shown in figure 6.18. The other two links shown in figure figure 6.19 already had excessive strength which is not surprising given the ratios of their dimensions.

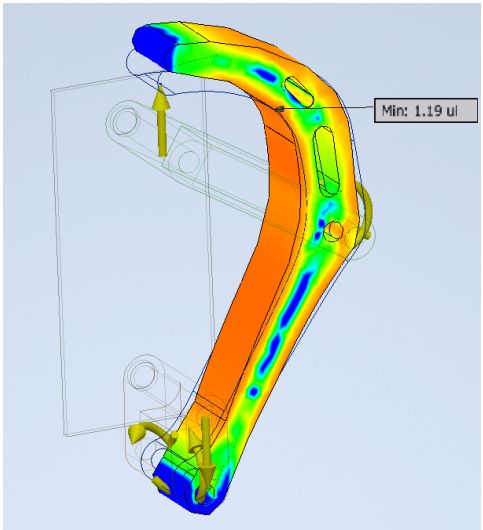

Figure 6.18: Safety factor distribution of the clamp finger. The mark indicates the minimum.

These results suggest that if the assumptions made are true, then the proposed mechanism is feasible to implement in comparable scale and without use of exotic materials. As such, future works are not expected to face excessive design challenges in this area. This achieves the primary goal of verifying feasibility.

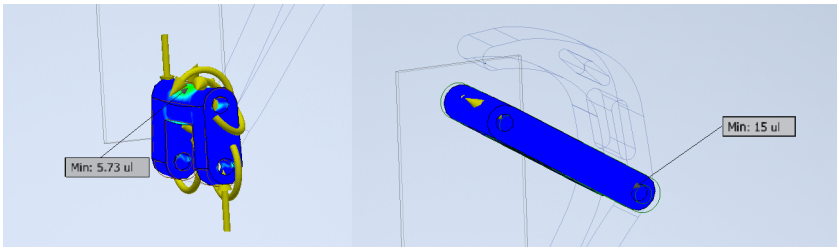

Figure 6.19: Safety factors of the driven link and the stabilizing link. The marks indicate the minima.

6.3. Integrated Simulations with the Faceplate

After the scale of the clamp linkages was verified, the mechanisms were packaged together with the passive faceplates to form the basis of the inner interface. The entire mechanical solution was then further simulated using the dynamic environment to verify that the desired alignment behavior has been achieved. Section 6.1.3 confirmed that the faceplates individually are expected to achieve the desired alignment and insertion properties if the closing force is assumed to be perfectly axial and balanced with respect to the centerline. It is to be verified that the behavior remains the same when the idealised closing force is replaced by the actual clamp linkages.

The resultant proof of concept active and passive sides of the inner interface are shown in figure 6.20. The passive side has been modified to include recessed target 'pockets' for the clamps. The dimensions of these pockets are enlarged beyond the target acceptance window of 5mm so as to respect the assumption of the clamps only providing a vertical force. In this arrangement, the clamp fingers can freely slide around the 'pockets' and thus should only generate forces normal to the bottom surface of the pocket aside from friction.

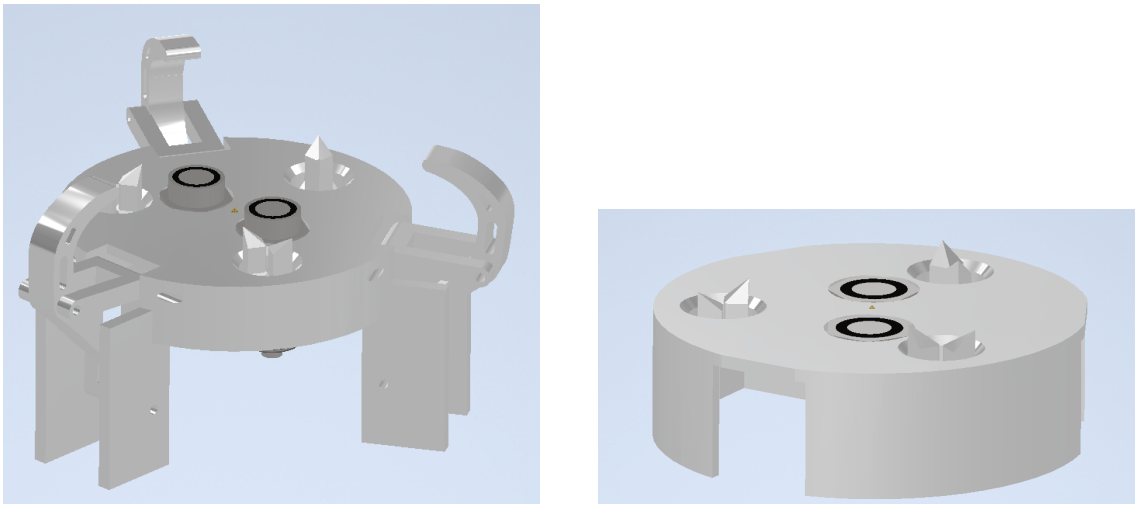

(a) Active side **(b)** Passive side

Figure 6.20: Latches integrated into active and passive sides of the inner element

6.3.1. Simulation setup

Mating of the interface was simulated directly by placing the passive side of the interface within the acceptance window of the active side and actuating the would-be driven link of the clamps' mechanisms. While the software is able to generate appropriate rotary joints for the linkages from the assembly data, additional joints need to be included to set up the full simulation case. These are the 6DOF spacial joint between the two halves of the interface and all the contacts as they are not implicit. To limit the computational complexity of the simulations only the expected contacting components were included as 3D contact joints. The full list of joint definitions (excluding the implicitly generated joints for the linkages) is following:

1. The faceplate of the active side of the interface is the grounded reference.
2. 6DOF spacial joint between centers of the active and passive faceplates' top surfaces.
3. 3D contact between each clamp finger and the passive faceplate. (3 contact definitions)
4. 3D contact between each pair of stabilizing structures. (3 contact definitions)
5. 3D contact between the two faceplates.

The parameters for the joints and the simulation environment were the following:

- 3D contact stiffness - 1e6 N/mm
- 3D contact damping - 1e4 N/mm/s
- 3D contact friction coef. - 0.2
- Gravity disabled
- Maximum timestep - 0.01s

The initial positioning of the two halves of the interface was achieved via altering the initial conditions of the 6dof joint.

6.3.2. Simulation results

The mechanism succeeded in achieving the desired capture and alignment behavior to a large extent. Specifically, the arrangement did behave as desired by remaining stable and ensuring tight planar alignment of the interface before any contact is made between the connectors, achieving the primary design objective. However, the reliable acceptance window of the mechanism was found to be smaller than expected at approximately 4mm rather than 5mm. This discrepancy is believed to arise from failure to account for the clamp fingers having thickness during the initial parameter synthesis, which partially upsets the overall geometry of the linkage. Although the error is obvious in hindsight, luckily the consequences of this mistake are not of crippling importance to this proof of concept and are expected to be fairly easily fixed by future iterations.

Due to the simulated scenarios only differing in the initial placement of the two interface halves, their results are extremely similar in nature. As such, two sample simulations will be discussed in detail as representing the typical results. One demonstrating a successful result and the second demonstrating a limit case at the edge of the acceptance window where the failure to account for clamp finger thickness leads to undesirable behavior.

First, the typical successful result. In this particular simulation the two halves were positioned within the allowable capture window, with an initial error of 4mm and 1° on the x axis, and the clamp mechanism was actuated from fully open position to fully closed over a period of 3s. A plot showing the alignment of the interface as the process progresses is given in figure 6.21 and corresponding images from the simulation of the device are provided in figure 6.22 for illustrative purposes. The axial separation in figure 6.21 is the physical distance between the two faceplates and becomes zero when the mating is completed. It can be seen that the arrangement successfully achieves approximately zero misalignment by the time it reaches the fully closed position. In addition, the mechanism also succeeds in achieving the goal of almost zero planar misalignment over the last $\sim 6mm$ of axial travel, which corresponds to the assumed insertion distance of the liquid connector. Therefore, the simulations verified the functionality of the proposed geometry if the starting conditions are within the acceptance window. If the initial conditions were outside the acceptance window, the passive side of the interface would simply not clear the opening provided by the clamp fingers and thus the mating would not commence.

In general, if the two halves were sufficiently aligned to fit through the clamp opening and enter the acceptance volume the rest of the mating process would succeed.

Figure 6.21: Axial separation and the planar misalignment of the two halves of the interface as the mechanism is closed over 3s. Starting condition within acceptance window.

The second example scenario near the edge of the capture window provides interesting observations on the current design as well as the simulation environment used. As for the previous example, the misalignment graph and the illustrative images from the simulation are shown figures 6.23 and 6.24, respectively. As can be seen in figure 6.23, the connection ultimately succeeds in this specific simulation but this still represents a scenario of the mechanism nearly failing. The root cause of these failures appears to be the previously mentioned failure to account for the clamp thickness which results in unwanted contact being made with the side surface of the faceplate. This can be seen in figure 6.24-2. This contact breaks the underlying assumption of the entire mechanism which is that of the clamp fingers only coming into contact with the top surfaces of their corresponding 'pockets'. The resultant sideways force knocks the interface to the side, imparting a large misalignment as can be seen in both figures 6.23 and 6.24. In this case, the mechanism still manages to constrain the motions sufficiently to complete the mating. However the behavior of the system is highly undesirable. Therefore, the observed acceptance window was approximately 4mm over the intended 5mm. This slight reduction is sufficient to avoid the premature contact of the clamp.

These edge cases also expose an weakness in the simulation setup. Because the interface is simulated in isolation, the passive plate can undergo excessive motion which could be considered infeasible in reality. In the physical world, the interface would be connected to a much larger structure, preventing it from essentially bouncing around like a hockey-puck within the volume it is constrained to. It could be argued that such a stabilizing effect would only be of benefit as a more inert system would suffer less from sporadic and 'bouncy' contact, making the entire mechanism better behaved. It could also be argued that this situation still demonstrates the inherent stability properties of the geometry arrangement.

Overall the simulations showed the desired behavior has been achieved within a reduced capture window of $\sim 4mm$, the results and the behavior were consistent for all initial positions tested that fell within this range. The simulated cases that started outside the intended acceptance window of 5mm expectantly failed by simply not clearing the opening gap provided by the clamps and as such being bumped off or otherwise ejected. The simulation cases that started near the edge of the intended acceptance window resulted in excessive unpredictable motions, but generally successful mating behavior. Inspecting the simulations it was noticed that at least a partial cause of this was due to clamp fingers making early contact with the structure. Although the initially synthesized 'ideal' linkage would correctly clear the geometry, the modelled part has non-zero thickness and as such the contact point is slightly offset from the intended location.

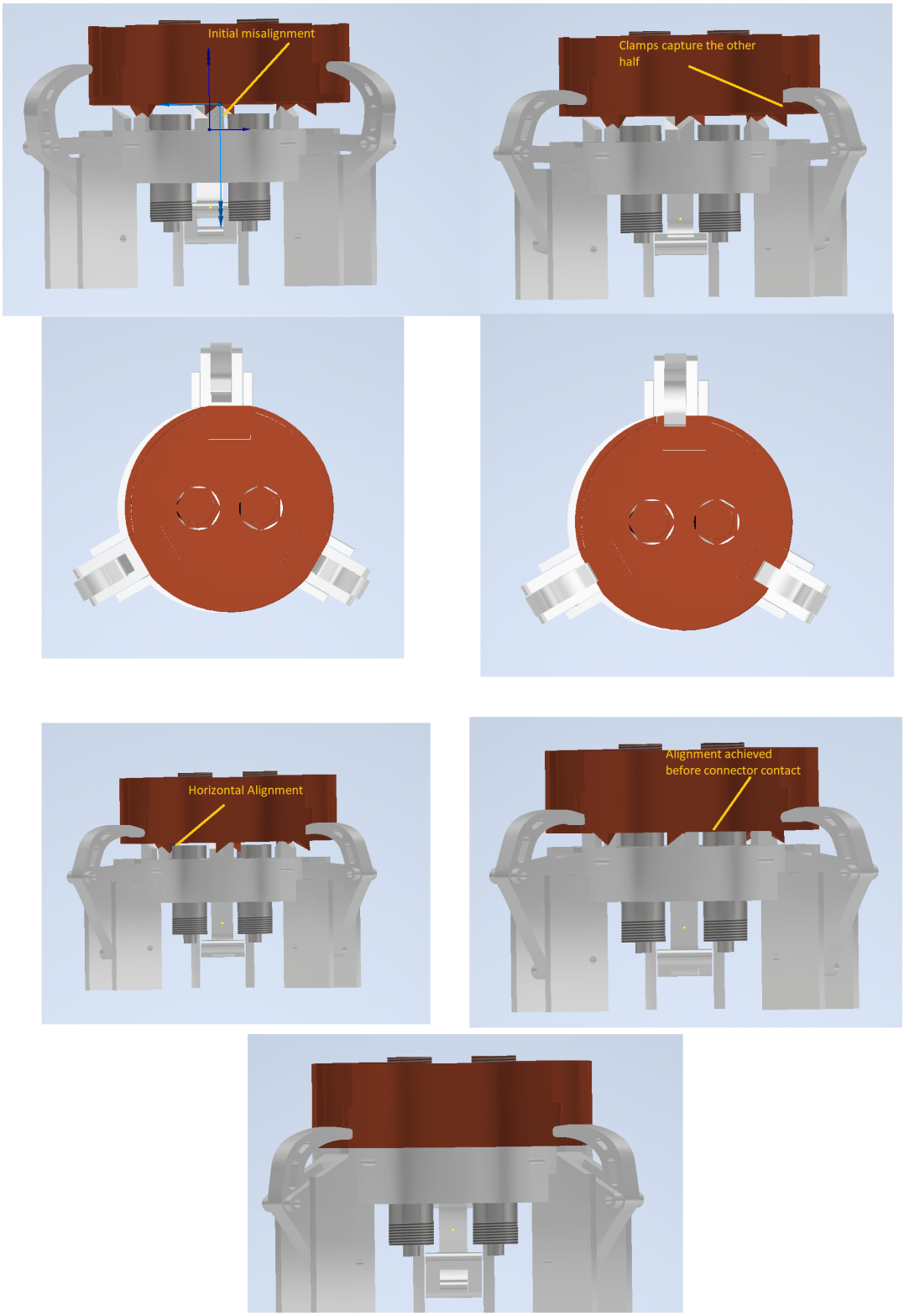

Figure 6.22: Example dynamic simulation of the interface mating. 1. Active side fully open. 2. The passive side is captured. 3. Stabilizers rapidly achieve horizontal alignment. 4. Stabilizers are horizontally aligned and only vertical travel is possible. 5. Fully closed

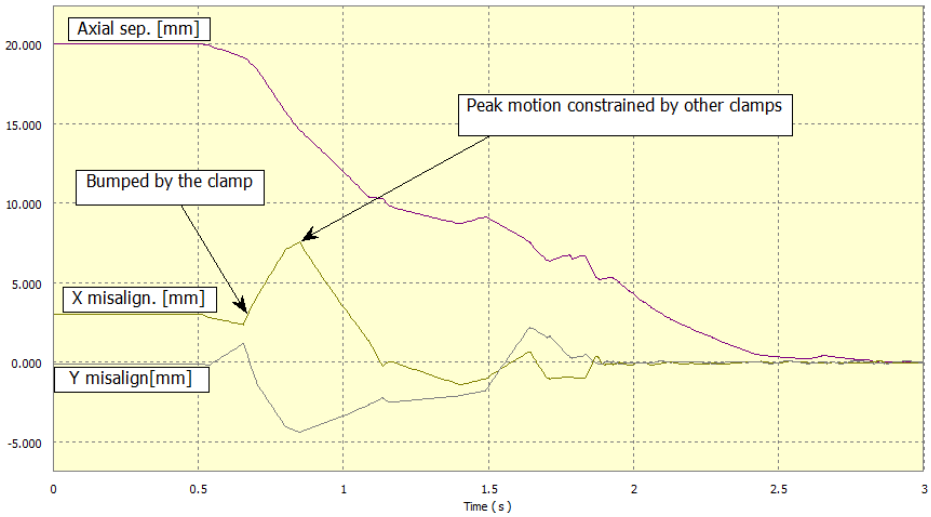

Figure 6.23: Axial separation and the planar misalignment of the two halves of the interface as the mechanism is closed over 3s. Starting condition on the edge of acceptance window.

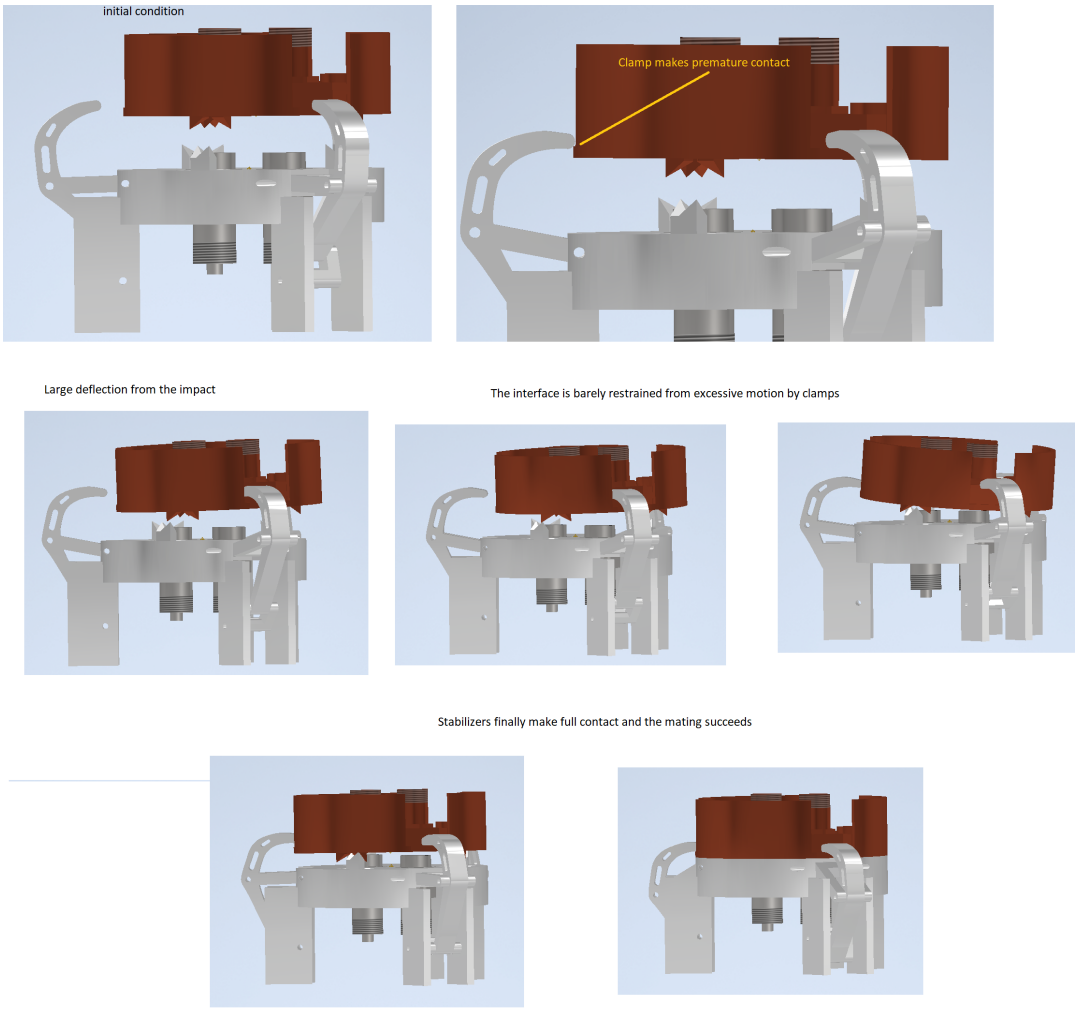

Figure 6.24: Example dynamic simulation of the interface mating. Due to failure to account for the clamp finger's thickness a large disturbance is imparted by premature contact.

6.4. 3D-printed Geometry Validation Model

The performed dynamic simulations of the mechanism predict that adequate alignment and insertion capabilities have been achieved. However, the motions of the structure observed during some of the simulations were deemed highly suspect. In order to increase the confidence in these results it was decided to simply manufacture the design utilizing 3D printing and thus validate the correctness of the the geometries directly.

The only intent of this 3D printed example is to validate that the geometry properties of the mechanism match those as predicted by the simulations. Due to the model being constructed out of PLA plastic rather than the intended metallic materials, it was deemed impractical to even attempt measurements on performance characteristics such preload forces, closing speeds, or similar. As a consequence, additional liberties were also taken in the drivetrain to greatly reduce the cost of construction by utilizing readily available hobby-grade components such as the motor.

To make the model feasible to 3D print, the drivetrain geometry has been altered. Primarily to utilize larger modulus gears, the enlarged teeth of which make it feasible to manufacture using hobby-grade 3D printers. The overall arrangement was maintained as proposed for the concept: all the clamp linkages are driven synchronously by a single shared drivetrain. Another simplification was that only a single small motor was used to actuate the mechanism. A basic microcontroller was used to control the motor speed and direction based on an input from a potentiometer. This provided a rudimentary level of control by the user such that the mechanism could be opened and closed without continuous input by the operator.

No alterations were made to the critical geometry of the faceplates or the clamp linkages. In order to avoid potential assembly errors and thus ensure the highest possible accuracy of the self-aligning geometry in question, the two faceplates were printed as monolithic components. Although this resulted in drastically increased printing times, the tradeoff was deemed necessary to avoid accidentally compromising the geometry due to assembly tolerances.

The manufactured device is shown in figure 6.25.

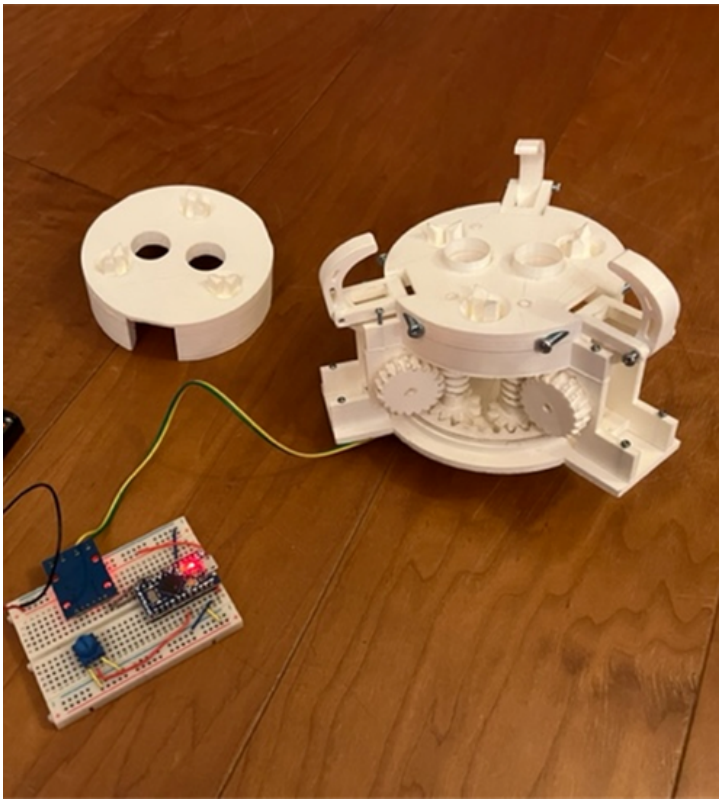

Figure 6.25: The 3D printed model of the inner interface

As a physical means of validating align-before-insert quality, connectors with tight alignment requirements were emulated by two cylindrical structures that have to be precisely aligned in order for the mechanism to successfully close the interface. A close-up of these structures is shown in figure 6.26. Due to inherent accuracy of 3D printing and slight warping of the material as it cools, it was decided to simply measure the final clearance of these inserts rather than attempt to manufacture to a precise tolerance. The manufactured inserts were measured to have $\sim 0.12mm$ radial clearance with their corresponding target recesses using a micrometer and this was deemed as suitable for the validation as such alignment would be exceedingly difficult to achieve if the structure did not have self-aligning properties.

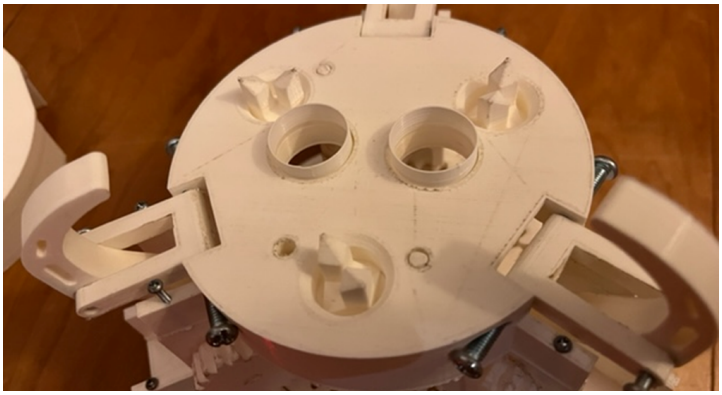

Figure 6.26: Tight-fitting cylindrical inserts emulate aligned insertion requirements of connectors

The manufactured model functioned correctly and especially the self-alignment properties were validated qualitatively by simple, albeit not very scientific, experiments. The primary means of testing was either 'handfeeding' the passive side of the interface to the mechanism or allowing the mechanism to pick up the passive side of the interface from a misaligned position. An example of the latter case is shown in figure 6.27. It can be seen from the images that the sequence of events progresses as intended. First, the two interface halves are positioned within the acceptance window and the clamp mechanism is actuated. Next, the clamp fingers reach their 'captured' position and the two halves will no longer separate. Then, as the clamps close, the alignment is gradually achieved by the stabilizing structures. The planar alignment is fully achieved before the interface is fully closed - at this stage horizontal motion is fully restrained by the alignment structures and only axial motion is possible. Lastly, the connectors are already aligned to below fractions of a millimeter and the interface smoothly closes.

The hand-held tests successfully validated that the alignment behavior observed in simulations was not a quirk of the simulation environment and is indeed inherent to the structure. The model mechanism was found capable to reliably self-align from considerable initial misalignment down to <0.1mm which is was required to smoothly insert the cylindrical protrusions emulating connectors.

These tests qualitatively validated the proposed design and, by extension, increased confidence that the approach and techniques utilized here could be repurposed as a starting point for future work aiming to fully implement such a device.

This is admittedly a fairly weak form of validation, but it was not done so without reason. Quantitative experiments should, without question, be performed by future works by utilizing a robotic manipulator or similar device in the setup to achieve precise control of the initial placement of the device under test. The reason such setup was not pursued here is simple - the performance requirements for this device are highly speculative. As such, even if much more detailed experimental measurements were made, the significance of the results would not benefit proportionally to the resource investment. After all, this is simply a proof of concept 0th iteration and the interest is to prove that qualitative features that make the proposed concept a suitable solution to the problem are achievable. The performance figures such as the acceptance window of 5mm are for the most part mere assumptions that simply serve a means to guide the proof of concept design into a more realistic scale. Chasing them to a very exact degree, while perhaps a nice result, would be rather foolish at this stage.

Figure 6.27: An example experiment where the passive side is picked up from a misaligned position.

6.5. Approximate Sizing of the Drivetrain

The final step that was done in verifying the feasibility of the proof of concept design was implementation of a suitable drivetrain. This was done to explore whether or not future efforts were likely to face sizing challenges arising from the gearing or the motors. Once again, the assumed scale of the required components is of question and whether or not they would define a critical dimension limit. If a potentially suitable gearing and motor combination were found such that required actuation torque and component longevity is achieved, and the scale of said components is that which could reasonably fit into the existing proof of concept, then the drivetrain will be deemed to not represent a critical limitation by future works.

The parameters to be achieved by this example for the drivetrain are the following:

- Achieve actuation torque of at least 1.33Nm for each of the clamp mechanism
- Achieve synchronicity between the clamp mechanism
- Achieve safe-life behavior in gearing.
- Redundancy for at least opening the mechanism.
- Achieve >1000hrs of expected endurance

The overall strategy behind the design is to share a single drivetrain between all of the linkages and utilize worm-gear pairs as a means to efficiently achieve high torque amplification in a small volume at the trade-off of speed. Doing so would assure synchronicity between the clamp linkages and allows to easily increase redundancy in the most likely area to suffer failure, which is the motor and related power electronics.

As the one expected to experience the heaviest loading, the first component to be selected were the worm-gear pairs that would directly drive the actuated link of the clamp linkages. These selections were made by scouting COTS part catalogues for parts with similar specification.

A particular issue with integrating the current design was immediately discovered - the size of the driven link was simply too small when compared to worm-gear pairs capable to handling the required torque. Because of the dimensions of the link, the driven gear would have to have an outer diameter of $<\sim 15mm$ to be reasonable to package within the driven link, otherwise it would not clear the other

components of the linkage. Unfortunately, no COTS worm-gear sets were found that even remotely approached this combination of small diameter and torque handling capabilities. Future iterations of the design should strongly consider introducing additional constrains to linkage generation that are based on feasible sizes of gears such that the overall mechanism would be more practical to implement. One of the smallest worm-gear pairs rated for sufficient torque that were found is manufactured by Framo-morat. The specific component codes for the gear and the worm are A17U-30/B[1]. This gear set was selected for use in this example because it offers a high gear ratio and sufficient torque handling rating. Worm-gear pairs of similar dimensions that offer a higher gear ratio had lower torque handling ratings, presumably due to the small tooth sizes becoming a limiting factor. The relevant specifications of the gears are provided in table 6.5.

Table 6.5: A17U-30/B worm-gear pair characteristics

Parameter	Value
Gear diameter	24.6 mm
Worm diameter	13 mm
Center distance	17mm
Torque rating	3.2Nm at 125RPM
Tooth safety factor	300%
Endurance rating	3000h
Gear ratio	1:30
Efficiency	45%

One unfortunate drawback of relying on worm gear sets is the inherently low efficiency of power transfer, especially at higher gear ratios. Due to very shallow contact angles, even small amounts of friction result in high frictional losses. In this particular case, if the gear geometry is assumed to utilize solid lubricant to support operation in vacuum, the expected efficiency of the wormgears is only $\sim 45\%$. There are no obvious alternative means to achieve comparable gearing reduction without resorting to multiple reduction stages either. As such, the motors are simply oversized to the degree that the output torque requirements would be satisfied even under such heavy efficiency losses.

The next major component are the motors. The motors selected for this example are is x208-047 stepper motor manufactured by Lin Engineering[2]. This was chosen as an example part because it is the smallest (and lightest) motor found that provides sufficient torque output and is also offered in vacuum-compatible variant by the manufacturer. Additionally, the overall geometry of this motor appears highly suitable for overall integration into the rest of the concept. The motor specifications are provided in table 6.6. Motors based on a smaller frame size are rated for drastically lower torque outputs while still maintaining comparable mass. Larger frame size motors likewise represented a drastic increase in mass. As such, this particular component was chosen as it was deemed to represent a decent balance between mass, size and torque output. Assuming the specification to be trustworthy, multiple of these motors in parallel would achieve sufficient torque output once paired with an additional $\sim 1:3$ gear reduction stage, even after the inefficiency of the worm gears is considered.

Table 6.6: Motor specifications

Parameter	Value
Frame dimension	24.6 mm
Length	46.50 mm
Torque Rating	0.05797 Nm
Mass	80 g
Endurance rating	5000h @ 1000rpm

The final combination of the redistributor gear and spurs were estimated using gear design tools in the CAD software that implement ISO6336:1996 standard. No concerning factors were found in this area and the specific resultant configuration is more akin to a visual aid for the concept than a concrete

[1] https://framo-morat.com/products/worm-gear-sets/worm-gear-sets-a17/

[2] https://www.linengineering.com/products/stepper-motors/hybrid-stepper-motors/x208-series/X208-047-01/X208-047-01

Table 6.7: Theoretical geartrain parameters

Gear pairs	Input [Nm]	Output [Nm]	Efficiency	Endurance [h]	Tooth Safety factor
Motor spur - distributor	0.06 (x2)	1.06	0.95	10000	4.5
Distributor - worm spur	1.06	0.33	0.98	10000	3.8
Worm - worm gear	0.33	4.45	0.45	3000	2.16
Entire drivetrain	0.06 x2	1.49 (x3)	0.41	$\sim$ 3000	-

sizing choice. The default material of heat-treated steel was applied to these components and the components were sized for 10000hrs of endurance in a loading condition representing a seized mechanism. The goal is to verify whether the arrangement could allow to safely stall the motor out at its maximum torque output without risking damage to any of the drivetrain components. This would suggest that there are no hard requirements for additional systems in order to avoid catastrophic damage.

The distributor gear and the pick-up spurs were roughly designed to provide an additional 1:3 reduction stage such that sufficient closing torque of >1.33Nm is achieved on the three clamp mechanism. Due to relatively large size of these teeth, there were no challenges observed in torque handling capacities during this naive approximate sizing. The gear synthesis tool predicted excessive strength for any gear geometry that would properly mesh under the assumed placement locations in this example. The predicted transfer efficiencies also raised no further concerns with the worm-gear pair remaining by far the major contributor to the overall inefficiency.

Table 6.7 shows the torque loads that were provided to the synthesis tool at each stage of gearing along with the predicted safety factor for the gear tooth failure. All the required gearing was successfully generated and achieved sufficiently high strength as to be considered safe-life. The worm-gear pair that was selected as a catalogue part was also used to verify the tool by manually inputting its geometry and selecting a similar brass-based material to check if the predicted strength resembled that as listed in the specifications. These predictions were found to be within approximately 20% of the listed value, depending on material choice in the software. The deviation was deemed acceptably low to assume some degree of confidence in the approximations produced for the other gears. An exact reproduction of the specification would be highly unlikely given the limited knowledge of the specific material used by the COTS part. However, this provided confirmation that the rest of the approximations are not likely to be excessively erroneous.

Figure 6.28 showcases how such a gearing and motor arrangement could be packaged into the proposed concept. As the size of the gears and the motor have been shown to be sufficient for enduring the operational loads, it can be assumed that future works should be successful in fully implementing such a mechanical arrangement. The conceptual assumptions made prior in chapter 4 were demonstrated to uphold with some degree of confidence and such arrangement does offer a reasonable promise of allowing convenient integration possibilities. Primarily, by leaving the central volume of the device vacant for placement of liquid transfer components it does not introduce additional complications.

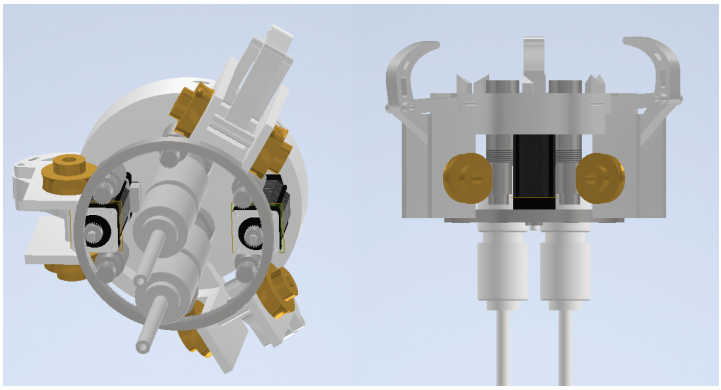

Figure 6.28: A mock-up of the unified drivetrain for the clamp mechanism.

6.6. Chapter Conclusions

In this chapter an example inner interface has been implemented to verify suitability of the proposed concept and investigate the potential feasibility of future efforts. Although the assumed specific performance figures were not fully achieved due to oversights in the design of the geometry, the fundamental functionality and layout features upon which suitability of the proposed concept hinges were successfully validated. In addition, the sanity checks for critical components indicate that the scale of the design is likely realistic. Rudimentary static stress analysis suggest that the linkage could achieve sufficient fatigue endurance without requiring significant upsizing. Likewise, an example drive train was successfully constructed out of catalogue COTS components and parametrically generated gears in a manner that satisfied endurance requirements and is of a scale suitable to package into this conceptual device.

The use of 3Dxface geometry was suggested as a possible stabilizing structure of choice due to its compact size and align-before-insert behavior. This choice has been validated by implementing a minimal model faceplate for interface, consisting of just a backplate, the approximate geometry of the liquid couplers and three sets of 3Dxface structures. By performing drop and insertion simulations, the example faceplate design was found to successfully achieve the alignment and insertion behavior suitable for the concept. A Python script was implemented to discover a possible geometry for the clamp mechanism. A four-bar mechanism was used as a starting point and appropriate link lengths and anchor locations were discovered to produce a target tip trajectory. Using Frechet distance as a measure of trajectory fitness and a multivariate optimization algorithm, a linkage with desired tip trajectory was discovered. The generated linkage was implemented in CAD software to verify the correctness of discovered parameters and that the overall arrangement leads to sane requirements for component strength and actuation torque. These two elements were successfully combined into a proof of concept construct which was demonstrated to achieve the desired behavior in terms of acceptance window and self-aligning properties via simulations. Due to some suspicious motions observed during the simulations, the studied design was also manufactured using 3D printing to qualitatively validate that the desired alignment properties of the mechanism are indeed present and were not simply a byproduct of the simulation environment.

In addition to demonstrating that the proposed concept is indeed a suitable and implementable solution with some level of confidence, a series of observations were made as areas of improvement for future work. First, the technique used to generate the geometry for the linkages should be extended to respect a predicted thickness of the clamp fingers as well be made aware of the scaling of the gearing. This is strongly recommended in order to avoid later design complications as were experienced during this 0th-iteration. The slight upsetting of the linkage geometry introduced by the clamp's thickness lead to unpredictable behavior of the mechanism in some cases that was not trivially fixable by minor tweaking of dimensions and margins, and as such should be included as a more fundamental design consideration. Likewise, the lack of awareness of a feasible size for the driving gear of the linkage resulted in the driven link being shorter than the radius of the gear that would be driving it. This lead to begrudged concessions in later packaging of the mechanism, as the driving gear was not feasible to house within the link itself. While not of critical importance in this proof of concept, this is definitely something that should be intentively monitored by any future work attempt, especially those attempting structural or layour optimisation on the mechanism. Second, almost the entirety of the dimensions of the 0th-iteration design can be traced back to the assumed dimensions of the liquid couplers. As such any future development of this mechanical concept should be postponed until the actual liquid couplers are developed to a sufficient degree as to have confident knowledge on their final dimensions, insertion tolerances and force requirements.

7

Proof of Concept Outer Element

In this chapter the idea to implement the outer element as a back-drivable stewart platform is demonstrated. Such concept is successfully used by the NASA docking system[79] but available literature only offers high level descriptions. To verify the expectation that the concept scales sensibly to our application, an approximation of the device is implemented using Simulink and directly tested in docking scenarios.

First, an estimate of desirable geometry of the capture structure is generated by rudimentary optimization aimed at minimising actuator force requirements. Next, the estimated platform was implemented as a mechanism in Simulink Multibody and a proof of concept control system was implemented which could handle the flexible behavior of the structure and provide adaptive damping during capture and docking. Third, an example docking scenario between two spacecraft representing an envisioned worst-case scenario was simulated to generate predictions of performance required by the actuators. Finally, it was verified that constructing such a modified actuator is within the realm of possibility as key components were found sufficient.

7.1. Finding a Desirable Geometry

The initial step is generating a plausible geometry for the hexapod platform. There do not yet exist any dimensional targets to be used as constraints, as estimating such target dimensions is the goal in the first place.

To arrive at some reasonable starting point for a geometry without simply guessing, an assumption was made that it is beneficial to minimize the actuation efforts required for a given load. This assumption is based on the observation that a hexapod platform consists almost entirely of actuators and an expectation that their mass is correlated with their actuation force. Similarly to the discovery of linkage parameters in section 6.2.1 a basic optimising script was implemented.

To estimate the actuation effort, the structure was solved for static equilibrium under an applied load. Equations for the equilibrium forces were referenced from supplementary material provided by a manufacturer of 6DOF platforms[90]. The equations were directly implemented in Python using Numpy library.

The solver positioned the platform at the neutral position and expected extremes of travel (combinations of axial and angular deflection). In each position, the structure was solved for equilibrium with unit loads applied at the origin of the top surface along the surface's normal vector and the two planar directions in sequence. For each evaluated geometry, position and load case, the maximum magnitude of the forces in the actuated links was recorded as the optimisation parameter to minimise. In addition, the maximum extension and contraction of each link was also recorded to eliminate geometries with unrealistic travel ranges for the actuators.

An approximate minimum diameter for the top part of the platform was set to $250mm$ based on the footprint of the inner interface and allowing for clearance during movement. The constraint for ratio of maximum to minimum allowed actuator length was introduced at 0.6 based on a quick survey of COTS actuators.

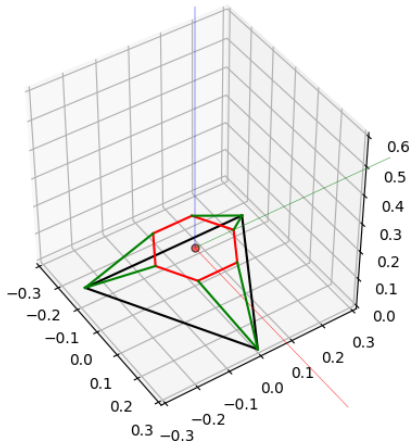

Figure 7.1: Resultant hexapod geometry

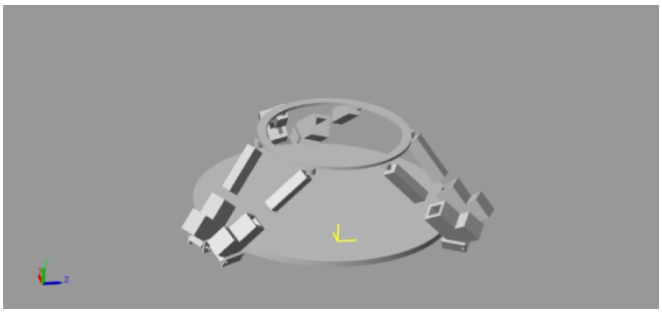

Figure 7.2: The hexapod platform implemented in Simscape Multibody

The geometry produced by this rudimentary optimisation is shown in figure 7.1. The general desirable features that reliably emerged during repeated executions of the script were the closely-spaced roots of the actuators, the evenly-spaced mounting points on the top ring. This base discovered geometry was thus adopted for use in the rest of this investigation.

Unfortunately due to the simplistic setup for the optimisation there are very limited conclusions that could be drawn in terms of optimality of the results, except perhaps, that they make intuitive sense. However, the goal was simply to decide on a starting geometry that is expected to not have degenerate properties which would hinder further work by means more grounded than simply guessing the dimensions. This was successfully achieved as the produced geometry is known to reach the desired travel range without unrealistic actuator extensions and is not expected to exhibit high levels of load amplification.

As it currently stands, the size of this geometry is bound by the required clearance zone around the inner interface element, required travel range, and the achievable ratio of extended to retracted length of the actuators. As such, it can also be argued that this example geometry is a decent representation of the minimal size required of such structure for this application. Factors such as structural integrity or actuator size limitations could very well require significantly enlarging the structure but it is much harder to envision a drastic reduction in size to be achievable without detailed future optimisation targeting a much more specific set of conditions.

This geometry was implemented as an idealised model in Matlab Simscape Multibody consisting of the capture ring, and six actuators, and is shown in Figure 7.2. The actuators are simulated as prismatic joints, have spherical joint connections to the top ring, and universal joints at the base connection. The prismatic joints representing actuators include motion limits equal to those as predicted by the generation script. The material of these components is assumed to be aluminium in order to provide known mass properties and make them suitable for dynamic simulation.

7.2. Conceptual Control Strategy

To demonstrate the proposed conceptual solution in a simulated environment, a control system was developed in Matlab to enable simulating an entire capture event in a closed loop scenario and demonstrate whether the proposed behavior can be achieved.

To achieve soft capture and impact through on backdrivability of the actuated links, the control system must tolerate a high degree of deformation and compliance from the structure. This makes the classical control approach for such structure where the actuators are simply commanded a desired extension not viable without modification. Simply due to the fact that the actuators in this concept are intended to behave as fairly soft springs and freely compress or extend based on experienced loads rather than maintain a position rigidly. By abandoning the typical design goal of ensuring stiff actuator behavior, the predictable positioning guarantees that enable this basic control strategy are lost.

An arrangement proposed by this work allows the actuators to behave as independent simple springs while the overall behavior of the structure is controlled by adaptively setting the neutral point. This arrangement is demonstrated to achieve the desired capture and docking capabilities without requiring any means of precise force feedback or complicated strategies to manage excessive forces in the structure.

7.2.1. Architecture of the control system

The developed demonstrator control system consists of three major elements: the quasi-soft actuators, a simple inverse kinematics solver and a posture controller. A high level diagram of the elements and their inputs is provided in Figure 7.3 and the conceptual arrangement is simple. The only feedback provided to the control system is the relative location and orientation of the approaching target, along with corresponding velocities. The posture controller calculates a desired target positioning of the capture ring based on this information. This stage determines an interception posture prior to making contact and dynamically steers the neutral point of the otherwise 'springy' structure to achieve damping of the impact. The target posture is then translated to target lengths for each actuator by the inverse kinematics code. These calculated target lengths are used to set the neutral points for each actuator, around which the actuators are controlled to behave as simple springs.

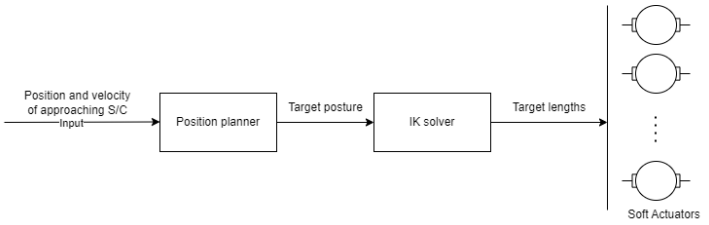

Figure 7.3: High level diagram of the control system

The first element to discuss are the actuators. Besides the conceptual modification of being smoothly back-drivable, the proposed arrangement only requires a means of position feedback from the actuators. The latter is not a novel feature and is commonly found in existing devices in the form of linear or rotary encoders, and is thus assumed present.

A spring-like behavior is achieved by pairing such conceptual actuator with a controller for the torque of the motor based on the position error of the actuator. By extension, this would directly control the actuator force assuming sufficiently small magnitude of backlash or similar effects. The conceptual actuator was implemented by augmenting each of the prismatic joints representing actuators with an independent PID controller that simply attempts to drive the joint to a desired position. The implementation is shown in Figure 7.4. The only feedback is the position of the joint and the only controlled parameter is the actuation force. The controller's proportional gain in this case directly correlates to the spring stiffness. Small integral and derivative terms were used to stabilize the loop, and the saturation limits of the controller block were utilized to emulate actuation force limits. The saturation limits were primarily included to prevent generation of unrealistically high forces and later served as a approximate means of determining expected requirements for the actuator by limiting the actuation forces until they were found insufficient.

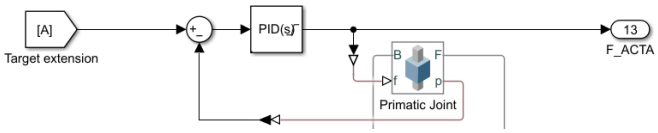

Figure 7.4: Internal actuator controller. Actuator only has position feedback and the stiffness is dominated by the proportional gain of the controller.

The inverse kinematics solution is a straightforward implementation of the classical control strategy for hex platforms. A function was implemented in Matlab that directly solves required actuator lengths given a desired position and orientation of the capture ring relative to the base as input. For clarity, the steps of the algorithm are as follows:

1. Generate the set of six points corresponding to actuator connection points of the top surface
2. Generate the set of six points corresponding to actuator anchor points on the bottom surface
3. Rotate the set of top points to the desired orientation
4. Translate the set of top points to the desired position
5. Calculate vector distance between corresponding pairs of the top and bottom points
6. Calculate the magnitude of these distances, which represents the required actuator lengths

The developed pose controller is more intricate and the means by which target interception and damping were achieved are explained in the following sections.

7.2.2. Estimation of impact point

One of the reasons the hexapod platform concept was suggested was the promise that pre-contact alignment of the capture ring could be achieved thus avoiding a requirement of great leniency within the securing mechanism. To fulfill this, the capture structure must be correctly positioned before any contact is made. This applies both to impact and zero-impact docking, as in the latter case the capture platform would have to 'reach out' and reach the target.

In this demonstrator example, the control employs a simple strategy of extrapolating the approaching vehicle's motion to determine where to position the capture structure. The approaching vehicle's orientation is matched such that the top of the capture structure will be facing normal to the target ring at the point of contact. Based on the findings from section 2.2 it is assumed that the relative pose and velocities of the target are known to a high degree of accuracy during at least the last 1m of separation, and by means independent from the interface itself. Specifically, the existing optical tracking solutions are expected to achieve accuracy of at least <0.1mm and <0.2° in this range. It is also assumed that an accurate estimate of motion would likewise be constructable from these measurements.

To find the intersection point, a ray is cast along the path of the approaching vehicle's capture structure's path and is checked for intersection with a cylinder representing the capture volume. The implemented algorithm attempts to find the interception point that is furthest from the bottom position of the mechanism as to allow for maximum remaining travel for bringing the spacecraft to rest. This estimate is continuously updated. If contact has already been made (i.e. the target ring is within the capture window), then this estimate coincides with the current location.

Two examples of the raycast are shown in Figure 7.5 as illustration.

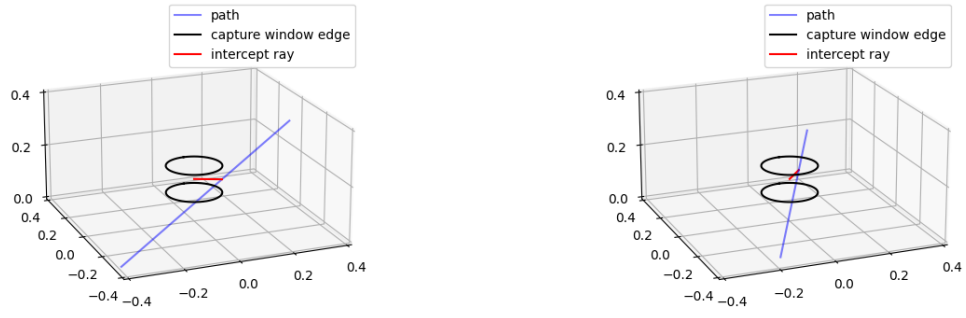

(a) High lateral velocity; Intercept is along vertical edge of the window.

(b) High axial velocity; Intercept is on top surface of the window.

Figure 7.5: Expected interception points in case of two approaches

7.2.3. Dynamic braking and damping

To generate damping and breaking forces during the docking maneuver, the desired neutral point of the structure is continuously steered in a manner that opposes the direction of motion. The simple approach of locking a desired pose and relying on the spring-like actuators was found to lead to excessive uncontrollable oscillations and otherwise highly unpredictable behavior if the structure sufficiently deflected from the commanded pose. The latter could perhaps be likened to buckling as the structure would deform sufficiently for the reaction forces of the actuators to drive it further away from the setpoint rather than being corrective, and cause it to snap to an undesirable pose.

The solution that was implemented is perhaps best described as a 'virtual' stiffness offset. The pose of the structure is continuously retargeted by taking the current position and offsetting it in the direction opposing the velocity vector by a fixed distance. This results in the target pose always remaining within close proximity of the actual, and thus resulting in predictably bound extension errors for the actuators. As a result, an overall behavior of the structure is achieved such that it behaves as a highly directional damper during the impact, the aggressiveness of which can be directly controlled by magnitude of this offset. In mathematical form, these calculations unsurprisingly resemble the equations of an ideal damper element.

The position offset to achieve linear damping during offset is included as:

$$\vec{P_{target}} = \vec{P_c} - K_l \hat{v_{rel}} \tag{7.1}$$

Where $\vec{P_{target}}$ is the position vector of the resultant target pose, $\vec{P_c}$ is the current position of the capture ring, $\hat{v_{rel}}$ is the unit vector of relative motion, and K_l is the damping offset.

The the angular offset is calculated in identical fashion but using quaternions to simplify the operations:

$$\mathbf{q}_{target} = \mathbf{q}_c \cdot \mathbf{q}(K_a \omega_{rel}) \tag{7.2}$$

Here $\mathbf{q}_{target}$ is the quaternion of the target pose orientation, $\mathbf{q}_c$ is the current orientation, ω_{rel} is the vector of relative 3D angular velocity, and K_a is the damping coefficient. Important to note is that the $\cdot$ operator in equation 7.2 is quaternion multiplication and not a vector dot product.

7.2.4. Staged operation

The implemented control system operates in five discrete stages. The are the following: idle, the approach, the arrest, the alignment and the parking.

Idle

The idle state is rather self-explanatory. It is the resting state of the interface. The capture platform is parked in a retracted position to minimize size and to remain mostly outside the approach window as to allow for near-miss approaches, especially for excessive lateral motion. The target of the approach is tracked, and once a likely interception point that is within the actuation limits of the platform is predicted, the interface transitions to the approach phase.

Approach phase

During the approach phase, the predicted intersection is used to preposition the capture ring to intercept the target in a well-behaved manner. Given the limit approach velocity is 10cm/s and the suitably accurate tracking is expected during at least the last meter of separation, this phase generally lasts a few seconds. During this time, the interception estimate is continuously updated in order to achieve good alignment of the capture ring against the passive target ring. During this time only basic control of the structure is active.

Arrest phase

Once contact is made, the capture platform transitions into the arrest phase during which the primary goal is to achieve zero relative motion between the spacecraft. During this phase the damping controllers become active and remain so throughout the sequence. At this stage the control system does not make additional efforts to control the position of the structure, only to arrest the motion. Once near zero velocity is achieved the structure remains in the position it was deflected to.

Reposition phase

Once relative motion is arrested, the alignment phase begins. During this phase the capture platform is gently commanded to its natural zero position over a predefined period of time. The starting point is the final resting pose after the arrest phase ended. This phase ends when the capture platform resides roughly in the center its actuation volume and is aligned with with the base of the capture structure.

Parking phase

This is the final phase of the sequence. During this phase, the capture platform is gently actuated back to its parking position near the bottom of its travel volume. This brings the inner interface elements together such that they are able to complete the final connection.

7.3. Simulink Model

7.3.1. Model setup

The outer element mechanism (hexapod platform) was assembled in Simulink out of rigid components connected through standard joints and attached to corresponding rigid bodies emulating large spacecraft. The described control strategy was implemented as Matlab function blocks to command the platform during these simulations.

Figure 7.6 shows a simplified global view of the model. The two bodies representing spacecraft are connected to the world frame through unconstrained 6DOF joints allowing free movement. One of the bodies has the capture platform rigidly attached, and the other has the corresponding target ring. An additional unconstrained 6DOF joint between the reference point of the capture platform and the target ring is used to sense relative position and velocity, and emulates feedback from a tracking system. As will be explained in section 7.3.2, the restraining mechanism between the two rings is idealised to a locking joint that is engaged upon contact, which is a tremendous simplification. When locked, it also creates a small separation between the two rings, allowing to avoid continuous contact between geometries and dramatically improving simulation time. These simplifications still allow to observe the actuator force requirements and expected loads on the restraining mechanism, estimating which is the primary interest.

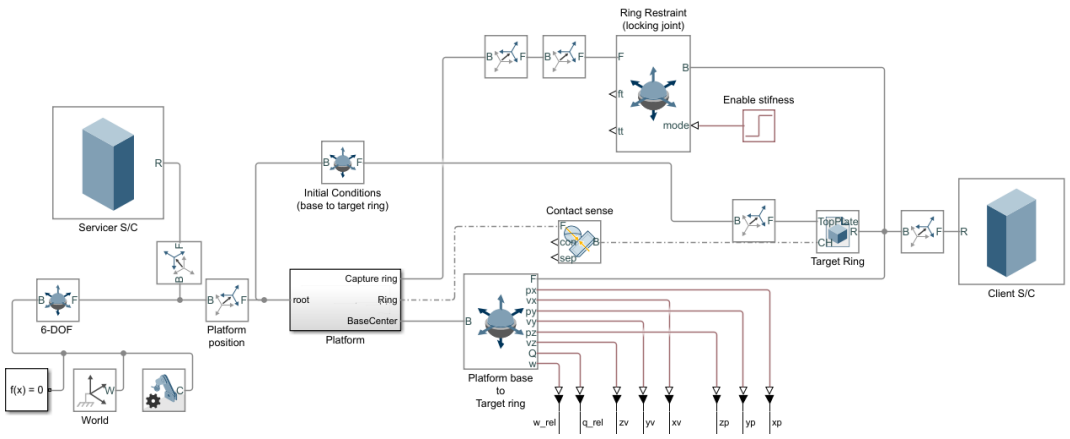

Figure 7.6: Model overview

The measured relative position of the target ring relative to the base of the capture platform is used by the pose controller and IK solver to generate target extension lengths for all 6 actuators as shown in figure 7.7. The output commands to the actuators are limited in slew rate to emulate actuator travel speed limitations. The contract signal is an additional input to the pose controller that is used as a workaround to provide some memory to the function block for interpolation and similar purposes. The code inside these blocks is provided in the appendix.

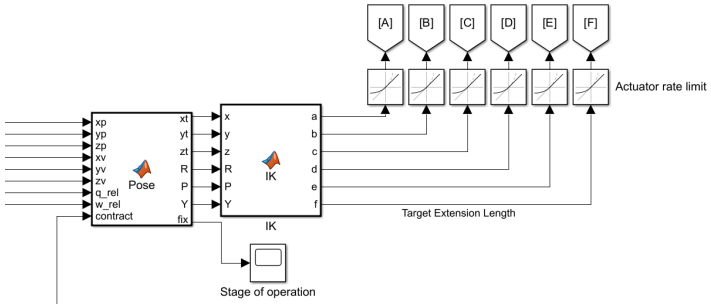

Figure 7.7: Pose and IK solver inputs and outputs

Shown in figure 7.8, each of the actuators is constructed out of a universal joint, a prismatic joint and a ball joint. Attached to these elements are simplistic rigid bodies that give the mechanism non-zero mass. Each actuator also equipped with a simple internal position controller that causes it to act as a spring and the saturation limits of this controller are used to introduce actuator force limitations into the system.

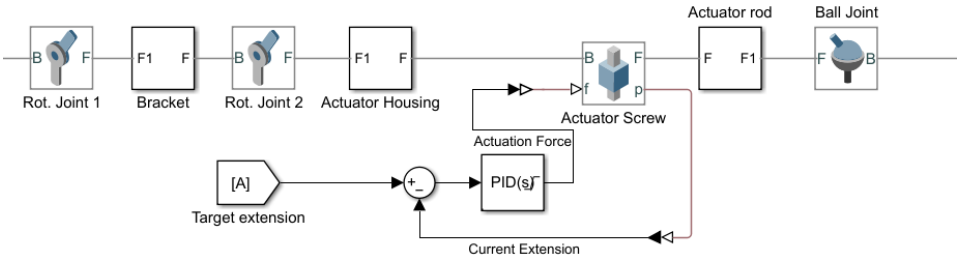

Figure 7.8: Simulated actuator

7.3.2. Omission of direct simulation of the restraining mechanism

Unfortunately this effort failed at integrating a direct simulation of the capture ring's restraining mechanism. This is a major concession made by this work in order to enable the rest of the system to be studied. Instead of directly simulating a restraining mechanism, the capture ring and the target ring are connected by a spacial joint with dynamic stiffness. Initially at zero stiffness, after a delay, this joint is toggled to gain stiffness, restraining the two capture rings together. This setup represents a large compromise, however it allows the rest of the docking sequence to be studied and at the very least observe the expected target requirements for a restraining mechanism. For example, the expected required positioning tolerance and load carrying capacity can still be predicted.

The primary reason behind this omission is that the Simulink software used does not provide innate means of simulating contact between complicated geometries. The spacial contact block present in the standard library only supports convex geometries, meaning any shape is effectively collapsed to its bounding volume. This made the block unsuitable for simulating all the important features of the restraining ring such as alignment petals or latches. This limitation is acknowledged in the documentation for the spacial contact block with possible workarounds listed as constructing these features from basic primitives or utilizing point cloud approximations. The problem and the workarounds are illustrated by the sketch featured in Figure 7.9.

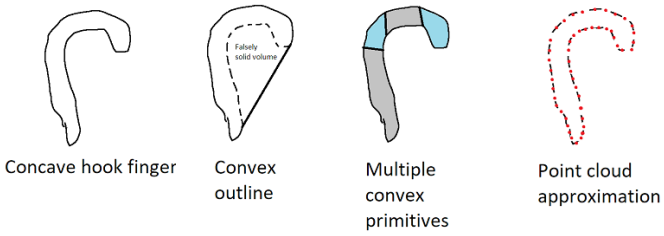

Figure 7.9: Convex geometry limitations and suggested workarounds

These workarounds were attempted with limited success. First of all, they were found to be extremely time consuming and prone to errors if done manually, and attempts to automate them trough scripting proved non-trivial and quickly represented a massive time investment for a questionable benefit. Given this work is not focused on validating an existing design but to provide first estimate of the requirements for such design in the future, this incapability to iterate made it not viable as an approach for discovery. Second, and perhaps much more importantly, the introduction of the excessively numerous non-linear elements into the simulation had crippling consequences in terms of solver performance. Having dozens of such elements in simultaneous contact resulted in simulation step time dropping to sub-microsecond intervals. Despite this, they still suffered from convergence issues as the miniscule timesteps lead to numerical stability errors and simulations would often fail. Particularly when floating point underflow seemingly resulted in divisions by zero within some library blocks. Usage of different solver algorithms and attempts to limit the minimum timesteps failed to solve this problem as well. Ode23t solver recommended by the documentation of contact primitive library[91] indeed behaved the best but the simulations still ran at upwards of a week of walltime per few seconds of simulated time. If the timestep was limited to the degree that a somewhat reasonable solve time was achieved (i.e. half a day), the results were simply nonsensical experiencing artifacts such as random and spontaneous ejection or excessive clipping.

Even after considerable time investment this area of the simulation proved too hard of a challenge to address in the timeframe of the project and was relegated for future work. This failure is also unlikely to be indicative of unsuitability of the software used as similar types of simulations have been reported successful[92].

The decision was thus made to reduce the scope of the project by idealizing the restraining mechanism and assume it somehow capable of providing the necessary connection. This concession allowed to simulate the rest of the capture system and predict the required performance of future implementation of the restraining mechanism.

7.4. Estimation of Parameters Simulations

The current simulation setup was still found to be rather computationally expensive, however sufficiently fast to at least explore the concept. Without concrete optimisation goals to target, wide global coverage of the parameter space was not attempted. Such search would require dramatic further optimisation or simply a large investment of computational time, both of which simply fall out of the timescale of this work. The goal is to verify the sanity (or lack there of) of the proposed concept and thus warrant or dismiss such time investment from future work.

As a means to answer the question of feasibility, rudimentary predictions of the required performance of components were achieved by experimenting on system's constrains in a few select scenarios. These experiments included introducing limitations on key characteristics of the system such as extension speed of the actuators, their force limits, or the sampling rate of the relative position data. Effectively this process attempted to find the minimum bounds for such parameters under which the concept did not operate reliably, even under the idealised conditions.

The first demonstrate that the solution does achieve the functionality as required by the concept. The last simulation case represents a capture and docking scenario near the proposed expected limits of the system. This case is used to provide estimates of the performance requirements for the actuators and the restraining mechanism.

In these simulations, the masses of the two spacecraft were assumed at 1e4kg each, representing the maximum expected masses as identified in chapter 3. As an idealisation, the two spacecraft were represented as two rigid cubes of constant density and the dimension of 3m.

7.5. Gentle Capture Cases

When gentle capture cases were simulated (i.e. near zero relative velocities), no interesting limiting requirements for the system were observed aside from the required actuator maximum travel speed. Conditions where it was limited to below $\approx$ 70mm/s resulted in inability to chase a laterally moving target such that the capture ring could properly intercept it. Otherwise, in these scenarios the system confirmed itself capable of reaching the target once within the capture window. The actuator force requirements were drastically lower than in the limit impact case, and only depended on the aggressiveness of the subsequent realignment after the initial arrest. As no requirement for a maximum duration of the docking maneuver has been defined, no further metrics could be estimated from these cases. As a consequence, most of the discussion will focus on the more interesting results from the hard impact simulation given in the following section.

7.6. Limit Impact Case

In the limit case, the two spacecraft of 10000kg of mass approach each other with maximum axial and lateral velocity, at a significant angular deflection, and the limit angular velocity. In this case, the parameters were experimentally found such that the target is arrested near the actuators exceeding their travel limits.

It was found that in this scenario the simulated actuators required to be capable of exerting a force in the approximate neighborhood of at least 500N each. The specific maximum force observed in the given example simulation was 422N but these results must be considered with great caution due to the highly idealised nature of the simulation. Only significant changes in actuator force limits could be considered observable and such reductions lead to consistent failure of the mechanism. For example, limiting the actuators to 300N lead to over excursion of the actuators or extreme difficulty in stabilizing the structure, especially against angular motions.

Although the simulated docking was successful, a worrying weakness was observed in form of low control authority against angular motion. The simulated mechanism only produced borderline sufficient torque to arrest the angular velocities and this tendency proved not easily counterable even in the idealized setting. This is likely a combination of deficiency in the fairly simple control strategy that was developed for this demonstration, as well as an inherent problem of the geometry found in section 7.1. The latter arising from erroneous simplifying assumptions during the geometry discovery which treated loading conditions in isolation. This is an important area to revise in the future. This major flaw aside, the docking concept performed sufficiently and without observed loads that would fail a sanity check.

7.6.1. Functionality

To aid as a visual reference for the rest of this discussion, sequences of images from the Simulink simulation are provided in figures 7.10 and 7.11. Figure 7.10 provides a wider view tracking both spacecraft, whereas figure 7.11 focuses on the capture platform. The side views demonstrate six key events in the sequence. The first is the initial condition, followed by the pre-positioning of the capture structure once an impact point has been estimated. Third shows the moment the capture rings make contact, and the forth is the position at which relative motion has been arrested. The fifth demonstrates the temporary realignment position before parking. And the sixth finally shows the final parking position where the entire structure is positioned within reach of the inner elements.

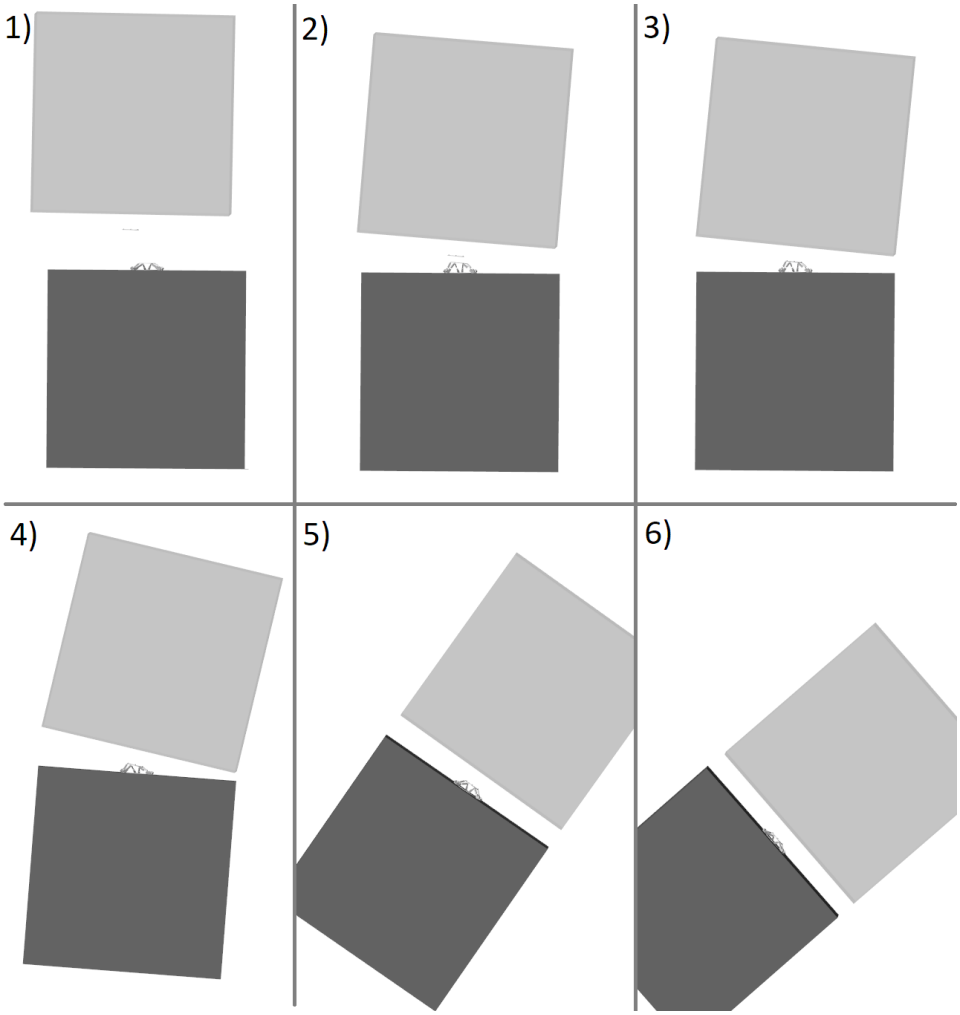

Figure 7.10: Wide view of the capture sequence.

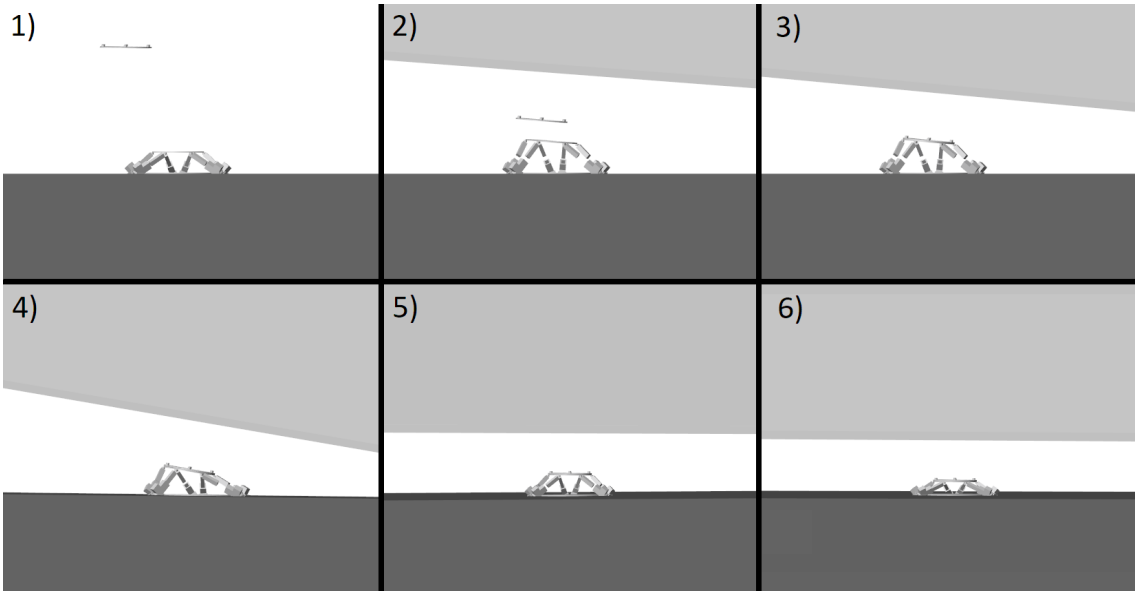

Figure 7.11: Close-up view of the capture platform during the sequence.

Figure 7.12 shows the relative linear motion of the target spacecraft. At $t \approx 5s$ contact is made with the other spacecraft at approximately 14cm distance from the base of the capture platform. As can be seen from Figure 7.12a and Figure 7.12b the linear velocities are quickly reduced from the initial values of 100mm/s axial and 50mm/s lateral. Likewise, from Figure 7.13a and Figure 7.13b show that the angular alignment was also achieved. At $t \approx 40s$ when the retraction to connect the inner interfaces begins, the two spacecraft are aligned well within the required 5mm and 1°, and the interface can still assist the final mating.

The proposed simple control system implemented to enable these simulations also proved capable of handling the highly deformable structure by steering a virtual neutral point of the structure. A sufficient degree of dynamic damping was achieved while still allowing the independent actuators to act as springs, and with no force feedback. To illustrate, Figure 7.14 shows the commanded actuator extension and the actual extension for one of the actuators.

Despite the success, the current arrangement struggled to arrest angular motions, as can be seen from Figure 7.13a and Figure 7.13b. This was further worsened by the fact that the initial lateral deceleration imparts a large amount of additional angular momentum, increasing the initial roll rate from $1°/s$ up to $1.4°/s$. Due to the flexible spring-like nature of this conceptual arrangement, the mechanism's efforts to produce angular deceleration likewise resulted in additional unwanted lateral deflection as can be seen in Figure 7.12a between 5s and 10s. While this 0th iteration of the control system can in fact handle the deformable structure and achieve the needed damping properties in the concept, it is clear that the independent handling of linear and angular damping is a major weakness. The control strategy would have to be improved to proactively include resistance against unwanted motions. Currently, the degrees of freedom that are close to their desired position exhibit near zero stiffness.

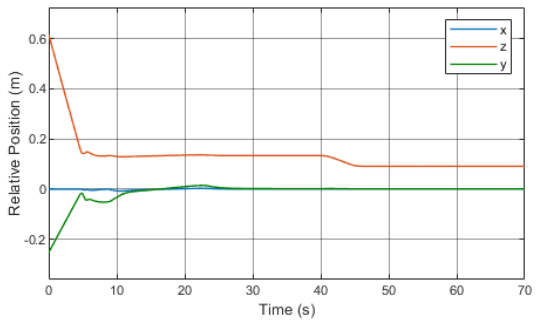

(a) Relative position

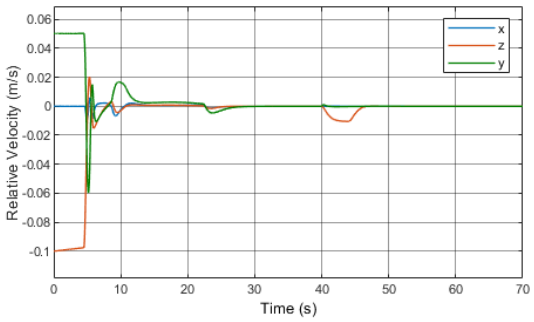

(b) Relative velocity

Figure 7.12: Linear motion of the target's capture ring relative to the base of the capture platform

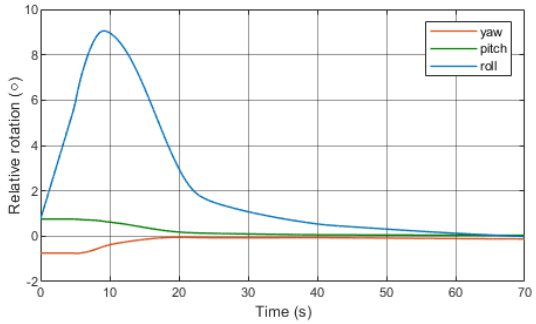

(a) Relative angles

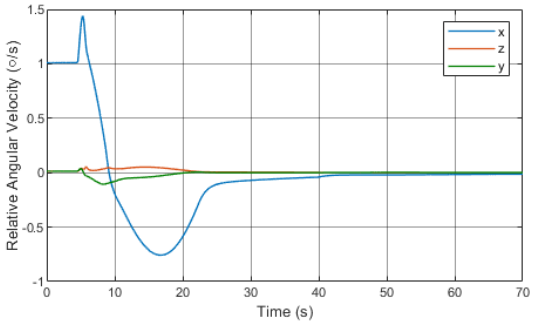

(b) Relative angular velocity

Figure 7.13: Angular motion of the target's capture ring relative to the base of the capture platform

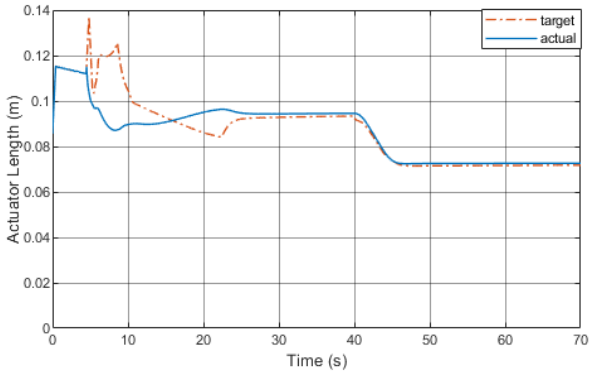

Figure 7.14: Commanded position vs. actual position

7.6.2. Estimated component loads

The final point of the discussion are the loads on the components. The areas of interest here are the actuators and the restraining joint between the two capture rings in particular.

The forces exerted by the actuators during the simulated docking sequence are shown in Figure 7.15. The distinct phases of the sequence can be clearly seen from the actuator force graphs. Once the contact is made at $t \approx 5s$, the system aggressively counteracts linear and angular motion until around 10s. It can also be seen that the previously discussed shortcomings of the control strategy are clearly visible in this graph, especially just after contact where linear damping effectively overpowers the angular and all actuators attempt to extend. This leads to the required actuation force being driven by the initial damping. As mentioned earlier, these results are to be considered with caution and large margins due to the highly idealised simulation. It can be seen in the figure that the peak pushing force reached by an actuator was 422N and peak retractive force was 368N, and similar levels of force are maintained for a prolonged duration.

In similar scenarios likewise similar peak forces in 300-400N range were observed depending on the approach. However, these rough estimates are rounded up to avoid introducing false confidence in the results by means of excess significant figures. Based on the simulated scenarios, the expected minimum force requirement from the actuators is suggested as $\approx 500N$.

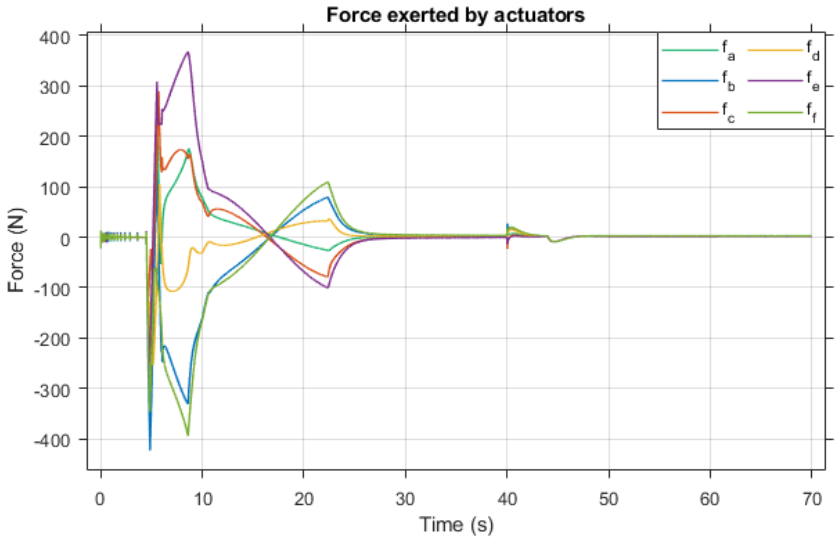

Figure 7.15: Linear forces provided by the actuators

The requirements for a the restraining mechanism for use in such configuration were also approximately identified. First, due to the achieved pre-positioning of the capture ring, the alignment error of the capture ring that was observed in the simulations was small. Any future conceptual solution for the restraining mechanism can safely assume that only a small misalignment tolerance would be required. The positioning error expected is on the order of the accuracy of the tracking data.

The restraint force requirements could be defined in more detail. Figures 7.16a and 7.16b show the restraining torque and force as measured by the idealised joint emulating a restraint mechanism between the two capture rings. In this specific simulation, the peak values reached 47Nm, 960N of axial force and 556N in lateral loads. Depending on the approach conditions the axial directions and the specific values changed, but the general magnitude remained the same. The compressive axial forces could perhaps be isolated separately as they were reliably observed to be approximately twice that of the axial tension, or the lateral. The result is not surprising, as the maximum axial approach velocity is twice that of the lateral, and the deceleration time is roughly identical as the current control scheme damps the total velocity vector, not the individual components in isolation.

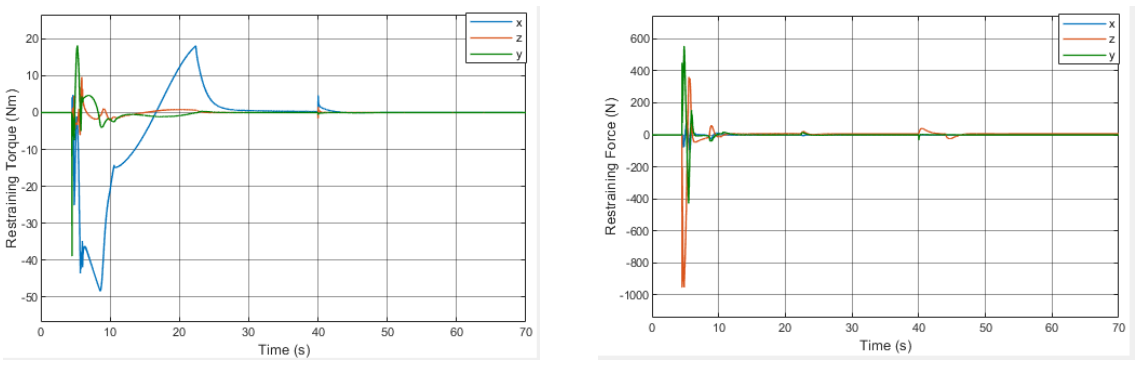

(a) Restraining torque

(b) Restraining force

Figure 7.16: Restraining loads

Once again caution is required in interpreting this data. The immediate results should by no means be considered a direct specification due to the accuracy of the simulations. However, these results

do suggest a set of characteristics of the restraining mechanism that future work could consider as an initial design target. Once combined with previous findings, any concept for the mechanism should posses the following characteristics:

- Ability to support order of $\sim 1e2Nm$ of restraining torque along any axis
- Ability to support order of $\sim 1e3N$ of restraining force laterally or in axial tension, twice that in axial compression
- Small misalignment tolerance (likely $< 10mm, < 1°$)
- Life cycle count of >1000
- Dual redundant in release
- No active elements on the target

7.7. Sanity Check of the Back-drivable Actuator

Based on the loads observed during simulations it was suggested that at the very least the actuators would have to achieve $\sim 70mm/s$ of extension speed and be capable of $\sim 500N$ of actuation force while being smoothly back-drivable. The feasibility of these parameters warrants a sanity check before any further time investment into the development of such an actuator. In essence, what are plausible sizes for the ball-screw and the motor, and whether or not these components would be of suitable scale as to not kill off the concept. Two aspects are considered here: the availability of a suitable ball-screw and availability of a brushless motor that could drive it in a direct fashion without relying on a multistage gearbox. An example of ball-screw suitable for vacuum applications and rated for sufficient load capacity was found to be available commercially at a suitable size. The particular component is listed as a custom option from NSK catalog No.1258[1]. The vacuum suitable version uses solid lubrication and would achieve sufficient lifetime. The smallest offered solid lubricated screw has a shaft diameter of 10mm, nut diameter of 22mm and a dynamic load rating of 1210N, which is considerably higher than required. This component should not present a limitation.

Based on the ballscrew specifications, a approximation for a matching motor could be BL17E19 from Lin Engineering [2]. The motor likewise is offered in vacuum compatible option and if paired with $\approx$ 1:3 gear reduction could provide sufficient travel speed and actuation force.

As part of this sanity check the two components were packaged in a mock-up actuator that would allow the required travel range, at least in terms of respecting the basic geometric constraints of the components.

The in-CAD mockup of the conceptual platform utilizing the estimated actuator is shown in figure 7.17. The mocked-up actuator was found to be well within reason of what could be expected to package into such design, under the assumption that it represents at least roughly correct dimensions. A later design deviating from this size to an extent extreme enough to warrant unsuitability (i.e. doubling) is unlikely however, as the screw and the motor are the largest elements.

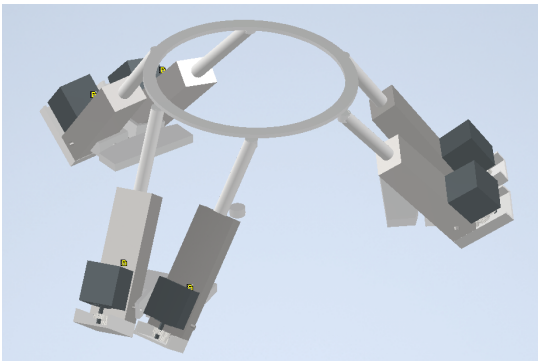

Figure 7.17: Linear forces provided by the actuators

[1] https://www.nsk.com/products/precisionmachine/ballscrew/

[2] https://www.linengineering.com/products/brushless-motors/standard-bldc-motors/bl17-series/bl17e19-02/BL17E19-02

7.8. Chapter Conclusions

The work presented in this chapter verified that the proposed conceptual solution of a capture mechanism based on backdrivable stewart platform could in fact be a feasible solution. The critical areas of uncertainty of this concept of achieving suitable actuation and minimisation were demonstrated to be within the realm of possibility by directly simulating an idealised worst case scenario. Aside from emulating a restraint mechanism via a locking joint, the rest of the mechanism was simulated more directly.

A simulated platform mechanism was constructed and a demonstrator control system was created to manage it. One of the considerations for this concept was the control of the platform that no longer had positioning guarantees due to backdrivability of the actuators. The devised strategy successfully achieved sufficient levels of damping and positional control by means of steering a virtual neutral position of the structure, while the actuators operated independently and as pure springs of configurable stiffness. This verified that, as was earlier proposed, such a conceptual mechanism could in fact be used to smoothly dampen impact by allowing backdrivable actuators to passively yield and without any need of force feedback.

While this model design did overall perform sufficiently, an immediate weaknesses was observed. The mechanism had worryingly low control authority against angular motion, especially when compared to the relatively excellent linear behavior. In this specific example the shortcoming could be easily blamed on the choice of the actuator geometry and the fairly simple control scheme. However, this still provides valuable knowledge that this is an area of the design that needs warrants additional scrutiny by any future work.

Additionally, the simulations were also used to provide rough estimates for the performance requirements of the actuator. It is suggested that the backdrivable actuator should be capable of at least $\approx 70mm/s$ of extension speed and $\approx 500N$ of extension force as a minimum target. Such parameters were also found to be likely achievable in an actuator of a size that would not pose an integration challenge, at least in this demonstrator design.

Although this work failed in directly implementing and simulating a restraining mechanism, approximate design targets for it were estimated that could serve as a rough starting point for future work.

Overall, the proposed conceptual solution was found to be feasible, assuming the same holds for the restraining mechanism. Additionally, the key expectations upon which the suitability of this concept was proposed have been demonstrated. These include the actuation capabilities allowing to smoothly intercept the target and suitably position it for the inner elements, expected scalability to the required size, and the avoidance of shock loads during impact.

8

Design Summary

This chapter summarizes the early design of the refuelling interface. First, section 8.1 explains the reasoning behind mass estimates for the otherwise incomplete system. Following section 8.2 describes the parameters of this specific design which could serve as an early approximation of the system's size, mass and capabilities. Third section 8.3 highlights critical omissions and simplifications made in this proof of concept and considers the validity of the results. Finally, section 8.4 talks about general observations and learnings from this initial implementation.

8.1. Mass Approximations

The major actuated components of the concept along with those for the fluid transfer have been estimated in previous chapters. The proof of concept design can thus provide verifiable approximate size bounds for such a device but estimation of the mass is a separate challenge. Aside from those of the major components, the masses of internal details are not known. As such, the design is not sufficiently developed to provide precise estimates for the exact size of mass of the device but the minimum bounds can be established with some degree of confidence. These can be used to provide at least an educated guess at a target for the upper bounds of the complete design.

Currently, the inner active element stands at a mass of 1.1kg that is largely dominated by the fluid transfer components and the actuated latch mechanism. With the exception of the housing, the missing details are relatively minor in comparison: connection pins, electrical wiring, etc. To an extent, the simplified design also includes material that would be displaced by such features. As a possible reference, the SIROM interface is of comparable size and has an all-up weight of 1.45kg[64]. The specifics of its internal construction are not known, but as an extreme exaggeration one could assume that nearly all of its mass arises from the housing or other components that are not yet included in this design. In this case, the overall active inner element should be implementable within $\approx$2.5kg of total mass.

The passive side of the interface currently stands at 716g (in low-flow configuration), more than half of which is dominated by the mass of the valves. The dimensions of the capture ring are defined by clearance around the inner element, and the current structure can at the very least tolerate the previously predicted docking loads if they are applied in an idealised fashion (i.e. distributed along the contact surface). As such, extremely dramatic growth of this element is not expected. It could likewise target a mass budget of $\approx$2kg.

Finally, the outer capture element. The mass of the current approximate design stands at 4.3kg which is nearly fully concentrated in the actuators. The restraint mechanism of the active capture platform was not sufficiently developed to present it with any significant certainty. Therefore it is not included in the model, however each of the hook elements are unlikely to be excessively massive. Comparable force capacity has been achieved by the inner element already and the expected possible use of hooks instead of latches would also drastically reduce the overall mass of the mechanism. As a very cautious bound, the platform should be implementable within 10kg of mass budget, although it is likely to be much lower. Even if there is a significant increase it is unlikely to present drastic challenges to spacecraft integration. The considered spacecraft mass ranges are 1-10t, and the current ($\approx$ 10kg) capture platform was shown to have the expected capacity for the largest spacecraft. The actuators

could be drastically scaled down for the lighter spacecraft but even this cautious bound for the element only represents 1% of the smallest spacecraft mass. Even fairly drastic misprediction of this device's mass (i.e. doubling) would likely be absorbed within by the margins applied to the design of spacecraft.

8.2. Approximate Specifications

This section summarizes the findings of this work in a form that presents the current three elements as an approximate specification. This is meant to serve as a concise summary of the concept based on what functionality has been achieved or otherwise expected from further developments. These approximate specifications are meant to serve as a reference for initial concepts of the spacecraft that would form the HTP space depot systems, allowing to refine the concept.

First, the passive client interface. For visual reference, the current design is shown in figure 8.1. This element is thus expected to have following characteristics:

- Entirely passive mechanically
- Expected mass <2kg
- Expected footprint ∼25cm diameter (excluding clearance zones)
- Supports direct docking by suitable vehicles
- Suitable up to 100g/s of HTP transfer
- Redundant against leaking

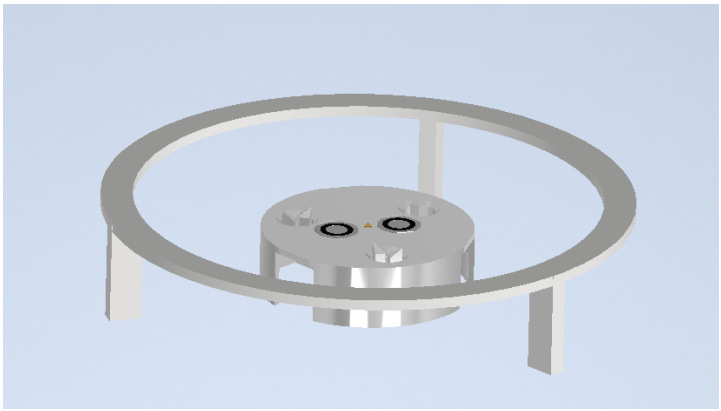

Figure 8.1: Passive universal client interface

Second, the active inner element of the servicer interface shown in figure 8.2.

- Expected complete mass <2.5kg
- Footprint diameter ∼15cm
- Positioning tolerance +-4mm, » 1°(any axis)
- Does not require external assistance to connect
- No power required to hold connection
- Damage tolerant for release
- Redundant against leaking
- Alignment enforced before connectors make contact (easy to expand)
- Lifetime >1000 cycles, 15years

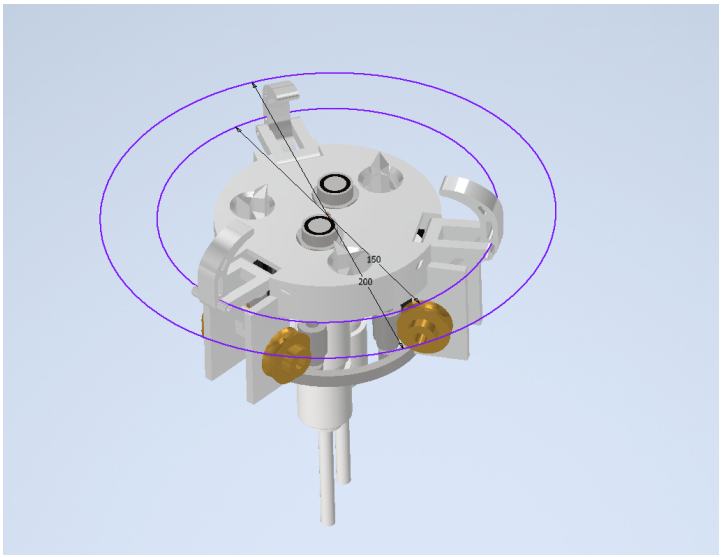

Figure 8.2: Active side inner element

Finally, the outer capture element. Shown in figure 8.3 together with the other elements. This element is expected to be:

- Entirely optional if servicer has other means to introduce the inner element to the client
- Expected mass <10kg
- Expected footprint ∼60cm diameter
- Allows soft (zero relative velocity) capture within a +-5cm, 5°window
- Can impart initial separation velocity
- Suitable for spacecraft 1-10t in mass, no shock loads
- Maximum impact velocities up to 5cm/s lateral, 10cm/s axial, 1°/s angular
- Lifetime >1000 capture/release cycles

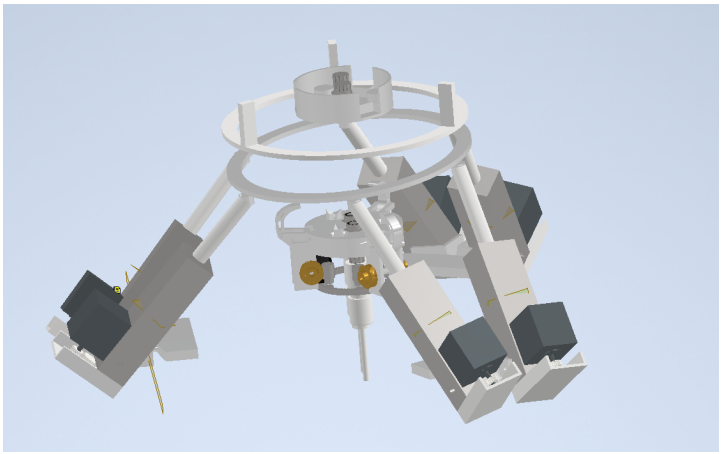

Figure 8.3: Full (direct shuttle) configuration

8.3. Design Omissions and Validity

These designs are by no means complete, lacking significant detail. The implementations only have sufficient detail to verify that the expected required functionality could realistically be achieved. The restraining mechanism for the capture platform is a large omission that has already been discussed. Following are other major areas that are likewise incomplete and must be paid future attention.

First and foremost, due to time constraints this work only investigated a subset of all components of the system for lifetime and load capacity. These were mostly the active components that presented an obvious opportunity for sizing concerns that could conflict with dimensions required for functionality. The latch mechanism, its geared drive and the platform actuators are the major examples that were investigated. Detailed sizing of other details like linkage pins, bearings, and especially the housings was not performed. This is the primary reason why the resultant proof of concept is considered a verification rather a validation of the solution. There are simply too many details omitted to draw concrete conclusions on true validity of the design. However, the work performed here at the very least demonstrated that further interest is at least warranted as there were no 'hard' limitations observed. Additionally, the knowledge of at least the approximate scale and arrangement of the device makes the more detailed investigations much more tractable in the future.

Second, some important secondary functionality was likewise simplified out to demonstrate the core working principles. A solution for covering the connectors when the inner element is not in use is one of such omissions. It is important to shield the connectors from UV radiation and space dust as these effects are particularly dangerous to seals[82]. Some experimentation with designs using various approaches like sliding or rotating doors, or an iris were attempted, both in passive and active forms. However, their feasibility was found excessively dependent on the geometry and arrangement of the connectors, which is not yet known, and as such they were not featured in the report. The construction of the liquid couplers will likely define the required solution to this problem in the future, or perhaps even manage to incorporate one directly into the connectors. In any case, this is an outstanding problem that will have to be reconsidered once a specific selection of connectors is known.

Third, the estimated lifetime is only based on generalised endurance of materials and coatings. A particularly key area to investigate in the future is more localised wear. Throughout this work it has been assumed that moving and sliding components will utilize solid lubricant coatings. These are expected to last sufficiently as there are no high speed mechanisms (i.e. reaction wheels). However, this is a critical assumption to validate as friction was found to be a critical parameter in the inner element. The probable localized wear on the alignment structures is cause for concern in particular. These structures are expected to experience point-like contact and must not exceed a certain threshold of friction to function. This can be accounted for in the geometry but the lifetime must still be validated. Another similar area is the over time damage to the surface of these structures itself, such as surface denting. The geometry of the surfaces is critical in driving the alignment but it is not known how much damage they can tolerate before loss of function. The 3D printed model was not smoothed, yet functioned correctly despite these surfaces being fairly rough and step-like from the print layers. This suggests the sensitivity is not extreme but otherwise remains unknown.

Answering these gaps in knowledge would require far more detailed iterations of the concept which are simply intractable within the timescale of this work. However, the successful partial verification increases confidence that the proposed concept is a plausible candidate to pursue. Future development is required before confident claims of validity could be made.

Ultimately the validity of the demonstrated concept and the approximations thereafter also hinge on the accuracy of the expected required functionality. As only partial analogs to the HTP depot concept were discovered, the requirements for the refuelling interface are likewise a rough estimate. As a form of validation, the produced approximate design could be utilized to construct an initial design of the HTP depot system and confirm that the offered set of capabilities is sufficient to enable such spacecraft. This was not tackled here because designs of other underlying systems of such spacecraft (i.e. the HTP storage system) were in progress and not yet defined. With these predictions available, future work could aim to close this iteration loop.

8.4. Observations for Future Iterations

8.4.1. Chain of dependency

The liquid connector was the critical component that defined most of the dimensions of the system, although not by its physical dimensions alone. It was primarily the required insertion distance that dictated the geometry of the alignment structures and the latching mechanism, and resulted in an indirect form of scaling. The required purely vertical travel range in particular affected the compactness of the linkage, which lead to the overall dimensions of the inner element in this design, which were then followed by the outer element.

Nearly all the dimensions of the proof of concept design can be traced back to the assumed representative stand-in for a liquid connector that is yet to be developed. This results in the entirety of the rest of the predictions hinging on this sole assumption. As such, this is by far the critical component to establish before any future work could proceed on a reliable foundation. It is therefore strongly recommended that the development of a suitable liquid coupler should be the immediate interest of any future work regarding this concept. At the very least knowledge of bounds on key parameters of insertion distance and preload force are required. The arrangement is much less sensitive to the overall physical dimensions of the connectors as neither the alignment structures nor the latch mechanism require precise placement.

Assuming the specific connector is known, the development of the inner and outer elements could be done largely in parallel. The outer element only requires knowledge of an approximate size of the inner one to determine the minimum possible size of the capture ring to avoid interference. After that, the outer element is free to scale up and outwards as necessary.

8.4.2. Linkage generation

The created the proof of concept design of the linkage, while sufficiently functional, had flaws that required later fix-up and can be traced to the initial technique used to generate the geometry. A series of improvements can be immediately suggested that should lead to more accurate results.

First, the generation code must respect the fact that linkage elements have thickness and the contact point may not coincide with a given vertex. At the very least, this must not be ignored for the extended link that forms the clamp finger. In the proof of concept design the failure to account for this fact lead to a reduction in the acceptance window.

Second, the linkage generation should be made aware of at least approximate sizing of related elements. An issue that was found during implementation of the linkage was that the driven link was too short to accommodate an integrated gear, which would have greatly simplified packaging. The links also caused minor clearance problems once thickened sufficiently to house a suitably strong shaft. The current implementation of the linkage generator could be extended to calculate static loads in the linkage. Doing so would provide means to incorporate at least approximations of required driving gear size and the pivot joints, allowing to constrain optimization to avoid these problems.

Third, the current design of the mechanism could be easily shielded from external particles by extending the housing such that only the latches are exposed. This is, admittedly, largely by chance. Future iterations have to bring this into consideration at earlier stages. Especially the triplet of the driving gear, the driven link and the environmental shielding options should not be treated in isolation. For example, if the driven link is optimised to use only a single gear, a mid-plane placement of it would be convenient. This, however, would dramatically complicate environmental protection of the drive train from particles.

9

Summary and Conclusions

9.1. Conclusions

This work successfully answered the need of a refuelling interface concept suitable for long life HTP refuelling system. Starting from a blank slate, the goal was to discover a possible solution for this need and to identify possible limiting factors. To achieve this goal, the functionality required from such a conceptual device was identified, followed by construction of a conceptual solution. The proposed solution was partially implemented and studied in proof of concept simulations to verify its feasibility. A limiting factor was found in the lack of a quick-connect fluid coupler that is both suitably HTP compatible and of sufficient endurance. The rest of the mechanical concept did not present immediate limiting factors. It successfully achieved the required functionality in simulations and the critical components were found to be possible to construct.

Until the long-life depot concept is sufficiently developed to provide concrete requirements, a cautious predicted set of capabilities was established based on existing literature. Conceptually, such an interface should target 15 years of lifetime and 1000 servicing cycles, and the interface should be suitable for both robotic manipulators or for directly docking by shuttle spacecraft. This cross-compatibility between the servicing models must be achieved by a universal client-side interface that is of low complexity and mass. Approximate upper bounds for the related performance specifications were also established.

A mechanical concept for the interface was proposed as consisting of two independent elements positioned concentrically. A small, latch-based inner element suitable for manipulator use, and an optional outer element based on a Stewart platform to facilitate direct docking in shuttle applications. These elements are easily scalable, were already used successfully in other applications, and the outer element could be entirely eliminated on manipulator based deployments. By partial implementation this mechanical concept was demonstrated to be implementable to satisfy the estimated required functionality, and in a relatively compact scale not infeasible to integrate into spacecraft of expected mass.

The most immediate limitation has been identified to be the availability of a sufficiently robust, quick-insert fluid coupler that is of aluminium construction to achieve the required lifetime. This is a critical challenge to address before future iterations on the refuelling interface are performed.

9.2. Research Questions

This section concludes on the answers found to the research questions raised at the start of this research.

9.2.1. What is the required functionality?

The capability scope of the refuelling interface device was found to be that consisting of the means to capture, arrest and connect the spacecraft for fluid transfer. There was no immediate reason found to consider additional functionality, such as the guidance or proximity tracking systems. These elements are generically shared between any servicing operations and already have suitable existing solutions that are largely standalone.

A possible set of early requirements for such a device was successfully proposed in section 3.8. The most particular features that would make a refuelling interface suitable for a long-life servicing application were found to be a lifetime of at least 15 years, and cross-compatibility for direct docking and manipulator access on the same client. The device must also not rely on external forces or impacts to achieve the connection.

The approximate upper bounds of expected mechanical performance requirements were successfully defined. The device is expected to require 5mm and 1°of positioning tolerance when accessed by manipulators. For direct docking, it should offer a zero force capture window of at least 50mm and 5°. As a limit case, an impact between spacecraft of 10 tons of mass up to 100mm/s axial and 50mm/s lateral velocity should be safely handled.

Regarding the fluid transfer capabilities, it was found that the interface must contain at least two fluid transfer lines that are highly compatible with HTP. As an initial target, these lines should be capable of operating at up to 20bar of pressure and be capable of up to 100g/s of flowrate.

9.2.2. How could such an interface be implemented?

This question was answered by proposing conceptual solutions to the fluid transfer lines and the interface mechanism, and verifying they are feasible ideas to implement.

The expected features for fluid transfer lines could be implemented if each side of the interface includes a quick-connect fluid coupler, a control valve, a relief valve and a pressure sensor. In order to achieve the required 15 years of lifetime, a fully aluminium construction of these components was found required. No suitably robust aluminium construction fluid coupler was discovered and this component thus represents a critical limiting factor for the concept and needs to be developed. Aluminium fill-drain valves were found to exist so this is likely feasible. It is suggested that such coupler could perhaps be constructed similarly to a discovered industrial automation part which satisfies all the expected requirements aside the construction materials. This discovered part is already highly HTP compatible but still insufficient for full 15 years of lifetime.

It is proposed that a two-element design for the interface is a suitable mechanical concept. Consisting of a latch-based 'inner' element and an 'outer' hexapod docking mechanism, this arrangement directly achieves the anticipated required features. In addition, these elements are inherently robust, and offer high potential for scalability and adaptability which is preferable given the early stages of the concept.

By partially implementing the mechanical concept it was demonstrated that such arrangement could in fact satisfy the required functionality and uphold the assumptions upon which it was proposed. The device functioned sufficiently in dynamic simulations, and the scale of the proposed concept was not found limited by feasibility of the critical components.

Based on the partial proof of concept design, generous upper bounds for the mass and volume such a device were predicted. Depending on the targeted flowrate, the client side passive interface could target a footprint of $\sim$250mm and $\sim$1-2kg of mass. The inner active element can expect a foot print of $\sim$150mm and achieve mass of $<$2-3kg. The capture platform is likely achievable <10kg and would require $\sim$ 650mm of footprint. Overall the proposed concept of the refuelling can achieve the required functionality in a scale and mass that are not excessive.

9.3. Achieved Goals

This work achieved the primary goal of producing a '0th' iteration of a refuelling interface suited for the long-life HTP depot concept. This provides a starting point for future considerations by providing a concrete, albeit approximate, design for such device. Having a specific set of capabilities attached to a specific design allows to begin making trade-offs and iterations. This design is unlikely to prove an optimal solution, however it proves a sufficient solution is achievable.

The identification of the need for an aluminium quick-connect fluid coupler is also a highly valuable result. Especially when combined with the gained experience on how heavily the specifics of the chosen connector affect the rest of the design. This provides clear direction for any future efforts; this is the challenge that must be addressed first. If the assumption that a restraint mechanism for the capture platform is in fact feasible holds, the rest of the interface design was not found to raise an immediate concern that would prevent iteration.

The design approach and techniques used to produce the initial proof of concept design succeeded

in yielding a sufficient design and could be reused in the future. Numerous areas of improvements for the tools utilized were proposed but the fundamental approach proved successful.

9.4. Future Work and Recommendations

Although continued work in refining the proof of concept by implementation of the missing details is an obvious possibility, it is suggested that this is not the best course of action. Based on the experience gained from this initial design, there are outstanding questions that would be wise to address beforehand.

First and foremost, a critical area to address is the development of a suitable fluid coupler. It is known with certainty that it must feature aluminium and PTFE construction, be suited for quick automated connection, and offer extended life cycle count. The specifics of it will heavily influence the design and thus have to be known to proceed with the concept.

Next, before proceeding with further iterations, the requirements for the interface system should be refined by targeting a specific mission. The current set of estimated requirements was proposed to be widely applicable and not discriminate between conceptual strategies of providing space refueling services found in literature. Future work should investigate the specifics of the depot-based refuelling ecosystem, especially the expected interactions between spacecraft. What would be the strategy of delivery, how many types of servicing vehicles would be deployed, what is the expected cooperation level of the clients; these are all open questions that have potential to significantly redefine the requirements. Of particular interest are more confident estimates of required transfer rate and docking capabilities.

A separate investigation focused on the refining the outer element is also a possible in parallel to the investigations above. The assumption that a restraint mechanism for the capture ring is in fact achievable within the assumed size is likely true as this problem lends itself well to the use of hook-based solutions. However this has not been directly demonstrated so far. A focused effort on this single subsystem could implement the concept in greater detail and thus greatly increase the confidence level in the solution. As the outer element is intentionally independent from the inner, this allows largely independent investigations.

Another open question also remains regarding the environmental protection of the couplers. This is a key area to address in the inner element but the solutions experimented with in this work were extremely dependent on the specifics of said couplers. As such, this problem is better postponed until a specific coupler design is available but must be addressed early in subsequent revisions of the inner element. Depending on the geometry of produced couplers, achieving the environmental shielding may require abandoning the passive align-insert behaviour and utilize extendable connectors as seen in other existing designs.

References

[1] John Whitehead, Michael Dittman, and Arno Ledebuhr. “Progress toward hydrogen peroxide micropropulsion”. In: (1999).

[2] John C. Whitehead. “Hydrogen peroxide propulsion for smaller satellites (SSC98-VIII-1)”. In: *12th Annual American Institute of Aeronautics and Astronautics/Utah State University Conference on Small Satellite*. July 1998. URL: https://www.osti.gov/biblio/3450.

[3] Botchu Vara Jyoti et al. “Hypergolicity and ignition delay study of gelled ethanolamine fuel”. In: *Combustion and Flame* 183 (2017), pp. 102–112. DOI: 10.1016/j.combustflame.2017.05.007.

[4] Andrew M. Long, Matthew G. Richards, and Daniel E. Hastings. “On-orbit servicing: A new value proposition for satellite design and Operation”. In: *Journal of Spacecraft and Rockets* 44.4 (2007), pp. 964–976. DOI: 10.2514/1.27117.

[5] Lindström Gustav. “The galileo satellite system and its security implications”. In: *European Union Institute for Security Studies: Occasional Papers* 44 (2003).

[6] Stephen Jacklin. *Small-Satellite Mission Failure Rates*. Tech. rep. NASA Ames Research Center, 2019.

[7] David Akin and Brook Sullivan. “A survey of serviceable spacecraft failures”. In: *AIAA Space 2001 Conference and Exposition*. 2001, p. 4540.

[8] H. C. Koons et al. “The Impact of the Space Environment on Space Systems”. In: *Proceedings of the 6th Spacecraft Charging Conference. November 2-6, 1998.* Pp. 7–11.

[9] Donald Kessler et al. “The Kessler Syndrome: Implications to Future Space operations”. In: *Advances in the Astronautical Sciences* 137 (Jan. 2010).

[10] Brook Rowland Sullivan. “Technical and economic feasibility of Telerobotic on-orbit satellite servicing”. PhD thesis. Digital Repository at the University of Maryland, 2005.

[11] Nicholas M. Jedrich et al. “Cryogenic cooling system for restoring IR science on the Hubble Space Telescope”. In: *SPIE Proceedings* (2003). DOI: 10.1117/12.461805.

[12] Daniel E. Hastings and Carole Joppin. “On-orbit upgrade and repair: The Hubble Space Telescope Example”. In: *Journal of Spacecraft and Rockets* 43.3 (2006), pp. 614–625. DOI: 10.2514/1.15496.

[13] Karl Hille. *The hubble story*. Sept. 2018. URL: https://www.nasa.gov/content/about-the-hubble-story (visited on 01/2023).

[14] Bryan L. Benedict. “Rationale for need of in-orbit servicing capabilities for Geo Spacecraft”. In: *AIAA SPACE 2013 Conference and Exposition* (2013). DOI: 10.2514/6.2013-5444.

[15] Joshua P Davis, John P Mayberry, and Jay P Penn. “On-orbit servicing: Inspection repair refuel upgrade and assembly of satellites in space”. In: *The Aerospace Corporation, report* (2019).

[16] Ronald L Ticker, Frank Cepollina, and Benjamin B Reed. “NASA’s in-space robotic servicing”. In: *AIAA Space 2015 Conference and Exposition*. 2015, p. 4644.

[17] Nicholas Cohen et al. “Extending Satellite Lifetimes in Geosynchronous Orbit with Servicing”. In: *AIAA SPACE 2011 Conference & Exposition*. 2011, p. 7302.

[18] Alex Ellery, Joerg Kreisel, and Bernd Sommer. “The case for robotic on-orbit servicing of spacecraft: Spacecraft reliability is a myth”. In: *Acta Astronautica* 63.5-6 (2008), pp. 632–648.

[19] David A Whelan et al. “DARPA Orbital Express program: Effecting a revolution in space-based systems”. In: *Small Payloads in Space*. Vol. 4136. SPIE. 2000, pp. 48–56.

[20] David A Barnhart and Rahul Rughani. “On-orbit servicing ontology applied to recommended standards for satellites in earth orbit”. In: *Journal of Space Safety Engineering* 7.1 (2020), pp. 83–98.

[21] The Orbital Index. *Issue no. 124*. July 2021. URL: https://orbitalindex.com/archive/2021-07-07-Issue-124/ (visited on 01/2023).

[22] Jeff Foust. *Orbit Fab demonstrates satellite refueling technology on ISS*. June 2019. URL: https://spacenews.com/orbit-fab-demonstrates-satellite-refueling-technology-on-iss/ (visited on 01/2023).

[23] Sandra Erwin. *Orbit Fab to launch propellant tanker to fuel satellites in geostationary orbit*. Sept. 2021. URL: https://spacenews.com/orbit-fab-to-launch-propellant-tanker-to-fuel-satellites-in-geostationary-orbit/ (visited on 01/2023).

[24] Orbit Fab. *Orbit Fab to publish Satellite refueling interface designs*. Oct. 2021. URL: https://www.prnewswire.com/news-releases/orbit-fab-to-publish-satellite-refueling-interface-designs-301392335.html (visited on 01/2023).

[25] *Lockheed Martin Linuss™ small satellites ready for 2021 launch*. URL: https://news.lockheedmartin.com/linuss-small-sats-mission (visited on 01/2023).

[26] Avni Shah. *USC launches its 3rd Satellite into Space - USC Viterbi: School of Engineering*. Jan. 2022. URL: https://viterbischool.usc.edu/news/2022/01/usc-launches-its-3rd-satellite-into-space/ (visited on 01/2023).

[27] *Satellite Solutions*. Jan. 2022. URL: https://lockheedmartin.com/en-us/products/satellite.html (visited on 01/2023).

[28] *Refueling satellites in space*. Sept. 2021. URL: https://www.lockheedmartin.com/en-us/news/features/2021/refueling-satellites-in-space.html (visited on 01/2023).

[29] *Northrop Grumman and Intelsat make history with docking of second mission extension vehicle to extend life of satellite*. URL: https://news.northropgrumman.com/news/releases/northrop-grumman-and-intelsat-make-history-with-docking-of-second-mission-extension-vehicle-to-extend-life-of-satellite (visited on 01/2023).

[30] *Mission extension vehicle: Breathing life back into in-orbit satellites*. URL: https://news.northropgrumman.com/news/features/mission-extension-vehicle-breathing-life-back-into-in-orbit-satellites (visited on 01/2023).

[31] Chelsea Gohd. *A Northrop Grumman Robot successfully docked to a satellite to extend its life*. Apr. 2021. URL: https://www.space.com/northrop-grumman-mev-2-docks-intelsat-satellite (visited on 01/2023).

[32] Astroscale US. URL: https://astroscale-us.com/wp-content/uploads/2021/09/LEXI-Fact-Sheet_September-21.pdf (visited on 01/2023).

[33] *Astroscale U.S. and Orbit Fab Sign First on-orbit satellite fuel sale agreement*. Jan. 2022. URL: https://astroscale.com/astroscale-u-s-and-orbit-fab-sign-first-on-orbit-satellite-fuel-sale-agreement/ (visited on 01/2023).

[34] V Dubanchet et al. “EROSS project–European Autonomous Robotic Vehicle for on-orbit servicing”. In: *International Symposium on Artificial Intelligence, Robotics and Automation in Space,(i-SAIRAS'20). USA: Pasadena, California*. 2020.

[35] *One more step*. URL: https://archive.ph/20120524111321/http://www.spacenews.com/satellite_telecom/intelsat-signs-for-satellite-refueling-service.html (visited on 01/2023).

[36] *DARPA Selects SSL as Commercial Partner for Revolutionary Goal of Servicing Satellites in GEO*. Sept. 2017. URL: https://www.darpa.mil/news-events/2017-02-09 (visited on 01/2023).

[37] Sandra Erwin. *Maxar's exit from DARPA satellite servicing program a cautionary tale*. Feb. 2019. URL: https://spacenews.com/maxars-exit-from-darpa-satellite-servicing-program-a-cautionary-tale/ (visited on 01/2023).

[38] *Northrop Grumman's wholly owned subsidiary, SpaceLogistics, selected by DARPA as commercial partner for Robotic Servicing Mission*. URL: https://news.northropgrumman.com/news/releases/northrop-grummans-wholly-owned-subsidiary-spacelogistics-selected-by-darpa-as-commercial-partner-for-robotic-servicing-mission (visited on 01/2023).

[39] *NASA's Exploration & in-Space Services*. URL: https://nexis.gsfc.nasa.gov/osam-1.html (visited on 01/2023).

[40] Lynn Jenner. *NASA's on-orbit servicing, assembly, and Manufacturing 1 Mission Ready*. May 2021. URL: https://www.nasa.gov/image-feature/goddard/2021/nasa-s-on-orbit-servicing-assembly-and-manufacturing-1-mission-ready-for-spacecraft (visited on 01/2023).

[41] Rani Gran. *NASA satellite servicing technologies licensed by Northrop Grumman*. Jan. 2022. URL: https://www.nasa.gov/feature/goddard/2022/nasa-satellite-servicing-technologies-licensed-by-northrop-grumman (visited on 01/2023).

[42] Scott Rotenberger, David SooHoo, and Gabriel Abraham. "Orbital Express fluid transfer demonstration system". In: *Sensors and Systems for Space Applications II*. Vol. 6958. SPIE. 2008, pp. 41–49.

[43] D Reintsema et al. "DEOS–the German robotics approach to secure and de-orbit malfunctioned satellites from low earth orbits". In: *Proceedings of the i-SAIRAS*. Japan Aerospace Exploration Agency (JAXA) Japan. 2010, pp. 244–251.

[44] *ESPI report 76: In-orbit services. Policy and business perspectives*. Tech. rep. European Space Policy Institute, 2020. URL: https://espi.or.at/news/new-espi-report-in-orbit-services.

[45] Simon George et al. "Phantom Echoes 2: A Five-Eyes SDA Experiment on GEO Proximity Operations". In: *Proc 22nd AMOS Conf*. 2021.

[46] Michael Machula and Gurpartap Sandhoo. "Rendezvous and docking for space exploration". In: *1st Space exploration conference: continuing the voyage of discovery*. 2005, p. 2716.

[47] William Easdown and Leonard Felicetti. "A mission architecture and systems level design of navigation, robotics and grappling hardware for an on-orbit servicing spacecraft". In: (2020).

[48] John Leif Jørgensen and Mathias Benn. "Vbs-the optical rendezvous and docking sensor for prisma". In: *NordicSpace* (2010), pp. 16–19.

[49] Camille Sébastien Pirat et al. "Guidance, navigation and control for autonomous cooperative docking of CubeSats". In: *The 4S Symposium 2018*. CONF. 2018.

[50] James Bultitude et al. "Development and Launch of the World's First Orbital Propellant Tanker". In: (2021).

[51] Alberto Medina et al. "Towards a standardized grasping and refuelling on-orbit servicing for geo spacecraft". In: *Acta Astronautica* 134 (2017), pp. 1–10.

[52] P Rank et al. "The DEOS automation and robotics payload". In: *Symp. on Advanced Space Technologies in Robotics and Automation, ASTRA, the Netherlands*. 2011.

[53] Mate Kisantal et al. "Satellite pose estimation challenge: Dataset, competition design, and results". In: *IEEE Transactions on Aerospace and Electronic Systems* 56.5 (2020), pp. 4083–4098.

[54] Matthew G. Richards. "On-orbit serviceability of Space System Architectures". PhD thesis. 2006.

[55] Jing Yu and Dong Hao. "Optimal mission planning for refuelling LEO satellites with peer-to-peer strategy". In: *IOP Conference Series: Materials Science and Engineering*. Vol. 715. 1. IOP Publishing. 2020, p. 012045.

[56] J Vinals et al. "Future space missions with reconfigurable modular payload modules and standard interface–an overview of the SIROM project". In: *In Proceedings of the 69th International Astronautical Congress (IAC-2018)*. 2018, p. 11.

[57] Brook Sullivan and David Akin. "Satellite servicing opportunities in geosynchronous orbit". In: *AIAA SPACE 2012 Conference & Exposition*. 2012, p. 5261.

[58] Jean-Francois Castet and Joseph H Saleh. "Satellite and satellite subsystems reliability: Statistical data analysis and modeling". In: *Reliability Engineering & System Safety* 94.11 (2009), pp. 1718–1728.

[59] M Kortman et al. “Building block based iBoss approach: fully modular systems with standard interface to enhance future satellites”. In: *66th International Astronautical Congress (Jerusalem)*. 2015, pp. 1–11.

[60] Kieran Wilson and Hanspeter Schaub. “Impact of electrostatic perturbations on proximity operations in high earth orbits”. In: *Journal of Spacecraft and Rockets* 58.5 (2021), pp. 1293–1302.

[61] Rainer Krenn et al. “Docking Simulations for ASSIST System Verification”. In: *Proceedings of the i-SAIRAS*. 2016.

[62] Casey Clark. “Dynamics of Spacecraft Orbital Refueling”. Florida Tech, 2018.

[63] R Carr et al. “A simulink-based satellite docking simulator with generic contact dynamics capabilities”. In: *6th Int. Symp. on Artificial. Intel., Robotics & Auto. in Space, CSA, St-Hubert, Quebec*. 2001.

[64] Javier Vinals et al. “Multi-functional interface for flexibility and reconfigurability of future european space robotic systems”. In: *Advances in Astronautics Science and Technology* 1.1 (2018), pp. 119–133.

[65] Huang Jianbin et al. “Docking mechanism design and dynamic analysis for the GEO tumbling satellite”. In: *Assembly Automation* (2019).

[66] Shane Stamm and Pejmun Motaghedi. “Orbital express capture system: concept to reality”. In: *Spacecraft Platforms and Infrastructure*. Vol. 5419. International Society for Optics and Photonics. 2004, pp. 78–91.

[67] David J Chato. “Cryogenic fluid transfer for exploration”. In: *Cryogenics* 48.5-6 (2008), pp. 206–209.

[68] MT Constantine and EF Cain. *Hydrogen peroxide handbook*. Tech. rep. Rocketdyne Canoga Park CA Chemical and Material Sciences Dept, 1967.

[69] Lockheed Martin. *LM 2100 Payload Accommodation*. URL: https://www.lockheedmartin.com/content/dam/lockheed-martin/space/documents/openspace/LM-2100-payload-accommodation.pdf (visited on 01/2023).

[70] Orbit Fab. *RAFTI specification sheet*. 2019. URL: https://www.satcatalog.com/component/rafti-service-valve-low-pressure/ (visited on 01/2023).

[71] Orbit Fab. *RAFTI Block 2 Spec Sheet*. Jan. 4, 2022. URL: https://www.orbitfab.com/raftib2 (visited on 01/2023).

[72] James Bultitude et al. “First Flight of RAFTI Orbital Refueling Interface”. In: *72nd International Astronautical Congress (IAC)*. Oct. 2021.

[73] Orbit Fab et al. *A CubeSat Compliant Interface to Enable Spacecraft Docking and Fuel Transfer*. Apr. 23–25, 2019. URL: http://mstl.atl.calpoly.edu/~workshop/archive/2019/Spring/Day%202/Session%203/JamesBultitude.pdf.

[74] Juan Sánchez García Casarrubios et al. “Standardization of Thermal Interface for Future Space Missions”. In: *8th European Conference for Aeronautics and Space Sciences*. July 2019.

[75] *Sener aeroespacial finishes validation of Robotic interface sirom*. URL: https://www.aeroespacial.sener/en/press-releases/sener-aeroespacial-finishes-the-validation-of-the-robotic-interface-sirom-for-the-project-eross-h2020 (visited on 01/2023).

[76] Wiebke Brinkmann et al. “Mechanical, thermal, data and power transfer types for robotic space interfaces for orbital and planetary missions - a technical review”. In: June 2017.

[77] Brandon N Dick, Nathan Mauch, and Timothy Rupp. “Capture Latch Assembly for the NASA Docking System”. In: *Aerospace Mechanisms Symposium*. JSC-E-DAA-TN51644. 2018.

[78] Hua Chen, Weishan Chen, and Junkao Liu. “Optimal design of Stewart platform safety mechanism”. In: *Chinese Journal of Aeronautics* 20.4 (2007), pp. 370–377.

[79] Justin McFatter, Karl Keiser, and Timothy W Rupp. “NASA Docking System Block 1: NASA’s new direct electric docking system supporting ISS and future human space exploration”. In: *Aerospace Mechanisms Symposium*. JSC-E-DAA-TN51081. 2018.

[80] R Eberhardt and T Tracey. “Orbital spacecraft resupply technology”. In: *22nd Joint Propulsion Conference*. 1986, p. 1604.

[81] *Material Compatibility for Bioquell Technology*. Tech. rep. Bioquell, 2019. URL: https://labotal.co.il/wp-content/uploads/2020/05/TD041-SP-001-VHP-Material-compatibility.pdf (visited on 12/2022).

[82] Leonard D Jaffe and John B Rittenhouse. “Behavior of materials in space environments”. In: *ARS Journal* 32.3 (1962), pp. 320–346.

[83] SSTL. *Space Propulsion Innovation Award*. 2014. URL: https://www.slideshare.net/Stellvia/space-propulsion-innovation-award (visited on 12/2022).

[84] Nick Eckenstein. “High-Dimensional Design Evaluations For Self-Aligning Geometries”. PhD thesis. University of Pennsylvania, 2019.

[85] Robert Connelly and Erik D Demaine. “9: Geometry and topology of polygonal linkages”. In: *Handbook of discrete and computational geometry*. Chapman and Hall/CRC, 2017, pp. 233–256.

[86] Eric W. Weisstein. *Circle-Circle Intersection.* URL: https://mathworld.wolfram.com/Circle-CircleIntersection.html (visited on 12/2022).

[87] Rachel M Holladay and Siddhartha S Srinivasa. “Distance metrics and algorithms for task space path optimization”. In: *2016 IEEE/RSJ International Conference on Intelligent Robots and Systems (IROS)*. IEEE. 2016, pp. 5533–5540.

[88] Maria Pikoula Spiros Denaxas. *Frechet library Discrete Fréchet distance*. URL: https://github.com/spiros/discrete_frechet (visited on 12/2022).

[89] Maxim Murashkin et al. “Fatigue behavior of an ultrafine-grained Al-Mg-Si alloy processed by high-pressure torsion”. In: *Metals* 5.2 (2015), pp. 578–590.

[90] *Hexapod: Forces*. July 2020. URL: https://www.jpe-innovations.com/precision-point/hexapod-forces/ (visited on 01/2023).

[91] Michael Grant and Stephen Boyd. *Simscape Multibody Contact Forces Library*. https://github.com/mathworks/Simscape-Multibody-Contact-Forces-Library/releases/tag/22.2.5.1. 2022. (Visited on 06/2022).

[92] R Carr et al. “A simulink-based satellite docking simulator with generic contact dynamics capabilities”. In: *6th Int. Symp. on Artificial. Intel., Robotics & Auto. in Space, CSA, St-Hubert, Quebec*. 2001.